Therapeutic Liposomes for Prostate Cancer Targeted by Phage Fusion Coat Proteins

by

Prashanth K. Jayanna

A dissertation submitted to the Graduate Faculty of
Auburn University
in partial fulfillment of the
requirements for the Degree of
Doctor of Philosophy

Auburn, Alabama
December 18, 2009

Approved by

Valery A. Petrenko, Chair, Professor of Pathobiology
Calvin M. Johnson, Professor of Pathobiology
Stuart B. Price, Associate Professor of Pathobiology
Dawn M. Boothe, Professor of Anatomy, Physiology & Pharmacology
Robert L. Judd, Associate Professor of Anatomy, Physiology & Pharmacology
Tatiana I. Samoylova, Associate Research Professor of Pathobiology

Abstract

Cancer diagnosis and treatment is complicated by the molecular similarity of the malignant cells to normal cells. This creates a constant need for the development of probes accurately distinguishing between diseased and healthy cells. I describe here the selection of phage probes for prostate carcinoma cells and further demonstrate the potential of these probes as navigating ligands for therapeutic liposomes.

Landscape libraries, our primary tools in the identification of ligands for a variety of targets are defined by their diversity and repertoire. We used two landscape libraries to identify phage probes for PC3 cells. The specificity and selectivity of these probes was demonstrated with cell association assays, fluorescence microscopy and flow cytometry.

Landscape phage particles are composed of 4000 units of the major coat protein pVIII with unique membranophilic properties. We hypothesized that once extracted from the phage particle these entities could serve as targeting ligands for liposomes. In a streptavidin based model we were able to demonstrate that streptavidin-specific pVIII units insert into liposomes and invest the same with affinity towards streptavidin. We adopted the same technique to derive PC3-specific phage coat protein units from the previously identified phage probes to be used as targeting ligands for fluorescently-labeled and drug-loaded liposomes.

Targeting has been shown to improve the therapeutic efficiency of liposomal drugs. We hypothesized that liposomal therapeutics targeted to PC3 cells via PC3

specific phage coat protein would achieve improved cytotoxic effects as against non-targeted formulations. In fluorescence microscopy and flow cytometry studies we demonstrated that targeted labeled liposomes associated with the target PC3 cells better than the control cells. Further, we demonstrated that grafting of the PC3-specific phage fusion protein units onto DOXIL improves the cytotoxic performance of the liposome encapsulated doxorubicin using *in vitro* cytotoxicity studies.

The identification of landscape phage probes for different carcinomas from landscape phage libraries may provide an impetus for harnessing the same in various diagnostic and therapeutic applications. Further, the simplicity of our approach for the construction of targeted liposomal formulations allows for the creation of a combinatorial system of production of therapeutic liposomes for different types of cancer.

Acknowledgments

The author would like to thank the members of his committee for their discerning guidance all through this project. He is exceptionally grateful to Dr. Petrenko for his astute advice and direction. The author would like to acknowledge the valuable intellectual contributions of his co-authors in his various publications; Dr. V.P. Torchilin, Dr. G.A. Kuzmicheva, Dr. I.B. Sorokulova, Dr. D. Bedi, Dr. R.C. Bird, Ms. Patricia Deinnnocentes and Ms. Tao Wang. The author would also like to thank the families of Donegan and Oliver for their undying support and encouragement. He also expresses deep gratitude for his family for their faith in him.

Table of Contents

List of Tables

List of Figures

CHAPTER 1

INTRODUCTION AND REVIEW OF LITERATURE

1. Introduction

Prostate cancer has emerged as a looming medical problem in recent years with improved diagnostic methods partially contributing to the increased incidence as well a better A survival rate after treatment. Given the observed chemoresistance of the tumor, treatment modalities for this cancer have traditionally been radiation therapy and radical surgery. Chemotherapy was relegated to a supporting palliative role in the advanced stages when the tumor becomes non-responsive to hormonal manipulations, a condition described as Hormone-Refractory Prostate Cancer (HRPC). However, the results of recent phase III trials with docetaxel, a taxane microtubule stabilizer, demonstrated that it can lead to a significant survival benefit and these observations led to the approval of docetaxel with prednisone by the FDA as the standard of care for HRPC (Pomerantz and Kantoff, 2007). The success of docetaxel opened up new opportunities for hitherto ignored chemotherapeutic options and at the same time brought to light problems associated with their use. Many of the hypersensitivity reactions associated with docetaxel administration were imputed to be caused by its formulation containing tween 80 and thus liposomal incorporation of docetaxel was suggested as a possible way to overcome this problem. Given their biocompatibility and ability to passively accumulate

in tumor interstitium by virtue of the Enhanced Permeation and Retention phenomenon (EPR), liposomes constitute a very attractive platform for tumor drug delivery.

To further amplify tumor selectivity and control drug unloading within tumors as well as improve therapeutic efficacy of drugs, liposomes can be conjugated to targeting ligands. Numerous ligands including antibodies, peptides, oligosaccharides, aptamers, and growth factors have been proposed and it has been repeatedly demonstrated that active targeting of drug delivery vectors such as liposomes significantly improves therapeutic performance of the drug even going so far as to overcome resistance mediated by efflux pumps due to an endocytosis-mediated intracellular delivery while simultaneously decreasing possible side effects by reducing the IC_{50} values (Goren *et al.*, 2000; Banerjee *et al.*, 2004; Elbayoumi *et al.*, 2007; Elbayoumi and Torchilin, 2007; Sawant *et al.*, 2008; ElBayoumi and Torchilin, 2009).

Within this context, we propose landscape phage fusion proteins – substitute antibodies with high selectivity, affinity and stability as advanced navigating ligands for liposomal vehicles bearing antitumor drugs. The tumor-specific peptides genetically fused to all 4,000 copies of the phage's major coat protein pVIII can be affinity selected from multibillion clone libraries by their ability to bind very specifically cancer cells, penetrate into the cells or accumulate in the tumor-surrounding vasculature. The selected tumor-specific phage can be converted into the drug-loaded vesicles in which the fusion phage proteins span the lipid bilayer of liposomes displaying the tumor-binding peptides on the surface of the vesicles. Thus, the major principle of the proposed approach is that fusion phage protein-targeted therapeutic liposomes recognize the same receptors, cells, tissues and organs that have been used for selection of that particular landscape phage.

We hypothesized that targeting of drug-bearing liposomes with the prostate tumor-specific phage proteins may significantly enhance the therapeutic efficiency of the drug contained within by virtue of the selective delivery of cytotoxic cargo. To test this hypothesis, we undertook experiments that demonstrate that landscape libraries are indeed an exemplary source of tumor-specific probes, that phage major coat protein can serve as an efficient targeting ligand and that this targeting has a definite beneficial effect on drug efficacy in a model system utilizing Doxil.

The first chapter of this dissertation reviews prostate cancer as a medical entity, treatment options for prostate carcinoma, current expansions in chemotherapeutic possibilities for advanced stages as well as a review of liposomes and targeted liposomes as carriers of drugs. In addition, this chapter also considers details of phage biology, the concept of landscape phage display and the unique properties of the phage major coat protein which merit its consideration as a novel targeting ligand for liposomes.

The second chapter of this dissertation provides the justification for using multiple libraries in selection procedures by comparing two landscape libraries and their evolution during selection. Specific aims included:

I. Compare the amino acid diversities of two landscape libraries of similar size and complexity to identify the effect of censoring arising due to phage reproduction.

II. Compare the results of parallel selection of the libraries against common targets of increasing molecular complexity namely β-lactamase, streptavidin and *Salmonella typhimurium*.

The third chapter of this dissertation describes the selection of landscape phage probes for PC3 prostate carcinoma cells and their characterization. Specific aims included:

I. Identify specific and selective phage probes from two landscape phage libraries that associate with PC3 prostate carcinoma cells.

II. Characterize the specificity and selectivity of the identified phage probes in cell association studies.

The fourth chapter of this dissertation describes an efficient technique for obtaining phage major coat protein from phage particles as well as provides proof of concept for the use of phage major coat protein as a targeting ligand for liposomes. Specific aims included:

I. Isolate and purify phage major coat protein using sodium cholate.

II. Incorporate the isolated phage major coat protein into liposomes and test for streptavidin targeting.

The fifth chapter of this dissertation describes the production of phage coat protein-targeted PC3 specific liposomes using techniques outlined in the fourth chapter. Specific aims included:

I. Produce liposomes incorporating phage major coat protein as the navigating ligand.

II. Evaluate the cytotoxic potential of such targeted therapeutic liposomes over that of non-targeted liposomes *in vitro* against PC3 cells.

2. Prostate cancer

2.1 Prostate Cancer as a Medical Entity

The prostate is an exocrine gland and forms part of the male reproductive anatomy. It is responsible for the production of nearly a third of seminal fluid. The prostatic secretions are alkaline and help in maintaining the viability of the spermatozoa in the acidic female genital tract. Among the disorders of the prostate, prostate cancer has garnered the most attention due to its widespread prevalence as well as the enormous impact on the quality of life of patients, particularly post-treatment.

Prostate cancer remains the most common among the malignancies afflicting males and is almost considered a normal age-related phenomenon in society. The American cancer institute estimates that almost 200,000 new cases will be diagnosed and nearly 30,000 deaths will occur in 2008 (ACS, 2008). Routine screening for Prostate Specific Antigen (PSA) despite being controversial has resulted in an increase in the prevalence of prostate cancer creating a lifetime risk of diagnosis of 16%. However, the lifetime risk of dying from the disease is 3.4% (Wilt *et al.*, 2003). Even though the malignancy *per se* does not carry a serious fatality risk with it, it still represents a significant burden on the health care industry due to the long term management and follow-up involved.

Prostate cancer is an extremely heterogeneous disease with a spectrum of signs ranging from asymptomatic to a rapidly disseminating fatal condition. Most cases of prostate cancer are adenocarcinomas arising from the glandular epithelium (Mazhar and Waxman, 2002). The etiology of prostate cancer remains unknown, however, a number

of risk factors have been identified as having a bearing on the probability of developing prostate cancer. These include age>65, race, ethnicity, family history, presence of prostatic intraepithelial neoplasia and genomic predispositions like having the *BRCA1* and *BRCA2* genes. Age remains the most significant risk factor with the risk of diagnosis increasing exponentially with age and almost 85% of cases diagnosed are in men over 65 years (Wilt *et al.*, 2003). The unusual epidemiology and natural history coupled with a lack of adequate knowledge of the biology of prostate cancer has created controversies regarding an optimal approach to the clinical management of the malignancy. Presently, Gleason score based on the histopathological examination of glandular differentiation is considered to be the best prognostic indicator to date (Hughes *et al.*, 2005). Coupled with the TNM (Tumor, Node, Metastasis) staging system, the Gleason grading system has been used as a critical determinant for the choice of therapy. The PSA test with a cutpoint of 4.0 ng/ml for detecting prostate cancer has a sensitivity of only 20% which implies a gross overdiagnosis of patients with low grade carcinomas not requiring biopsies or treatment. Furthermore, the PSA values fail to predict the clinical outcome of the disease. Monitoring the PSA velocity (rate of PSA increase) has been suggested to overcome this deficit as a higher PSA velocity has been shown to have stronger correlation with more lethal types of prostate cancer (Taichman *et al.*, 2007). Despite these shortcomings of the PSA test, its widespread adaptation for prostate cancer screening has allowed for an earlier diagnosis of the disease as well diagnosis of earlier, more tractable stages of disease. This early diagnosis followed by appropriate therapy prevents mortality and is responsible for the tremendous improvement in the 5-year survival rate which almost approaches 100% (Hughes *et al.*, 2005). Despite therapy, approximately 10-20% of

prostate cancer cases proceed to metastatic disease and thence onto a unique stage referred to as Hormone Refractory Prostate Cancer (HRPC) or Androgen Independent Prostate Cancer (AIPC)(Chowdhury *et al.*, 2007). Prostate cancer cells start out as being dependent on androgens for their growth and sustenance. Thus, androgen depletion regimens have been a long-standing treatment option for advanced prostate cancers. However, as the disease progresses further, the cancer cells develop a gradual independence from hormonal influences. Though several genetic mutations have been implicated in the development of this condition, the most compelling is that of the androgen receptor (*AR*) gene. Cases of HRPC demonstrate an overexpression of the AR as well as mutations leading to hypersensitivity of the receptor, promiscuous activation or bypass activation (Feldman and Feldman, 2001). Many of the mutations are thought to be enforced by the hormone deficient conditions that exist during androgen ablation therapy which exerts a selective pressure for the creation of hormone insensitive populations of cells (Nieto *et al.*, 2007). In addition, hormone resistant cells have been demonstrated to overexpress antiapoptotic molecules to enhance their survival capabilities (Gao *et al.*, 2006). Another probable contributing factor to the emergence of androgen independence would be the presence of androgen-independent prostate stem/progenitor cells which continuously replenish the tumor mass (Collins and Maitland, 2006).

2.2 Treatment Options

In general, early stages of prostate cancer (localized disease) is treated with either surgery or radiation whereas the advanced forms of prostate cancer are dealt with using hormone ablation approaches or chemotherapy or a combination. Treatment of early

stages of prostate cancer can be curative whereas the therapies revolving around later stages are mostly palliative and symptomatic.

2.2.1 Localized prostate cancer

The treatment of localized prostate cancer is the matter of much contention as no single treatment modality is seen to have a clear significant advantage over the others. Each comes with its attendant advantages and pitfalls. The treatment options for localized cancer can be classified into the surgical and non-surgical arms. The surgical approach advocated for prostate cancer encompasses radical prostatectomy, transurethral resection of prostate and cryosurgery. Nerve sparing radical prostatectomy is considered by many surgeons to be the 'gold standard' for the treatment of prostate cancer (Goldstraw and Kirby, 2006) and indeed in a study performed to compare radical prostatectomy to deferred treatment (watchful waiting), the radical prostatectomy arm showed a higher survival advantage as well as decreased incidence of metastasis (Bill-Axelson *et al.*, 2005). However, the incidence of side effects arising from the procedure like erectile dysfunction and urinary incontinence was very high. The cost-benefit ratio of radical prostatectomy in terms of the side effects made it look superfluous in low-risk patients. This gains even more importance in view of the fact that PSA testing results in the diagnosis of lower grade tumors in younger men. Radical prostatectomy in such cases would have a serious impact on the quality of life of these patients. Watchful waiting as described in the above study entails no treatment until the onset of clinical progression. However, an improvement over this method called 'active surveillance' involves regular monitoring and institution of treatment prior to clinical onset of symptoms. However, a

singular problem that crops up is that of patient suitability to active surveillance. Algorithms based on clinical parameters have been developed to overcome this problem (Klotz, 2005). Apart from active surveillance, the other non-surgical approaches include radiation therapy. Radiation therapy may be external beam radiotherapy in which the source of radiation is produced outside the patient's body and directed towards the malignancy or it can be brachytherapy in which radioactive 'seeds' are implanted in the prostatic tissue so as to release radiation over a period of time. Impotence and urinary incontinence are often encountered as side effects. In conjunction with radiation therapy, adjuvant and neoadjuvant therapy involving androgen deprivation have been shown to improve survival rates (D'Amico *et al.*, 2004; Tanne, 2008).

2.2.2 Advanced, recurrent and metastatic prostate cancer

Following the groundbreaking studies of Huggins et al in 1941 (Huggins *et al.*, 1941) demonstrating that androgen suppression is advantageous to some extent in all forms of prostatic carcinoma for which they were subsequently awarded the Nobel prize, androgen ablation or androgen deprivation therapy (ADT) has become the mainstay in the treatment of advanced prostate cancers. Huggins and Hodges used surgical castration and diethyl stilbestrol (DES) to lower serum testosterone levels in advanced prostate cancer patients and found an alleviation of symptoms namely bone pain in both cases. Following this study, DES became the standard of care in advanced cases of prostate cancer though at higher concentrations it was found to be cardiotoxic (Byar and Corle, 1988). The availability of potent and long acting luteinizing hormone-releasing hormone (LHRH) agonists led to a complete displacement of DES in prostate cancer treatment.

These act by the negative feedback regulation of the pituitary LHRH receptors. Apart from the side effects which include loss of libido, impotence and hot flashes, a disadvantage associated with their use was the 'flare' phenomenon which is an initial surge of testosterone immediately after treatment (Waxman *et al.*, 1985). This may exacerbate the tumor leading to acute symptoms but can be avoided by the concomitant administration of an antiandrogen (Schulze and Senge, 1990). Recently, in a bid to overcome the flare effect, LHRH antagonists were developed which have been shown to bring down the serum testosterone to castrate levels more rapidly than the LHRH agonists (McLeod *et al.*, 2001). In addition, compounds that inhibit or block the androgen receptor called antiandrogens have been developed. These are classified as being steroidal or non-steroidal. The steroidal antiandrogens include megestrol acetate and medroxyprogesterone acetate whereas non-steroidal antiandrogens include flutamide, bicalutamide and nilutamide. Monotherapy with antiandrogens has shown to be less effective as either medical or surgical androgen ablation, thereby damping their primary use (Kaisary *et al.*, 1995; Iversen *et al.*, 1996). However, they have come to play a very important role in a treatment strategy known as complete androgen blockade (CAB). This strategy is targeted at the adrenal synthesized testosterone which has a significant effect on tumor tissue even in the absence of testicular testosterone. A combination of an LHRH agonist with an antiandrogen is used to achieve a complete abrogation of serum testosterone and has been shown to be more effective than castration alone in several studies (Crawford *et al.*, 1989; Janknegt *et al.*, 1993; Dijkman *et al.*, 1997). Despite hormone manipulations, most advanced cases of prostate cancer proceed to a hormone independent stage where in they no longer respond to mainline hormone therapy. A

therapeutic design aimed at delaying this progression has been developed and is termed intermittent androgen deprivation (IAD). Here the patient is subjected to the hormone therapy until the PSA reaches a nadir whereupon it is discontinued and reinstituted only when the PSA reaches a pre-determined level which is usually 5-10 ng/ml. Another obvious advantage is the reprieve from the side effects of long term continuous androgen ablation thereby ensuring a better quality of life (Bhandari *et al.*, 2005; Calais Da Silva *et al.*, 2006). One of the most debated issues in hormone therapy of prostate cancer is the onset of the therapy. The question as to whether therapy should be instituted immediately after diagnosis or should be deferred until appearance of symptoms has been extremely controversial. Most studies so far seem to indicate in favor of an early onset of ADT in terms of survival and disease progression though not always significantly so (Walsh, 1997; Messing *et al.*, 1999; SchrÖDer *et al.*, 2004).

In addition to hormonal therapy, several novel approaches involving chemotherapeutic agents, monoclonal antibodies as well as receptor antagonists in combination with ADT are currently under investigation (Brawer, 2006).

2.2.3 Androgen Independent or Hormone Refractory Prostate Cancer (AIPC OR HRPC)

Almost all advanced cases of prostate cancer proceed inexorably into a highly painful, therapeutically intractable stage referred to as AIPC or HRPC. Though the stage is referred to as hormone independent, some treatment modalites involving hormonal manipulations do produce results and is often referred to as secondary hormonal treatment. Ketoconazole used to suppress adrenal androgen production as well as second-line antiandrogens like Nilutamide have been shown to have favorable effects in the

reduction of PSA (Kassouf *et al.*, 2003; Small *et al.*, 2004). Apart from the secondary hormone therapy, no treatment options apart from the pain relieving corticosteroids were available to patients with HRPC. Studies conducted to evaluate the efficacy of chemotherapeutic possibilities had not provided promising results leading to the relegation of chemotherapy as being marginally effective (Yagoda and Petrylak, 1993). However, the development of surrogate endpoints for clinical trials like reduction of PSA, quality of life, pain alleviation and survival allowed for a much broader spectrum of patients to be included in the studies and provided an improved window to judge chemotherapeutic agents (de Wit, 2008). Subsequently, it was demonstrated that a combination of mitoxantrone, an anthracenedione in combination with corticosteroids provided better relief than corticosteroids alone though there was no significant improvement in overall survival (Tannock *et al.*, 1996; Kantoff *et al.*, 1999). Following promising proof-of-concept studies with docetaxel in 1999 (Picus and Schultz, 1999), two randomized phase III studies were undertaken to further evaluate the efficacy of docetaxel (Petrylak *et al.*, 2004; Tannock *et al.*, 2004). The results of these trials provided the first instance of survival benefit attributable to chemotherapy in prostate cancer and led to the approval of docetaxel with prednisone by the FDA as the standard of care for HRPC (Pomerantz and Kantoff, 2007). The major toxicities associated with docetaxel administration include hypersensitivity and peripheral neuropathy imputed to the excipient, Tween 80 (polysorbate 80), and routine premedication with glucocorticoids and antihistamines is advocated to decrease their incidence. As a more permanent and safer solution, alternative formulations to deliver the active drug to tumors are being investigated. Immordino et al have prepared and characterized docetaxel containing

PEGylated liposomes. Since the incorporated drug assumes the pharmacokinetic profile of its vector, docetaxel terminal half-life in liposomes demonstrated a nearly 13-fold increase whereas clearance and volume of distribution were decreased more than 100- and 6-fold, respectively, compared to the traditional formulation of docetaxel. Liposome incorporation did not affect the *in vitro* cytotoxicity of docetaxel (Immordino *et al.*, 2003). Furthermore, immunoliposomal docetaxel was shown to potentiate radiosensitivity of human colon cancer cells demonstrating that encapsulation entails no compromise in drug activity (Wang *et al.*, 2005). However, a limiting factor in liposomal preparations of docetaxel was the low loading efficiency observed (Immordino *et al.*, 2003).

Studies involving standard liposomal formulations of doxorubicin, which are already available in the market (Doxil®, Caelyx®), have demonstrated conflicting results. In a pilot study conducted by Hubert et al, Doxil® was found to be effective against HRPC but severe mucocutaneous toxicities precluded further investigations (Hubert *et al.*, 2000). In a later phase II study, Doxil® was observed to produce no objective response and a PSA response in only 3 out of 14 patients leading the authors to question the utility of the formulation in HRPC (McMenemin *et al.*, 2002). However, in another randomized phase II trial involving more patients a significant palliative response was obtained with Doxil®. The authors again reported the palmar-plantar erythrodysesthesia (PPE) but observed that the lesions were self-limiting and could be resolved by the topical application of 99% dimethylsulfoxide (Heidenreich *et al.*, 2004). Despite these contradictory results with Doxil, studies involving the active targeting of doxorubicin-loaded liposomes and Doxil®, both *in vitro* and *in vivo* have provided encouraging results. Banerjee et al demonstrated the feasibility of using small molecular

weight targeting ligands like anisamide to target liposomes to prostate cancer cell line DU-145 *in vitro* as well as anti-tumor activity of targeted liposomes *in vivo* in a mouse xenograft model of DU-145 (Banerjee *et al.*, 2004). The grafting of nucleosome-specific monoclonal antibody 2C5 (mAB 2C5) onto the surface of Doxil® resulted in enhanced cytotoxicity against a variety of cancer cells in comparison with untargeted Doxil®. There was significant lowering of the IC_{50} values (~8 fold) indicating a lowered toxicity profile with targeted formulations. Furthermore, the targeting antibody allowed for increased internalization of liposomes which may be critical in drug resistant tumors due to the bypass of drug efflux pumps (Elbayoumi and Torchilin, 2007). In an extension of these studies, the *in vivo* tumor accumulation of ^{111}In-labeled 2C5 targeted liposomes in various mouse models of human tumor xenografts was examined. Targeted liposomes showed a preferential accumulation in the tumors over untargeted liposomes (Elbayoumi *et al.*, 2007). Further, the *in vivo* therapeutic efficiency of 2C5 – modified Doxil was evaluated in a PC3 xenograft mouse model. It was observed that treatment with targeted liposomes resulted in lower tumor volumes and tumor weights as compared with unmodified Doxil (ElBayoumi and Torchilin, 2009). Taken together, these results indicate that targeting functions to increase the therapeutic efficiency of drugs at the same time reducing the toxicities associated with them. Thus, targeting may provide the reprieve required to overcome the hurdles facing the use of Doxil® in HRPC. In addition, the potential use of targeted Doxil as part of a combination therapy also has to be considered. For example, it was shown that doxorubicin amplified the apoptotic properties of Apo2L/TRAIL against PC3 xenograft models in nude mice (El-Zawahry *et al.*, 2005).

Thus, targeting provides a window of opportunity to recast the use of liposomal anthracyclines in the treatment of HRPC and provides an impetus to delve into improved methods of targeting liposomes to tumors. These observations along with the necessity to adopt a model system to prove our concept led us to incorporate Doxil in our studies.

3. Liposomes

3.1 Liposomes as drug carriers

Liposomes, spherical bilayered vesicles composed of phospholipids, were first described by Bangham in 1961. The unique architecture of these structures arising as a result of the amphipathic properties of its constituent molecules allowed for the creation of compartments within which both hydrophobic and hydrophilic pharmacologically active molecules could be accommodated, thus giving rise to the concept of liposomes as carrier vehicles. Liposomes as biological vectors held great promise as they were inert and completely biocompatible. Drugs entrapped into liposomes are shielded from degradative mechanisms and thus exhibit a greater residence time *in vivo*. Since liposomal encapsulation invests the drug with the vehicular pharmacokinetic properties, the therapeutic index as well as the bioavailability of the drug is improved. Advances in liposomal formulation techniques have made liposome production a routine procedure with ultrasonication, reverse phase evaporation and detergent dialysis being the most commonly employed techniques. In addition, the amenability of liposomal surface to modifications allow for the incorporation of various targeting molecules which again results in improved therapeutic indices of encapsulated drugs (Torchilin, 1985). Despite

these inherent advantages, the harnessing of liposomes in clinical therapy has not been impressive. One of the major reasons for this is the rapid recognition and subsequent clearance of liposomes from circulation by the monocytic phagocytic system (MPS) which led to Gregory Gregoriadis' epitaphic description, "…unstable, shortlived……doomed to decay in looming Kupffer cells" of these vesicles. However, a reprieve was obtained with the development of sterically stabilized liposomes in which surface grafting of liposomes with hydrophilic polymers helped prevent their uptake into the MPS, thereby increasing their circulatory times.

3.2 Sterically stabilized liposomes

Liposomes with low MPS uptake were first demonstrated by Allen et al who achieved this by decorating the liposomal surface with gangliosides. The presence of gangliosides effectively obviated liver and spleen uptake of liposomes and enabled prolonged circulation times (Allen and Chonn, 1987). Due to their ability to escape recognition by the MPS they were named 'stealth liposomes' (Allen *et al.*, 1989). Furthermore, stealth liposomes targeted with monoclonal antibodies were shown to circumvent the MPS and successfully accumulate in the target organ providing additional basis for the concept of targeted drug delivery vehicles for cancer therapy (Maruyama *et al.*, 1990). Following this study, Klibanov et al demonstrated that liposomes incorporating polymers like polyethylene glycols show a ten-fold increase in their circulation half-lives with minimal accumulation in liver and spleen (Klibanov *et al.*, 1990). They hypothesized that the increased hydrophilicity resulting from a PEG coating of the liposome may help in reducing nonspecific interactions with the RES and also

sterically hinder opsonization of liposomes thereby stabilizing them. Surface coating of liposomes with PEG dramatically altered the pharmacokinetics of liposomes transforming it from a saturable, dose-dependent and non-linear one to non-saturable, dose-independent, log-linear one with enhanced anti-tumor efficacy (Papahadjopoulos *et al.*, 1991).

3.3 Enhanced Permeation and Retention (EPR) effect in tumors

Another critical milestone in liposome-mediated anti-tumor treatment was the observation of the EPR phenomena described by Maeda et al (Maeda *et al.*, 2000). The phenomenon was first described to explain the increased deposition of macromolecular anticancer drugs in tumor tissue but was found to be true for various blood borne nanoparticles and lipidic materials. The increased permeation of tumors arises from the various anatomical anomalies that occur in tumor blood vessels. For instance, endothelial cells in tumor blood vessels show poor alignment with large fenestrations. Furthermore, there is a distinct lack of the perivascular cells and smooth muscle cells critical for generating and maintaining a constant blood volume flow to tissues. The causatives for enhanced retention are mainly a defective lymphatic drainage and a poor venous return. Taken together, these factors enable extensive extravasation of blood borne macromolecules into tumor tissue and their retention for protracted periods of time within the tumor interstitium (Iyer *et al.*, 2006), a phenomenon that results in passive targeting of liposomes. Liposomes were shown to extravasate and accumulate selectively in tumor interstitium of colon cancer-bearing mice as a result of the EPR effect (Huang *et al.*, 1992).

3.4 Targeted sterically stablilized liposomes

The conjunction of long circulating properties with the EPR phenomenon yielded a drug delivery system which combined the optimal pharmacokinetic qualities of liposomes with their tumor selective biodistribution to ensure a specific delivery of the encapsulated drug to tumor sites. The rapid realization of these milestones allowed for a liposomal anticancer therapeutic, Doxil® to be introduced into clinical practice with full FDA approval. Despite the success achieved with Doxil® (Haley and Frenkel, 2008), passive targeting does not avail a precise tumor targeting based on the molecular biology of the malignancy. Furthermore, EPR is efficient in bringing about the deposition of drug-loaded liposomes into tumor interstitium but once in the interstitium, further effects of the drug depends on the drug release from the carrier molecule. Mechanisms of drug release following liposome disassembly have not been clearly defined and lack a definite direction of drug release and hence are not well controlled (Noble *et al.*, 2004). Also, free drug in the tumor interstitium has a definite propensity to get removed by the tumor circulation. Thus, a precise intracellular unloading of drug would circumvent these problems and establish a liaison to deliver the liposomal payload to the site of action which requires that liposomes be targeted actively to tumor specific markers. The concept of targeting liposomes using tumor-specific ligands has been demonstrated (Banerjee *et al.*, 2004; Gabizon *et al.*, 2004; Lukyanov *et al.*, 2004; Pastorino *et al.*, 2006) and a plethora of ligands including antibodies (MAb) or fragments, peptides, growth factors, glycoproteins, carbohydrates or receptor ligands have been proposed (Immordino *et al.*, 2006).

3.5 Peptide targeting ligands for liposomes

Though most studies have used antibodies, these therapies show limited efficacy in solid tumors mainly due to their large size (~160 kDa) which precludes efficient penetration, a problem aggravated by the elevated tumor interstitial pressure (Jain, 1990). Furthermore, optimal tumor penetration may be hindered by a high affinity interaction between the antibody and the first few antigen molecules it comes in contact with thereby preventing uniform diffusion, a phenomenon first described as "binding site barrier" (Fujimori *et al.*, 1989) and later demonstrated conclusively (Adams *et al.*, 2001). Also, immunogenicity and non-specific uptake by the reticulo-endothelial system contribute to a less than favorable clinical outcome. Advances in antibody engineering have partly alleviated these problems by creating functional fragments of target-specific antibodies. Examples include single chain Fv fragments (~25 kDa) (Adams and Schier, 1999) as well as VHH domains or nanobodies (~15 kDa) (Cortez-Retamozo *et al.*, 2004) which are better able to cater to the needs of increased tumor penetration and decreased immunogenicity and non-specific removal. Research has indicated that pharmacokinetic properties are improved with the use of smaller ligands underscoring the need for smaller molecules for tumor directed therapies (Reilly *et al.*, 1995). Peptides being in the range of 1-2 kDa and demonstrating acceptable affinity and specificity to their targets represent an attractive alternative to antibodies. Much of the problems attendant with the larger sized antibodies appears to be resolved with peptides. They possess impressive tumor penetrating capacity, are generally not recognized by the MPS and are less likely to instigate immune responses. In addition, they exhibit a higher activity per mass and

greater stability (Ladner *et al.*, 2004). Their undoing, rapid proteolysis as well as poor affinity can be resolved by derivation of peptidomimetics by N and/or C terminal blocking, cyclization and incorporation of D-amino acids (Nilsson *et al.*, 2000; Aina *et al.*, 2002a; Borghouts *et al.*, 2005). Furthermore, the availability of combinatorial peptide libraries from which potential therapeutics can be extracted adds another availing dimension to the concept of peptidic biopharmaceuticals. The use of phage displayed peptide libraries for obtaining tumor-specific peptides and their application in tumor-targeting has been illustrated with several examples in recent reviews (Craig and Li, 2006; Krumpe and Mori, 2006). Liposomal targeting mediated by phage display-derived peptides has been amply demonstrated (Koivunen *et al.*, 1999; Medina *et al.*, 2001; Lee *et al.*, 2004; Pastorino *et al.*, 2006; Slimani *et al.*, 2006; Garde *et al.*, 2007; Lee *et al.*, 2007). A critical factor within this scenario is that of the conjugation chemistry required to attach the ligand to the liposomal surface. Numerous covalent coupling techniques including the formation of a disulfide bond, cross-linking between primary amines, reactions between a carboxylic acid and primary amine, between maleimide and thiol, between hydrazide and aldehyde or between a primary amine and free aldehyde can be used [reviewed in (Nobs *et al.*, 2006)]. The conjugation procedures adapted from the armentarium of organic chemistry are quite efficient for preparation of various targeted liposomes in small scale – for their preliminary laboratory and clinical study. However, the cost and reproducibility of these derivatives in quality and quantity sufficient for pharmaceutical applications are challenging problems.

Furthermore, the use of antibody conjugates may be less efficient at the scaling step, when very standardized and pharmaceutically acceptable preparations are required

(Nellis *et al.*, 2005b). For example, 2,085 mg of lipid conjugated with single chain antibody was obtained through a laborious procedure involving high volume propagation of bacteria, several chromatographic steps and sophisticated conjugation procedures yielding a preparation which had 93% purity (Nellis *et al.*, 2005a). Also, preparative conditions for the addressed vesicles differ idiosyncratically from one targeted particle to another. These considerations led us to evaluate the potential of phage coat proteins as easily available targeting components of drug carriers. We propose a new approach which relies on the use of phage coat proteins as the targeting probes of the drug-loaded liposomes and micelles and is predicated on the unique structural properties of the phage coat protein. In our approach the phage specific for the target organ, tissue or cell is selected from the multibillion landscape phage libraries, as described (Romanov *et al.*, 2001; Romanov, 2003; Samoylova *et al.*, 2003; Mount *et al.*, 2004) and is converted to the liposome exploiting intrinsic amphiphilic properties of the phage proteins (Figure 1). As a result, the targeting probe—the tumor-specific peptide fused to the major coat protein is exposed on the shell of the drug-loaded vesicle. In contrast to the sophisticated and poorly controllable conjugation procedures used for coupling of peptides and antibodies to the targeted vesicles, the new landscape phage-based approach relies on and mimics the extremely precise natural mechanisms of biosynthesis and self assembly of phage particles. When landscape phage serve as reservoir of the targeted membrane proteins one of the most troublesome steps of the conjugation technology is bypassed. Furthermore, it does not require idiosyncratic reactions with any new shell-decorating polymer or targeting ligand and may be easily adapted to a new liposome or micelle composition and a new addressed target. No re-engineering of the selected phage is

required at all: the phages themselves serve as the source of the final product—coat protein genetically fused to the targeting peptide. Indeed, a culture of cells secreting filamentous phage is an efficient, convenient and discontinuous protein production system. The yield of wild-type particles regularly reaches 300 mg/liter (20 mg/liter for the engineered landscape phage described here). They are secreted from the cell nearly free of intracellular components; further purification is easily accomplished by simple, routine steps that do not differ from one clone to another. The major coat protein constitute 98% of the total protein mass of the virion—the purity hardly reachable in normal synthetic and bioengineering procedures. As a normal intestinal parasite, phage itself and its components are not toxic and have been already tested for safety in preclinical and clinical trials (Krag *et al.*, 2002; Shukla and Krag, 2005b; Krag *et al.*, 2006). In contrast to immunization procedure, the phage selection protocol may require tiny amounts of a target material (thousands of tumor cells available in biopsy procedure (Shukla and Krag, 2005a) for obtaining the tumor-specific phage ligands, affinity and selectivity of which may be controlled, if necessary, by exploring well developed depletion and affinity maturation procedures.

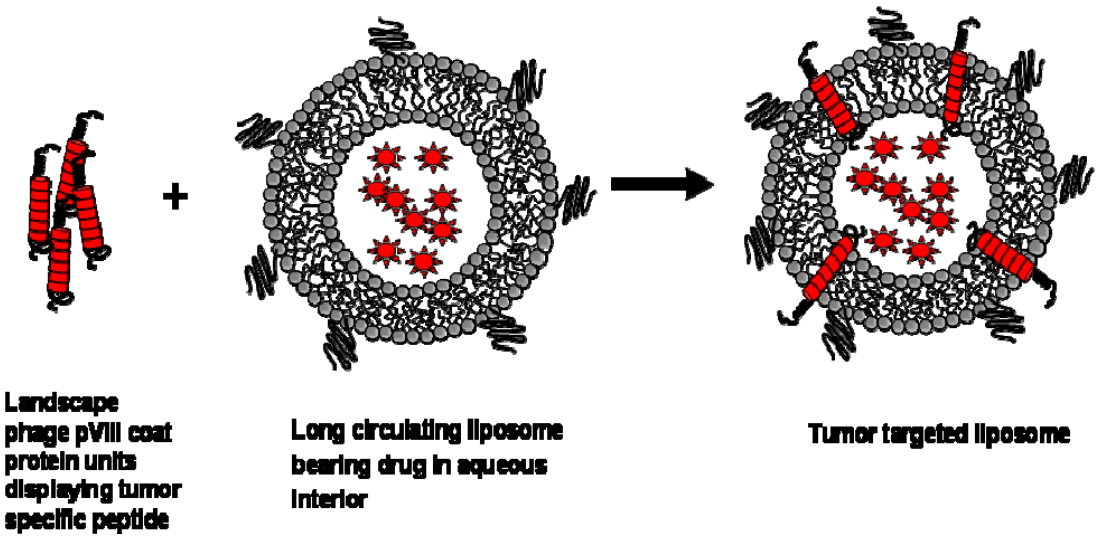

Figure 1. Drug-loaded liposome targeted by the pVIII phage fusion protein. The hydrophobic helix of the pVIII spans the lipid bilayer, and tumor-specific peptide is displayed on the surface of the carrier particles. The drug molecules are pictured as spiked circles.

4. Phage as Targeting Ligand for Liposomes

4.1 Phage display libraries

Fusion phage, the fount of phage display technology, was first described by Smith (Smith, 1985) and involves modifying the phage genome to achieve surface display of a peptide on the virion while maintaining its viability and infectivity. Phage display has since then evolved into a widely used screening resource for molecular targets supporting a burgeoning repertoire of applications (Sidhu, 2000; Arap, 2005; Kehoe and Kay, 2005; Merzlyak and Lee, 2006; Paschke, 2006). The potential of phage display libraries is founded on phage biology. Bacteriophages are viruses that infect bacteria and in

particular the phage vectors employed in phage display infect the bacterium *E.coli*. The filamentous phage of class Ff (M13, fd, f1) widely exploited to develop phage display systems possess single stranded circular DNA enclosed in a tubular capsid composed predominantly of pVIII major coat protein with few copies of minor coat proteins at the ends of the virion (Figure 2A). In-frame oligonucleotide inserts into one of the coat protein genes results in the expression of the foreign amino acids as part of the corresponding coat protein, creating a hybrid fusion protein displayed on the surface of the phage particles. Thus, the extraneous peptide is now linked to the phage genotype and this forms the cornerstone for the creation of phage display libraries. Phage display libraries are created by splicing unique randomized oligonucleotide inserts into individual phages so that each phage displays a unique peptide.

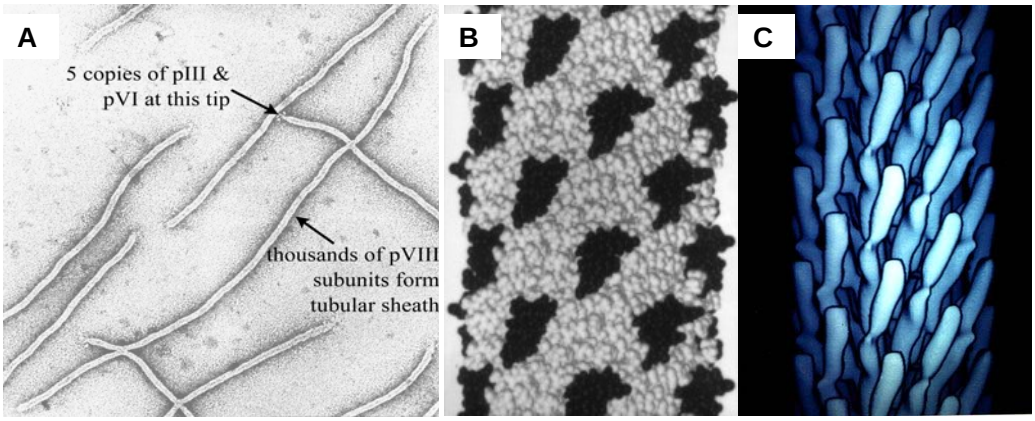

Figure 2. Filamentous phage. A: electron micrograph. The minor pIII proteins are pointed by arrow. B: Segment of landscape phage. Foreign peptides are pictured with dark atoms; their arrangement corresponds to the model of Marvin, 1994. C: Segment of ~1% of phage virion with the array of pVIII proteins shown as electron densities (Micrograph and model cortesy of Irina Davidovich, Gregory Kishchenko and Lee Makowski)

4.2 Landscape phage display libraries

In landscape phages, the degenerate oligonucleotide is inserted into the gene for the major coat protein pVIII. Thus, unlike conventional constructs, landscape phages display thousands of copies of the peptide comprising a major fraction of viral surface. The iterative close knit arrangement of the guest peptides dramatically alters the surface architecture of the phage creating defined organic surface structures (landscapes) to be used in multivalent interaction with an almost inexhaustible source of targets (Figure 2B). The phage is thus transformed from being a genetic carrier of foreign peptides to a

nanofilament with emergent physico-chemical characteristics. Multibillion collections of such singularly modified phages constitute a landscape phage peptide library. The multivalent display of peptides, apart from contributing to avidity allows for a greater freedom in manipulating the phage filament as a scaffold for biospecific interactions. The guest peptides that comprise 25% by weight of the phage particle and overlays 50% of its surface area can be easily prepared by cultivation of the infected bacteria and isolation of the secreted phage particles by precipitation. The surface density of phage particle is 300-400 m^2/g, comparable to absorbents and catalysts. Petrenko et al have successfully demonstrated the use of landscape phage as substitute antibodies (Petrenko and Smith, 2000) and because the phage filament itself acts as a framework for the random peptide "antigen binding sites" the most burdensome step of antibody technology, re-engineering of selected antibody genes for high expression levels is bypassed. Phage particles are very stable and can be stored indefinitely at moderate temperatures without a loss of infectivity. They are also resistant to organic solvents like chloroform and acetonitrile (Olofsson *et al.*, 1998; Petrenko and Smith, 2000). These attributes qualify landscape phage as unique selectable nanomaterials. Landscape phage have been used as diagnostic probes for bacteria (Sorokulova *et al.*, 2005; Carnazza *et al.*, 2007), spores (Brigati *et al.*, 2004), cancer cells (Romanov *et al.*, 2001; Romanov, 2003; Samoylova *et al.*, 2003) as components of gene and drug delivery systems (Mount *et al.*, 2004; Jayanna *et al.*, 2009), biospecific adsorbents (Samoylova *et al.*, 2004) and molecular recognition interfaces in detection systems (Petrenko and Brigati, 2007). More importantly, phage derived probes allow the fabrication of bioselective materials by self-assemblage on metal, mineral or plastic surfaces (Flynn *et al.*, 2003; Mao *et al.*, 2004; Sorokulova *et al.*, 2005; Olsen *et*

al., 2006). These observations allowed us to surmise the utility of derivatized phage components as targeting moieties of drug carriers.

4.3 Structural distinctions of phage major coat protein

Ability of the major coat protein pVIII to form micelles and liposomes emerges from its intrinsic function as a membrane protein judged by its biological, chemical, and structural properties. During infection of the host *Escherichia coli*, the phage coat is dissolved in the bacterial cytoplasmic membrane, while viral DNA enters the cytoplasm (Webster, 2001). The protein is synthesized in the infected cells as a water-soluble cytoplasmic precursor, which contains an additional leader sequence of 23 residues at its N-terminus. When this protein is inserted into the membrane, the leader sequence is cleaved off by a leader peptidase. Later, during the phage assembly, the newly synthesized proteins are transferred from the membrane into the coat of the emerging phage. Thus, the major coat protein can change its conformation to accommodate various distinctly different forms of the phage and its precursors: phage filament, intermediate particle (I-form), spheroid (S-form), and membrane-bound form. This structural flexibility of the major coat protein is determined by its unique architecture, which is studied in much detail. The structure of the major coat protein in the phage virions, micelles and bilayer membranes is well resolved (Lee *et al.*, 2003; Zeri *et al.*, 2003). The 50 amino acid-long pVIII protein is very hydrophobic and insoluble in water when separated from virus particles or membranes. In virus particles it forms a single, somewhat distorted α-helix with only the first four to five residues mobile and

unstructured (Marvin *et al.*, 1994). It is arranged in layers with a 5-fold rotational symmetry and approximate 2-fold screw symmetry around the filament axis (Figure 2C).

4.4 pVIII coat protein in liposomes

Liposomes displaying coat protein pVIII fixed in the lipid bilayers can be prepared by sonication of the virus with excess of phospholipids, such as dimyristoyl-sn-glycero-phosphocholine (DMPC) (Fodor *et al.*, 1981). In another procedure, pVIII protein can be reconstituted into phospholipids by dialysis, yielding liposomes with the molar lipid-to-protein ratio ~250 (Sprujit *et al.*, 1989). The membrane-bound form of fd coat protein in lipid bilayers is illustrated by Figure 3**.** The 16-Å-long amphipathic helix (residues 8-18) rests on the membrane surface, while the 35-Å-long trans-membrane (TM) helix (residues 21-45) crosses the membrane at an angle of 26 ° up to residue Lys40, where the helix tilt changes. The helix tilt accommodates the thickness of the phospholipid bilayer, which is 31 Å for the palmitoyl-oleoyl-phosphatidylcholine and –phosphatidylglycerol--typical lipids of *E. coli* membrane components. Tyr 21 and Phe 45 at the lipid–water interfaces delimit the TM helix, while a half of N-terminal and the last C-terminal amino acids, including the charged lysine side chains, and emerge from the membrane interior. The transmembrane and amphipathic helices are connected by a short turn (Thr 19–Glu 20).

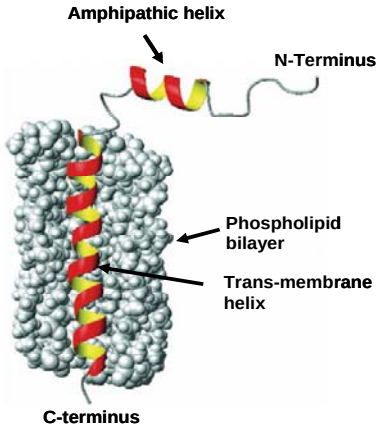

Figure 3. The model of pVIII in a lipid environment. (Adapted from Stopar et al. Protein–lipid interactions of bacteriophage M13 major coat protein, Biochimica et Biophysica Acta (BBA) - Biomembranes, 2003;1611:5-15.)

4.5 Spontaneous insertion of phage major coat protein pVIII into lipid vesicles

Prior to assembly of viral progeny, precursor coat protein pVIII integrates into inner membrane of the host bacterium and this process is believed to be mediated by interplay of electrophoretic influences (membrane potential), electrostatic forces (charges on membrane and protein) and hydrophobic interactions. The hydrophobicity of the transmembrane domain is chiefly responsible for driving the insertion of the coat protein to allow for thermodynamic equilibrium whereas the membrane potential and charges on the protein in question are the major determinants of the topology of the membrane associated protein (Kiefer and Kuhn, 1999). The spontaneous insertion of a membrane protein can be envisioned as a three-step process. The first step involves binding of the protein to the membrane parallel to the plane of the membrane. In the second ‘transition

step', the hydrophobic region and one of the hydrophilic tails is inserted into the hydrocarbon core of the lipid bilayer. The third step would involve the release of the hydrophilic tail into the *trans* side. The structural characterstics of the membrane-bound coat protein after spontaneous insertion was shown to be predominantly α-helical (Thiaudiere *et al.*, 1993). Association of coat protein with lipid vesicles has been determined by fluorescence energy transfer (FET) between the coat protein's tyrosine and tryptophan residues (donors) and a diphenylhexatriene (DPH) in the lipids (acceptor) (Soekarjo *et al.*, 1996).The membrane penetration of coat proteins depends on the concentration of lipids available and almost complete association is seen at high lipid to protein ratios. Furthermore, lipid membranes with negative charges demonstrate higher amenability to spontaneous insertion whereas rigid lipid membranes preclude spontaneous insertion. Also, coat protein insertion into liposomes follows an almost exclusive N terminus$_{out}$ topological preference. A mutant of coat protein Pf3 of the bacteriophage Pf3 having three additional leucine residues in the transmembrane region and a complete replacement of charged amino acids by aspargine (3L-4N) was shown to spontaneously insert into lipid vesicles (Ridder *et al.*, 2002). In an extension of this research, hybrid peptides comprising a fusion of a single IgG binding unit of Staphylococcal protein A attached to the N-terminus of the coat protein mutant was shown to spontaneously insert into liposomes and resulted in an emergent liposomal property that of antibody binding (Matsuo *et al.*, 2007).

CHAPTER 2

DIVERSITY AND CENSORING OF LANDSCAPE PHAGE LIBRARIES

1. Abstract

Libraries of random peptides displayed on the surface of filamentous phages are a valuable source for biospecific ligands. However, their successful use can be hindered by a disproportionate representation of different phage clones and fluctuation of their composition that arises during phage reproduction, which have potential to affect efficiency of selection of clones with an optimal binding. Therefore, there is a need to develop phage display libraries with extended and varied repertoires of displayed peptides. In this work, we compared the complexity, evolution and representation of two phage display libraries displaying foreign octamers and nonamers in 4000 copies as the N-terminal part of the major coat protein pVIII of phage fd-tet (landscape libraries). They were obtained by replacement of amino acids 2-4 and 2-5 of pVIII with random octa- and nonamers, respectively. Statistical analysis of the libraries revealed their dramatic censoring and evolution during amplification. Further, a survey of both libraries for clones that bind common selectors revealed the presence of different non-overlapping families of target-specific clones in each library, justifying the concept that different landscape libraries cover different areas of a sequence space.

2. Introduction

Ff class of filamentous phage includes three strains: f1 (Loeb, 1960), M13 (Hofschneider, 1963) and fd (Marvin and Hoffman-Berling, 1963). The wild-type phages are thread-like particles about 1 μm long and 7 nm in diameter. The bulk of their tubular capsid consists of 2,700 identical, largely α-helical subunits of the 50-residue major coat protein pVIII arranged in an array with five-fold rotational and two-fold screw symmetries. About half of the pVIII protein's amino acids are exposed to the solvent, the other half being buried in the capsid (Marvin, 1998; Marvin *et al.*, 2006). One tip of the phage outer tube is capped with five copies each of minor coat proteins pVII and pIX and another tip with minor coat proteins pIII and pVI. Viral DNA of varying sizes, including recombinant genomes with foreign DNA inserts, can be accommodated in the filamentous capsid whose length is altered to match the size of the enclosed DNA by adding proportionally fewer or more pVIII subunits during phage assembly (Hunter *et al.*, 1987).

In phage display constructions, foreign coding sequences are spliced in-frame into one of the five phage coat protein genes, so that the "guest" peptide, encoded by that sequence, is fused to the coat protein and thereby displayed on the surface of the virion (reviewed in (Smith and Petrenko, 1997)). A phage display library is a collection of such fusion phage clones, each harboring a different foreign coding sequence, and therefore displaying a different guest peptide on their surface. When a foreign coding sequence is spliced into the major coat protein's gene, *gpVIII*, the guest peptide is displayed on every pVIII subunit (Ilyichev *et al.*, 1989; Felici *et al.*, 1991; Greenwood *et al.*, 1991)

increasing the virion's total mass by up to 20% (Iannolo *et al.*, 1995). Such particles were eventually given the name "landscape phage" to emphasize the dramatic change in surface architecture caused by arraying thousands of copies of the foreign peptide in a dense, repeating pattern around the viral capsid. A landscape library is a large population of such phages, encompassing billions of clones with different surface structures and biophysical properties (Petrenko *et al.*, 1996; Iannolo *et al.*, 1997; Legendre and Fastrez, 2002; Petrenko *et al.*, 2002).

Different applications of phage display strategy in biomedicine and nanotechnology has promoted a fast growing interest in landscape phages as a new selectable nanomaterial. Depending upon the particular foreign peptide sequence inserted, the resulting landscape phage can bind organic and inorganic compounds, proteins and antibodies, induce specific immune responses in animals, or resist stress factors such as chloroform or high temperature. Landscape phages serve as substitutes for antibodies against cell-displayed antigens and receptors, diagnostic probes for bacteria and spores, gene- and drug-delivery systems and biospecific adsorbents (reviewed in (Petrenko, 2008a). Phage-derived probes inherit the extreme robustness of wild-type phage and allow fabrication of bioselective materials by self-assembly of phage or its composites on metal, mineral or plastic surfaces (Flynn *et al.*, 2003; Reiss *et al.*, 2004).

Although landscape phages retain their ability to infect *E. coli* and form phage progeny, it is not surprising that these chimeras, with the alien peptides composing up to one fifth of the phage mass, are defective to some degree when compared to parental wild-type strains. Some recombinant pre-coat proteins cannot be processed normally at

the inner bacterial membrane (Malik *et al.*, 1998) and it is likely that other types of defects are operative as well (Li *et al.*, 2003). Most guest peptides are not tolerated when displayed on every pVIII subunit in high-copy-number vectors, and it wasn't until the introduction of vectors based on the replication-defective phage fd-tet that multibillion-clone landscape libraries could be constructed (Petrenko *et al.*, 1996).

It was observed, however, that even in highly diverse libraries, different guest peptides are presented unequally (Petrenko *et al.*, 2002). The disproportionate representation of different phage clones in the original libraries and fluctuation of their composition that arises during phage construction and reproduction may affect efficiency of selection of clones with an optimal fitness. Therefore, there is a need to develop phage display libraries with extended repertoires of displayed sequences. In this work we compared the complexity, evolution and representation of two landscape libraries displaying foreign octamers and nonamers in the same register on the surface of the phage. They were obtained by replacement of amino acids 2-4 and 2-5 of pVIII with random octa- and nonamers, respectively. It was found that although these libraries have similar size and complexity, they represent phages that may belong to different families of homologous clones that were identified by parallel affinity selection with common selectors: β–lactamase, streptavidin and *Salmonella typhimurium*. These results justify development of separate landscape libraries covering different areas of a "sequence space".

3. Materials and Methods

3.1 Bacterial strains and general procedures

E. coli strains MC1061 (F^- *araD139* Δ*(ara-leu)7696 galE15 galK16* Δ*(lac)X74 rpsL* (Str^r) *hsdR2* (r_k^- m_{k+}) *mcrA mcrB1*) (Meissner *et al.*, 1987) and K91BlueKan (Kan^r Hfr-C thi *lacZ*Δ*M15 lacY::mkh* $lacI^Q$) (Smith and Scott, 1993) were obtained from George Smith (University of Missouri, Columbia, MO). *Salmonella typhimurium,* reference strain ATCC 13311, was obtained from the American Type Culture Collection (Rockville, MD). All general procedures employed for construction of the libraries, production and analysis of recombinant phages, DNA sequencing, media and buffers, selection procedures and analysis of phage binding by Enzyme Linked Immunosorbent Assay (ELISA) are detailed in recently published protocols (Brigati *et al.*, 2008) and previous publications (Sorokulova *et al.*, 2005).

3.2 Statistical analysis of phage populations

Phage populations in original landscape libraries and selected phage clones were analyzed using bioinformatics programs RELIC (Mandava *et al.*, 2004). A *population diversity* of libraries was estimated using the program POPDIV. *Positional amino acid diversity* in each randomized position was evaluated with program DIVAA and compared with parental primary libraries. Program INFO was used to calculate *information content* of selected peptides using the population of analyzed clones in primary libraries as a reference for calculation of amino acid occurrence probabilities. The AAFREQ program was used to analyze the frequency of amino acid occurrence in the random peptide inserts

including 73 clones from primary and 73 clones from amplified f8/8 libraries, 49 phage-producing clones from the pre-f8/9 library (clones obtained as colonies of transformed bacteria after their electroporation with mutagenized phage DNA) and 61 clones from primary f8/9 libraries. Since the observed frequency of amino acids at different positions of the insert does not implicitly follow the theoretical profile of frequency, we obtained an intuitive portrayal of this discrepancy using an adaptation of the one-sample tests for proportions (Rosner, 2006). Based on our assumptions, the observed value is expected to follow a binomial distribution based on a fixed number of clones analyzed (N) and expected frequency (E). The result of this analysis was designated as the "Frequency Disparity Index" and was calculated for each amino acid for each position in the insert as follows:

$$FDI = \frac{O - E}{\sqrt{E(1-E)/N}}$$

Where, the formula is an algebraic equivalent to that found in (Rosner, 2006)and

FDI - frequency disparity index, a measure of how much the expected frequency differs from the observed frequency

E - Expected frequency of an amino acid at a given position in the phage insert,

O - Observed frequency of the amino acid at the same position in the phage insert as noted for "E" above

N - The number of clones used to calculate the observed and expected frequencies

The FDI scores thus obtained have an expectation of being zero, negative or positive depending on whether the amino acid being considered occurred at the expected level, at a lower frequency than expected or at a higher frequency than expected, respectively. Thus, a graphical representation of such scores provides a picture of over-representation or under-representation of different amino acids at different positions of the phage inserts. Furthermore, since we analyzed a relatively large number of clones, we expect the FDI scores to approximately follow a normal distribution that allows using two tailed *p*-values obtained from a standard Z table (Rosner, 2006) to prove statistical significance of the difference seen between the observed and expected frequencies of an amino acid at a particular position.

4. Results

4.1 Complexities and diversities of phage libraries

Previous studies indicated that randomization of the N-terminal region of each copy of the phage major coat protein pVIII may be subject to some limitations in size and structure (Ilyichev *et al.*, 1989; Iannolo *et al.*, 1997; Rodi *et al.*, 2005). It has been demonstrated that phage M13 can tolerate a 6-mer peptide insertion at the beginning of the pVIII protein, but when the length of the peptide increases, the percentage of clones able to form infective phage particles drops significantly. Only 40% of clones with inserts corresponding to 8-mer peptides formed infective phage particles and this value decreased to 20% for 10-mer peptide inserts and to 1% for 16-mer peptide inserts (Iannolo *et al.*, 1997). Attempts to construct an 8-mer representative library in each copy

of the pVIII protein based on the multi-copy vector M13 failed (Petrenko and Smith, unpublished). The first comprehensive multibillion-clone landscape library was successfully constructed only when the very low-copy number vector f8-1 (AF218734), a derivative of the phage fd–tet with a defective origin of replication, was employed (Petrenko *et al.*, 1996). The replication defectiveness of the vector becomes an advantage as it averts a phenomenon called "cell killing". Also, toxic effects of fusion proteins may be better tolerated when carried by replication-compromised vectors such as fd-tet, which produce a very low number of replicative form (RF) DNA in infected bacteria (Smith, 1988). In this library a random octamer replaces amino acids 2-4 (EGE) at the beginning of the pVIII protein of the f8-1 vector extending the total length of the fusion pVIII protein by five amino acids (Figure. 4).

Here we have demonstrated that another amino acid (D5 at the beginning of the pVIII protein) could be also randomized. In the f8/9 library four amino acids (EGED) were replaced by random nonamers bringing a total length of the fusion pVIII protein to 55 amino acids, the same length as in the previously constructed f8/8 library (Petrenko *et al.*, 1996). For construction of the f8/9 library we used vector f8-6, derivative of f8-5 (AF464138) (Petrenko and Smith, 2005) (Figure.4). A characteristic feature in f8-6 – two amber TAG codons at the beginning of the gene *gpVIII*, ensures the absence of residual wild-type phage in the library. Such wild-type phage was shown to overgrow their recombinant counterparts during successive amplification that may hinder results of affinity selection. Double-stranded randomized DNA fragments were ligated into cleaved vector DNA followed by electroporation of resulting recombinant DNA molecules into MC1061 *E. coli* cells. A portion of transformed bacterial clones (named

the "pre-library") was grown on an indicator plate with tetracycline, and the major part of transformed bacteria were cultured in liquid media with tetracycline. The size of the pre-library (2×10^9 clones) was estimated in proportion to the number of clones that grew on the indicator plate. The phage library isolated from the liquid culture, containing ~4.4×10^{13} phage virions was named the "primary library". It was observed that about half of the transformed bacteria in the pre-library produced phage particles, in agreement with our previous observations (Petrenko *et al.*, 1996). It was determined by growing individual pre-library clones in liquid cultures, separating bulk cells by centrifugation and titering the phage remaining in the supernatants. The complexity (the size) of f8/9 library (1.2×10^9 clones) – the number of primary clones able to produce phage – was determined as a portion of the primary clones producing phage particles (61%) compared to the total number of primary clones (2×10^9 clones). The rest 39% of the pre-library clones did not produce phage in the host bacteria because they contained the stop codon TAG in different positions of the gene encoding fusion coat proteins that did not allow expression of the fusion pVIII protein and assemblage of the phage in the non-supressor strain MC1061. That was demonstrated by PCR amplification of the corresponding segments of double stranded viral DNA from tetracycline-resistant bacterial clones and their sequencing. Thus, we found that complexities of f8/8 and f8/9 libraries were similar to each other but both differ from their theoretical complexities (1.28×10^{11} for f8/9 library encoded by DNA's Gnk$(nnk)_8$ where n = G, A, T, or C and k = G or T; and 4.16×10^9 for f8/8 library encoded by DNA's Gnk$(nnk)_6$nnG).

Vector f8-6

*Pst*I *Bam*HI

..GCT.GCA.GAG.TAG.TAG.GAT.CCC.GCA.AAA.GCG.GCC...

A E Stop Stop D P A K A A...

1 2 5 6 7 8 9 10...

f8/8 library

*Pst*I *Bam*HI

..GCT.GCA.Gnk (nnk)$_6$ nnG.GAT.CCC.GCA.AAA.GCG.GCC...

A ------- X_8-------- D P A K A A...

1 a-h 5 6 7 8 9 10...

f8/9 library

*Pst*I

..GCT.GCA.Gnk ---(nnk)$_8$--- CCC.GCA.AAA.GCG.GCC...

A -------X_9------ P A K A A...

1 a-i 6 7 8 9 10...

Figure 4. Vectors and libraries. In the nucleotide sequences corresponding to the part of recombinant gene *gpVIII* encoding the N-terminal part of the major coat protein, randomized structures are designated as **nnk**, where **n** = A, T, G, or C, and **k** = G or T. Restriction sites for *Pst*I and *Bam*HI are underlined. N-terminal amino acid structures of mature recombinant pVIII proteins in libraries indicated by capital single letters according to amino acid abbreviations. Randomized amino acids are designated in small letters (**a-h** in the f8/8 library and **a-i** in the f8/9 library). Amino acids are numbered as in vector phage f8-5 (Petrenko *et al.,* 2002).

The quality of a phage display library can be characterized by its completeness or diversity - the proportion of all possible sequences actually present in the library. Population diversity of the libraries was estimated from the sequences of a limited

number of the members of the libraries (73 for f8/8 and 61 for f8/9) using the statistical program RELIC POPDIV (Mandava *et al.*, 2004). An algorithm of the program has been previously shown to provide reasonable estimates of population diversities even when based on as few as 50 peptides even though a high standard deviation is observed due to the low number of sequences analyzed (Makowski and Soares, 2003). Since both theoretical as well as observed diversities were calculated using the same algorithm using at least 50 peptides in each case, the estimates derived can serve as an acceptable measure of the population diversities of our libraries. Calculated population diversities of f8/8 and f8/9 primary libraries (0.0091 +/- 0.0045 and 0.0029+/-0.0016 respectively as per POPDIV), were 37 and 3 times lower than the observed diversities of these libraries ($1.4\times10^{9}/4.16\times10^{9} = 0.34$ and $1.2\times10^{9}/1.28\times10^{11} = 0.0094$ respectively) probably because of unequal presentation of different clones in the libraries and uneven positional distribution of amino acids in foreign peptides. It is interesting to note that population diversity of phage-producing clones in the pre-library f8/9 (0.0116+/- 0.0074) exceeds the diversity of the primary library f8/9 (0.0029+/-0.0016) four times, indicating that occurrence of unique clones in the library change during its growth in the liquid medium because the efficiency of phage assembly and export is different for different clones. An even more dramatic change in population diversity was observed when a portion of the primary library f8/8 was used for amplification in the presence of fresh *E. coli* K91BlueKan cells (0.0091 +/- 0.0045 and 0.0012+/-0.0006 for the primary and amplified libraries respectively). The decrease in population diversity of the library more than 7 times during its amplification can be attributed to differences in infectivity of individual

clones in the library toward the host bacterium and differences of biosynthesis of distinct phage particles inside the bacterial cell during phage assembly and export.

Positional diversity is a statistical measure of the proportion of the 20 possible amino acids that are observed at any given position (Mandava *et al.*, 2004). If a position in the peptide is populated by equal proportions of all 20 amino acids then the diversity is equal to 1 (20/20). If a position in the peptide is populated by only one amino acid in all sequences, then the diversity is 0.05 (1/20), as is the case for the 9^{th} position in the f8/8 library which is always occupied by aspartic acid. We estimated positional diversity of both libraries using the statistical program RELIC DIVAA. The positional diversities of both libraries exhibited similar patterns (Figure 5) with the diversity in position one for f8/8 and f8/9 libraries and position eight for the f8/8 library being significantly lower than in the other positions because they have codons Gnk and nnG, encoding 5 and 13 amino acids, respectively.

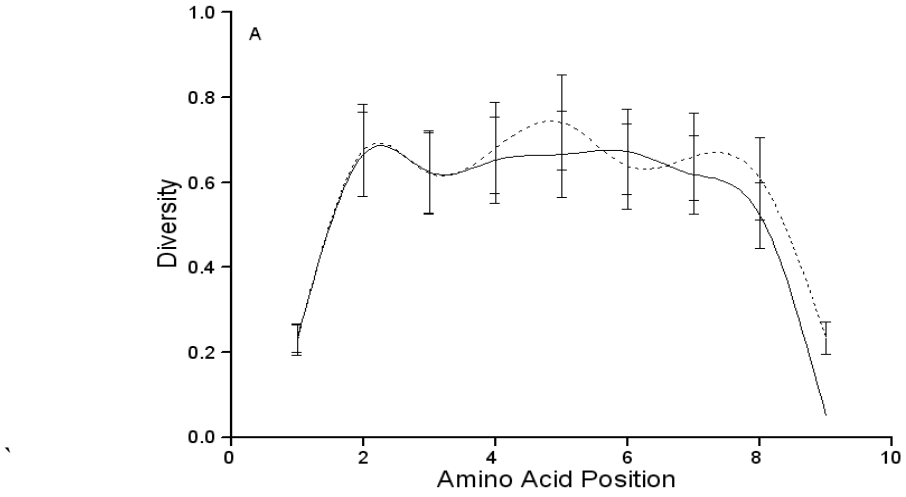

Figure 5. Positional diversities of libraries used in the study as determined by the program DIVAA of the RELIC suite. Diversity of f8/8 and f8/9 primary libraries; X - amino acid position, Y - diversity measure. Solid line corresponds to f8/8 library, dashed line – to f8/9 library.

4.2 Biological censoring of phage libraries

We assumed that the diversities of f8/9 and f8/8 libraries were affected by biological censoring of phage-producing clones during phage amplification. To check this hypothesis, amino acid profiles of the theoretically randomized 8-mer and 9-mer libraries were compared with amino acid profiles of the obtained libraries (Figure 6) using the RELIC program AAFREQ (Mandava *et al.*, 2004). Further, an adaptation of the one-sample test for proportions was used to obtain a statistical measure (FDI) of the divergence from the theoretical diversities as follows;

$$FDI = \frac{O - E}{\sqrt{E(1-E)/N}}$$

Where, the formula is an algebraic equivalent to that found in (Rosner, 2006) and

FDI - frequency disparity index, a measure of how much the expected frequency differs from the observed frequency

E - Expected frequency of an amino acid at a given position in the phage insert,

O - Observed frequency of the amino acid at the same position in the phage insert as noted for "E" above

N - The number of clones used to calculate the observed and expected frequencies

We found that the observed frequency of amino acids at different positions of the randomized area does not implicitly follow the theoretical profile of frequency. Based on the formula applied for our calculations, a frequency disparity index (FDI) of 0 would imply that the occurrence of the amino acid at a given position follows the expected frequency. A positive FDI score (with the bar above the X-axis) would imply that the amino acid is over-represented at a given position whereas a negative FDI score (with the bar being below the X-axis) would imply an under-representation of the amino acid at a given position. Furthermore, at an α level of 0.05, an FDI score of 1.96 would represent significant deviation of amino acid frequency from the expected with the amino acid being either overrepresented or underrepresented depending on the sign of the FDI score. A critical issue is that even though the graphical representation shows the amino acids to be grouped together for ease of comparison, the occurrence of each amino acid at each individual position in our approximation is an independent event and cannot be correlated

to either neighboring positions or to other amino acids. This means that the degrees of over- and under-representation are unique for each amino acid at each position. Also, no adjustments were made for multiple comparisons as our focus was on individual amino acids at individual positions. A special case to be considered is the amino acid cysteine which is conspicuously absent in all clones of the library due to structural restraints. This absence is accurately depicted as under-representation in our analysis supporting the prediction of independence of each amino acid and position in our analysis. Our observations based on the above technique can be summarized as follows:

4.2.1 Evolution of pre-library f8/9 during its amplification

Distribution of FDI scores in the f8/9 pre-library and f8/9 primary library are very similar (Figure 6, panels D and C respectively). In both libraries, the acidic amino acids aspartic acid (D) and glutamic acid (E) are significantly overrepresented while the positively charged amino acids lysine (K) and arginine (R) are relatively underrepresented. Glycine (G), asparagine (N) and serine (S) are overrepresented in several positions while leucine (L) and tryptophan (W) are relatively underrepresented. Only few statistically significant changes in amino acids distributions were observed during amplification of the pre-library f8/9. For example, aspartic acid (D) in position "i" is much less overrepresented in the primary library; isoleucine (I) is underrepresented in most positions of the primary library, while similar amino acids leucine (L) and valine (V) are less underrepresented. Thus, noted above the difference in diversities of the pre-library and primary f8/9 libraries can be attributed to the changes in their amino acid

distribution, probably influenced by biological mechanisms of phage assembly and secretion.

4.2.2 Evolution of the f8/8 library during its amplification

Distribution patterns of amino acids for the f8/8 primary library and amplified f8/8 library are very similar (Figure 6, panels B and A respectively). In both libraries aspartic acid (D) and asparagine (N) are overrepresented in the N-terminus of the peptide inserts whereas glutamine (Q) is overrepresented at the C-terminus. Proline (P) and threonine (T) are overrepresented at various positions except the first. Serine (S) is overrepresented in the first few positions. Arginine (R) is underrepresented in the first and last positions. Glycine (G), leucine (L), arginine (R), valine (V), and tryptophan (W) are underrepresented at several positions. The amplification of the primary library leads to "contrasting" of the biased distribution of amino acids in different positions changing overall library's diversity, as noted above.

4.2.3 Comparison of the primary libraries f8/8 and f8/9

Frequencies with which the amino acids occurred in both libraries are quite different with a distinct preference toward negatively charged amino acids D and E in the f8/9 library and very different patterns of glycine (G), proline (P) and threonine (T) distribution in both libraries (Figure 6, panels B and C for the primary library f8/8 and primary library f8/9 respectively). Comparison of the amino acid profiles for the f8/8 and f8/9 libraries against theoretically randomized libraries provides evidence of censoring of the real libraries. Randomization of an additional amino acid (D5) in phages belonging to

f8/9 library also affected amino acid frequency profiles and library evolution with a preference towards better surviving clones during amplification of the library.

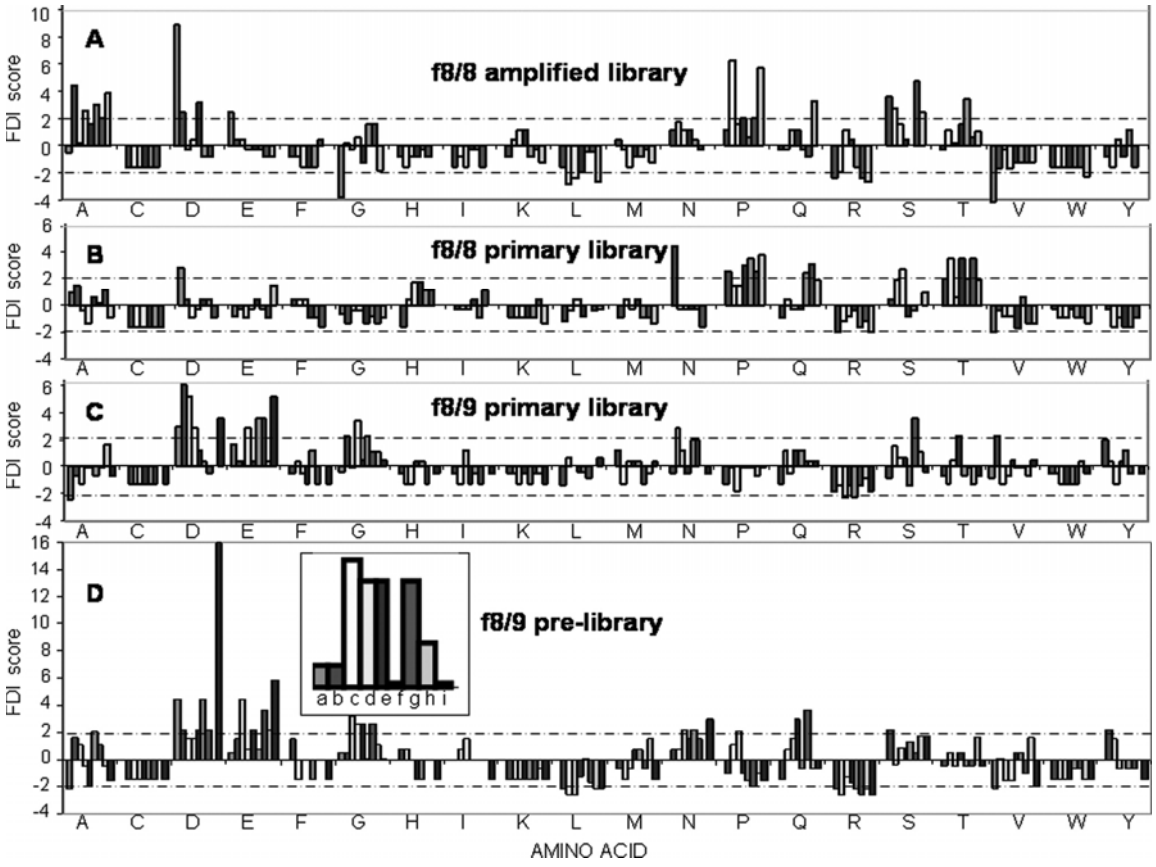

Figure 6. Frequencies of amino acids at different positions in peptide inserts. The expected frequency of amino acids and the observed frequency calculated using the AAFREQ program of the RELIC suite (Mandava *et al*, 2004) were used in an adaptation of the one-sample tests for proportion (Rosner, 2006). The results of this analysis were expressed as a *frequency disparity index FDI* which is a measure of how much the observed frequency deviates from the expected. Amino acids at various positions of the peptide inserts are arrayed along the X-axis whereas the Y-axis represents the FDI. FDIs for each amino acids are presented by clusters of columns, in which positions of each

column correspond to the amino acid's position in the peptides (a-h for 8-mer libraries, and a-i for 9-mer libraries, see Fig. 1 and insert lower panel). The dashed line represents statistical significance of a frequency disparity at the α level of 0.05. **A** - f8/8 amplified library; **B** - f8/8 primary library; **C** - f8/9 primary library; **D** - f8/9 pre-library.

4.3 Selection of phages from primary libraries f8/8 and f8/9 that bind model targets

We hypothesized that using different landscape phage libraries may be advantageous in the search for specific ligands by affinity selection against different targets because the range of clones belonging to the same sequence "family" in each library may be different. Selection of both libraries with the same target should yield a greater variety of structurally non-overlapping clones. To prove this hypothesis, we surveyed both primary libraries in selection of binding phage against the same selectors: monomeric TEM-1 β-lactamase, tetrameric streptavidin and whole *Salmonella typhimurium* cells.

4.3.1 TEM-1 β-lactamase-binding phages

The simplest target we chose was TEM -1 β lactamase, a monomeric bacterial protein which has been used to select phage binding clones also by Huang et al (Huang *et al.*, 2003). Phage libraries were depleted against plastic and bovine serum albumin to eliminate phages binding to these entities during the selection process. Three rounds of affinity selection were performed to obtain phage clones with a putative propensity to bind β-lactamase. Fifty clones, randomly picked from the last round of selection were

sequenced for each library. Most of the sequences of the selected peptides from both libraries (Table 1) demonstrate the clustering into families, with a few "orphans" that did not belong to any identifiable family structure. Positional diversity of amino acids in affinity selected guest peptides was distinct from diversity of the guest peptides in the original library and showed a predictable decrease in all positions except for position 7 in the octamer library (Figure 7) and position 6 in the nonamer library (data not shown).

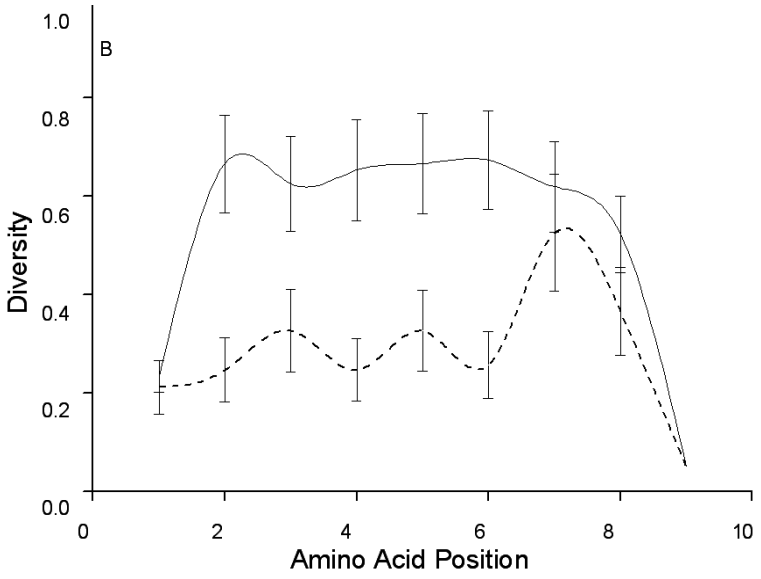

Figure 7. Positional diversities of amino acids in selected β-lactamase-binding peptides. X - amino acid position, Y - diversity measure. Diversity of primary library f8/8 (solid line) and selected β-lactamase binding clones (dashed line).

Table I. Phage displayed peptides selected from landscape phage libraries.

	β-lactamase	Streptavidin	*S. typhimurium*	
			Acid	DOC
Library f8/8	**DPKP**TA**A**A[4] **DPRP**ES**A**P **EPKP**TP**A**A[2] **DP**PK**R**PDV[5] **DP**SS**R**QTP **EHP**Q**P**PT**P** **ERP**A**P**QL**P** **DR**VQ**P**AMQ[3] SD**TSSPGQ** VN**TSSPGQ**[6] **VSP**P**S**H**ST** **VT**GS**PP**S**T**[2] **VTP**S**P**TPQ **V**P**PQS**N**S**M APVHQESS DNASAPRS	**VP**E**GAFS**S[7] **VP**E**GAFT**S[3] **VP**E**GAF**GS **VP**E**GAFS**T **VP**E**GAFS**Q **VP**E**SAF**AQ **VP**D**GAFS**T **VP**DS**AF**NT **VP**D**GAFS**Q[2]	**VTPP**Q**S**S**S** **VTPPTS**PQ **VTPSSP**H**S** **VTP**QG**SH**P **VS**TQ**STH**P **TP**GQP**SH**P **VPPPS**PQ**S**[2] **VPPPS**PH**S**[3] **VPPPS**AS**S** **VPPPS**QSQ[2] **VPPPS**NP**S** **VPPP**GQHQ **VPP**S**S**SSP **VP**QQDKAQ	**DPK**G**P**HSM **DPK**S**P**LHT **DPK**S**P**QQT **DPRSP**ASL[2] **DPRP**A**Q**HT **DPH**K**A**GGL **EPR**L**A**HGA **EPH**R**A**ASV **DP**S**KRTQ**P **EP**N**KHSQ**S DRPSPNTV VTPPQQGS DNKMTSHS
Library f8/9	**A**R**SVAMSDS** **A**S**SVAMSDS** **D**FGYA**KEDT** **D**QRGD**RDDT** **DH**L**N**VA**SSD** **ERTQ**DG**SSD** **DQSG**AVGMG **ENTG**TSIPE **V**L**SSDHNED** **VSSSDHNED**[2] **V**PSGDV**SME** **V**QGYGP**SMD** **VS**MEVA**PD**A **VS**SGTG**PD**G GMGPEYGGD VTAPSTAED AIETTVGDD EPQTLYGTQ GHTGGLEED VHNGNLRLD GDSGTGDSH EMDTGKDGN ATFSVPEAD ASSPGIGSE	**VP**V**GAYS**DT[21] AALGHPAMD[22] ETHLDPNRT[4] EYVLHGSED	**ELPL**AF**G**N**D**[2] **ELPL**DP**G**L**D** GS**YSDM**VDN[2] GV**YSD**I**S**GD VN**YDDMT**ST[2] VP**YA**D**MS**ES[2] AGMTYDLPD[2] DAFSQSATD[2] VAEPVDLPA	**VH**G**E**T**S**NQD[2] **VH**S**E**G**S**VNT **VH**S**D**H**S**ISD **DK**N**S**G**G**GES[4] **DK**A**S**P**G**SSD[2] **DK**HEGSNTD DDYNFYGVN

a) Common motifs in families are indicated by bold letters.

b) Superscripted arabic numbers show how many identical clones were identified in the group of the sequenced phages.

4.3.2 Streptavidin-binding phages

Streptavidin was chosen as a more complex target possessing a tetrameric structure with four potential binding sites. It has commonly been used as a model for analysis of random peptide libraries and several consensus motifs such as HPQ (Devlin *et al.*, 1990; Kay *et al.*, 1993; McLafferty *et al.*, 1993; Giebel *et al.*, 1995), GDF/WXF, PWXWL (Roberts *et al.*, 1993), EPDWF/Y (Caparon *et al.*, 1996) and DVEAWL/I (Lamla and Erdmann, 2003) that bind streptavidin have been identified.

Streptavidin-binding phages were selected in the same set up as described above for TEM-1 β-lactamase (Table 1). Fifty clones that were isolated and sequenced contained 6 unique sequences: VPVGAYSDT, AALGHPAMD, DQFSLQSQD, ETHLDPNRT, EYVLHGSED and VGGFGHPDD with a predominance of two clones, VPVGAYSDT (21/50) and AALGHPAMD (22/50). In the phage capture ELISA with the fixed concentration of the phages, phage VPVGAYSDT bound streptavidin 162 times stronger, phage EYVLHGSED – 30 times stronger, phage AALGHPAMD -13 times stronger and phage ETHLDPNRT – 10 times stronger than negative control (vector f8-5). Phage VPVGAYSDT resembles the structures of clones with the motif (VPxGA Y/F S/Txx) isolated previously from the f8/8 library (Table 1) (Petrenko and Smith, 2000). The best binder of this family, phage VPEGAFSS, demonstrated a 168 times higher binding efficiency than the control phage in the same experiment with the rest of the binding clones selected from f8/9 library.

Affinities of two representative phages from different libraries, VPEGAFSS from the f8/8 library and VPVGAYSDT from the f8/9 library, were compared in a competition

ELISA, in which the previously characterized streptavidin-binding phage VPEGAFSS was immobilized and used as a detector for streptavidin. The surveyed phages were pre-incubated with AP-SA in solution and applied to the wells containing immobilized detector phage (Figure 8). Phage VPVGAYSDT bound to streptavidin (AP-SA) with about 50 times higher affinity than phage VPEGAFSS (estimated as the proportion of phage concentration when 50% of AP-SA is bound to the immobilized detector phage). Numerical data from these assays can be found online as supplementary material. These data confirmed the assumption that the use of separate phage libraries can be beneficial for selection of phages with higher level of binding to a corresponding selector.

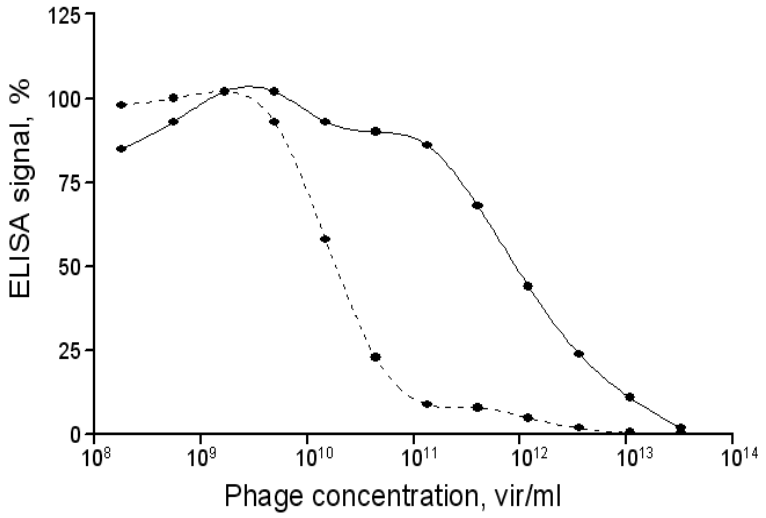

Figure 8. Competition ELISA of streptavidin-binding phages. Streptavidin-conjugated alkaline phosphatase (AP-SA, final concentration in the mixture – 0.67 μg/ml),) was mixed with gradually increasing concentrations (from 9.7×10^{13} vir/ml to 0.55×10^{9} vir/ml) of phage VPVGAYSDT (dashed line) and phage VPEGAFSS (solid line) and tested on ELISA plates with immobilized detector phage VPEGAFSS. ELISA signals of

characterized phages were presented as a percentage of ELISA signals of the samples without phage, which were considered as 100%. (Details for the procedure described in (Petrenko and Smith, 2000)).

4.3.3 *Salmonella typhimurium*-binding phages

The affinity selection regimen for our library analysis culminated with the most complex target, *Salmonella typhimurium*. As described above, phage libraries were depleted against plastic and bovine serum albumin to eliminate phages binding to these entities during the selection process. Two elution strategies were employed to recover the phages – using acid and deoxycholate buffers (the last allows isolation of membrane-bound or cell-penetrating phages). Most clones randomly chosen after the fourth round of affinity selection from the f8/8 library congregated into 3 families (Table 1). Almost all clones recovered bound *S. typhimurium* cells more strongly than control vector f8-5 in cell capture ELISA (Sorokulova *et al.*, 2005). Clones from Acid and DOC fractions encoded no apparent overlapping structures of the displayed peptides except for clone VTPPQQGS, originating from the f8/8 library, which was found in the DOC fraction and shared the common motif VTPPxxxS with a family found in the Acid fraction. Most clones selected from the f8/9 library (12/16) could be clustered into four families with structures distinct from those identified in the f8/8 library.

Several phage clones from the f8/8 and f8/9 libraries which demonstrated high ELISA signals were evaluated in co-precipitation assay (Table 2). In this test, selected phage particles were incubated with *S. typhimurium* cells in solution, unbound phage was removed by centrifugation followed by washing, and bound phage was eluted with

deoxycholate buffer and titered. Yields of recovered phages were compared with the yield of negative control phage f8-5. Six ELISA positive clones from the f8/8 library and two clones from the f8/9 library demonstrated binding with *S. typhimurium* cells in solution (Table 2). Numerical data from these assays can be found online as supplementary material. As in two preceding examples, the use of two separate libraries for selection of Salmonella binders permitted increasing diversity of bacterial binders.

Table II. Co-precipitation assay of *Salmonella typhimurium*-binding phages.
Phage suspensions were mixed with suspension of bacterial cells, incubated and phage–bacteria complexes precipitated. Phages were recovered by elution buffer. Phage inputs and recoveries were determined by biological titering (Brigati and Petrenko, 2005; Sorokulova *et al,* 2005).

Library	**Peptide insert**	**Yield, recovery/input in %**
f8/8	DRPSPNTV	8.0×10^{-1}
	VPQQDKAQ	6.0×10^{-2}
	VTPPQSSS	5.0×10^{-2}
	DPKSPQQT	1.9×10^{-3}
	VTPQGSHP	8.2×10^{-4}
	VSTQSTHP	2.5×10^{-4}
f8/9	VNYDDMTST	7.0×10^{-2}
	AGMTYDLPD	2.3×10^{-4}
	ELPLDPGLD	$< 1.2\times10^{-4}$
	VHSEGSVNT	$< 1.2\times10^{-4}$
Control	EGE (f8-5 vector)	1.2×10^{-4}

4.4 Analysis of a possible correlation between information content of the selected peptides with their binding ability

Bioinformatics has enabled analysis of information relating to the physico-chemical properties of biologically relevant molecules in a relatively short span of time. These tools, though extremely useful, provide only a theoretical picture, the merit of which could be considerably improved if it could be translated to a practical application estimating predictability of peptide binding affinity to a specific target. Toward such a goal, we analyzed data generated from the INFO program of the RELIC suite for affinity selected peptides and attempted to correlate results from theoretical predictions with our experimental observations.

The information value of a given peptide arises as a functional extension of the theory of information, the basic precept of which is that information is a decrease in uncertainty (Shannon, 1948). Accordingly, information calculated by the program INFO is a measure of the probability of encountering a particular peptide in a pool of affinity selected peptides due to random chance (nonspecific binding or good growth characteristics) as opposed to ligand affinity. It is equal to the negative logarithm of the probability of its natural occurrence. INFO uses the program AAFREQ to calculate position-specific frequencies of each amino acid at each position of the insert and uses this data to the generate the probability of random observation of the insert as a whole by multiplying the probability of each amino acid occurring at each position within the peptide. The lower the probability of occurrence is, the higher the information value will be as its presence in the affinity selected sub-library is likely due to its ligand affinity

rather than good growth characteristics or nonspecific binding. The higher the probability of occurrence, the higher is the chance is that the peptide will be carried over to the subsequent rounds due to favorable viral growth rather than ligand affinity and thus lower is the information value. Similarly, peptides with high information content are rare in the parental library and therefore their increased presence in the affinity selected sub-libraries should be due to affinity to their target and vice versa. We estimated information content of the selected clones from affinity selected phage populations (shown in Table 1) and compared them to the information content of the clones from the original landscape libraries. The analysis revealed that in each case information content profiles of the clones from the selected population was different from that of the original libraries. We postulated that the increased occurrence of a clone with high information (as calculated by the INFO program) is a function of its binding affinity as demonstrated by ELISA. It was predicted that a set of clones with high information content would emerge during selection and that the best binder would be among these selected phages. This expectation was fulfilled in the selection against streptavidin (Figure 9; the best binder is starred) and partially in the selection against *Salmonella* (data not shown), although in selection against β-lactamase the best binder demonstrated relatively low information content (data not shown). Though these results indicate a possibility of a direct relationship between the theoretical information that a peptide contains and the practical rendering of this information into a binding signal, it may not be universally true. Within their own realms, both information content of a peptide and the cognate binding signal are complex factors which are dependent on multiple sub-factors. Thus, a more complicated model may be better able to define the relationship between these two entities and enable the use of

information content of a peptide as a predictor of the binding signal it will eventually produce in an assay.

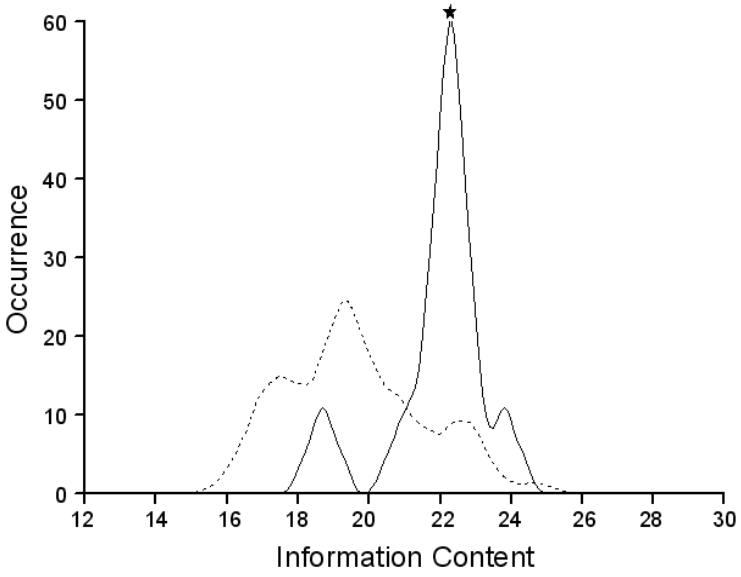

Figure 9. Shift in the Information profile of the f8/8 library following affinity selection against streptavidin. The information content is a measure of the probability of encountering a particular peptide in a pool of affinity selected peptides due to random chance (non-specific binding or good growth characteristics) as opposed to ligand affinity. Thus, the profile of information is supposed to change as a result of affinity selection which is demonstrated in the above figure with shift to the right. Also we predicted that increased occurrence of a clone with high information (as calculated by the INFO program) is a function of its binding affinity as demonstrated by ELISA. The Information profile of the parent f8/8 library is shown as dashed line; information content profile of affinity selected clones clones is shown as solid line. X – information content of peptides, Y – occurrence of peptides in populations of the primary library f8/8 and

selected clones. The star represents the best binder identified by the binding assays (VPEGAFSS).

5. Discussion

The ultimate goal of most phage display selection projects is identification of peptide ligands that bind strongly and specifically to a target receptor. It may be assumed *a priori* that in every population of random peptides there are peptides with ideal fitness and highest affinity to the target, so called leading peptides. A collection of structural homologues to a leading peptide would therefore form a structural family within a library and would be expected to possess lower fitness and thereby lower affinity to the target. A model of such relationships, suggested previously (Smith and Petrenko, 1997) can be envisioned as an affinity cone with the lead peptide sequence occupying the peak and different members of the family occupying different and descending levels in the cone based on a hierarchical gradient of affinity to the target (Figure 10).

In an ideal situation, the leading peptide should be revealed by affinity selection (biopanning) as we have demonstrated. However, in practice, the leading peptide may be absent from the selected pool of phage clones because the theoretical complexity (total number of all possible peptide structures) of the library exceeds the actual observed complexity. For example, there are 1.28×10^{11} possible peptide structures for the 9-mer library $Gnk(nnk)_8$ which is about 60 times higher than the actual number of clones we have observed in this library. Furthermore, since the peptide is genetically coupled to a biological entity, the phage, the availability of this peptide for selection is

contingent upon the growth capacities of its carrier phage. For example, a phage clone may be a moderate binder but yet be selected and propagated by virtue of its better multiplicative potential. Thus, more abundant phage clones in the lower echelons of the affinity cone would be more likely to be selected.

To address this problem, we hypothesized that the chances of revealing the leading ligands may be considerably increased by using "separate libraries". These are libraries enriched with clones that belong to different families. To explore this hypothesis, we obtained the landscape library f8/9 by randomizing position 5 in the major coat protein pVIII normally occupied by aspartic acid (D). This change represented an increase in the number of randomized amino acid residues compared to our previous landscape library, f8/8, in which positions 2, 3, and 4 of the major coat protein had been randomized. Our primary observation was that, in addition to enhancing the diversity of the random peptides displayed on the phages, the type of amino acid in position 5 also played a functional role in determining the viability of the phage. A direct evaluation of the diversity of peptides generated by the randomization of amino acids at position 5 would require statistical analysis of thousands of clones. Instead, we chose to analyze the common shift in the peptide diversity as a result of the randomization of position 5 in the major coat protein. Despite some bias in amino acid selection at this position, such as a complete absence of cysteine, an under-representation in hydrophobic and basic amino acids, and an increased representation in acidic acids, the novel library differs considerably from the former f8/8 library. Distinguishing characteristics of the new 9-mer library included an even greater bias against positively charged amino acids (K and R), an increased number and distinct dispersion of negatively charged amino acids (D and

E), a change in frequency and dispersion of valine, a decreased number of alanines and prolines and an increase in the number of glycines. Overall, we demonstrate here that both libraries encode unique amino acid sequence profiles suggesting the prevalence of different families of phage clones represented in each library.

To further characterize the sequence repertoires encoded and the behavior of the libraries during affinity selection, we screened the libraries against three selectors with a gradient of structural complexity: TEM 1 β-lactamase, streptavidin and *Salmonella typhimurium*. Analysis of the unique clones obtained during affinity selection against TEM 1 β-lactamase revealed non-overlapping and dissimilar families of peptides and sometimes even individual phages within each library. A significant observation was that the diversity of the clones selected from the f8/9 library was higher than diversity of clones selected from the f8/8 library. Thus, the use of both libraries in selection protocols against the same target is justified as this would provide with a greater chance of finding a peptide with high affinity and specificity. Furthermore, selection with "separate libraries" such as the one used in our experiments is warranted based on the increased diversity that is generated in the selected clones.

Affinity selection against streptavidin has already been done in our laboratory using the f8/8 library (Petrenko and Smith, 2000). Here, we used the novel f8/9 library and contrasted the results obtained with those previously obtained for the f8/8 library. A predominant family of clones with the motif VPxGAY/FS/T had been previously identified in the f8/8 library as being specific for streptavidin. Among the highly diverse affinity selected clones from the 9-mer library, only one clone showed homology with this family. This clone displayed an affinity to streptavidin which was 50 times higher

than the best binder from the f8/8 library. Thus, separate libraries create greater diversity in the repertoire of the clones represented in the library, provide a wider range of alternative clones and allow phage clones with maximal affinity to a particular target to be selected.

Phage display is rapidly being adapted as a high throughput screening system for affinity ligands against biologically relevant targets like tumor receptors, surface components of bacteria and others. With these applications in mind, we decided to test our hypothesis by screening both the f8/8 and f8/9 libraries against a complex target, *Salmonella typhimurium* cells, exposing numerous binding receptors on their surface. As with our earlier targets, we identified non-overlapping and highly divergent sets of clone families in each library and isolated unique clones with a variety of binding capacities.

In summary, we have demonstrated that the use of separate landscape libraries enhances the likelihood that novel ligands can be isolated including some with very high target affinities and simultaneously increase the diversity of the target-specific ligands that can be selected. It has been previously demonstrated that landscape libraries with high diversity are a rich source of specific binders with applications in cancer cell recognition, gene- and drug delivery systems, diagnostic probes against pathogenic bacteria and spores, etc. Such a wide range of potential applications for this technology has generated a considerable demand for many new target-specific ligands. Techniques that enhance the repertoire of peptide ligands during affinity selection would help quench this demand and create new novel adaptations of phage display technology.

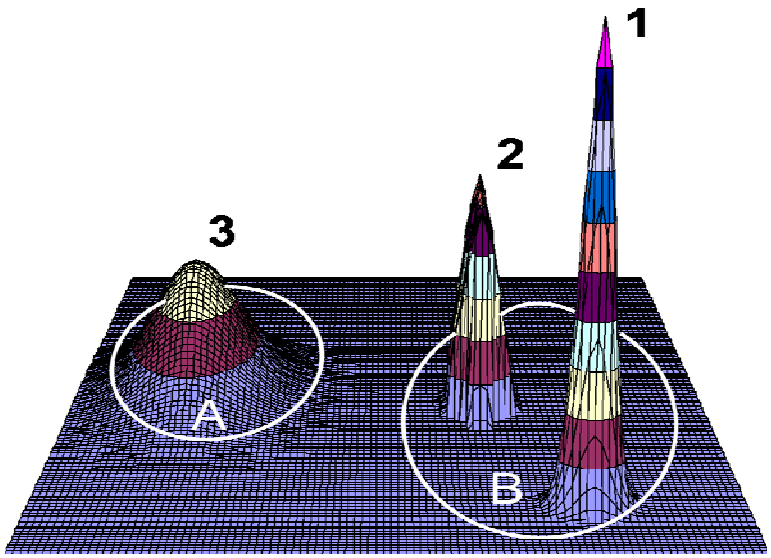

Figure 10. Hypothetical three dimensional representation of peptide population in a sequence space. Following a previously suggested model (Smith and Petrenko, 1997), a highly simplified two dimensional tableau of all possible combinations of amino acids for a given number of randomized positions can be represented as a grid with each position in the grid standing for a unique combination of amino acids (e.g., 4.16×10^9 or ($5x20^6x13$) for f8/8 library encoded by DNA's $Gnk(nnk)_6nnG$). For convenience, we assume that points that are close in our two-dimensional representation indicate similar amino acid sequences. To make the model more illustrative, we can represent the possible sequences for a hypothetically 4-mer library in two non-overlapping subsets of the randomized positions along the axes of the plane, for example subset of 400 sequences or (20 ×20) (positions 1-2, along the X axis, and subset of 400 or (20×20) (positions 3-4, along the Y axis**.** In phage libraries displaying longer peptides, the sequence space would be considerably larger (e.g. 4.16×10^9 for the 8-mer library and

1.28×10^{11} for the 9-mer library). Real phage libraries, which hardly reach the theoretical diversities, would be seen as a collection of random points in sequence space and be expected to form overlapping domains within such a grid as depicted (**A** and **B)**. An additional dimension is superimposed onto this grid when phage libraries are considered in the context of their affinity towards a target. Thus, we would expect to find structurally related peptide clusters stratified on the basis of their target affinity so as to form "affinity cones" (**1**, **2**, and **3**) with affinity increasing from the base to the peak of each cone. Hence, the peptide with the highest affinity to the target ("leading peptide") would form the peak of the cone.

CHAPTER 3

LANDSCAPE PHAGE PROBES FOR PC3 PROSTATE CARCINOMA CELLS

1. Abstract

Prostate carcinoma, a medically and economically significant malignancy, represents a complex clinical entity due to the broad spectrum of the disease-related factors associated with its diagnosis, management and treatment, creating the need for probes capable of distinguishing different forms of the cancers at the molecular level. Phage display technology with its high throughput capacity for analysis of random peptides possessing specific binding properties represents a very attractive tool in the quest for molecular probes. Herein we describe the use of two landscape phage libraries to obtain probes against PC3 prostate carcinoma cells. Following a very stringent selection scheme, we were able to identify three phage probes, two from the 8-mer library and one from the 9-mer library that demonstrated specific and selective affinity to PC3 cells. The probes thus identified will be used as navigating modules in both therapeutic and diagnostic approaches to prostate carcinoma.

2. Introduction

Following skin cancer, prostate cancer remains the most common cancer diagnosed in American men and is the second leading cause of cancer-related mortality. An estimated ~187,000 new cases are expected to be diagnosed during 2008 (ACS, 2008). Though an earlier diagnosis of cancer correlates with a better survival rate, it is accompanied by a host of attendant problems involving clinical assessment, treatment selection, post-therapeutic evaluation that emerge due to the nascency of the neoplasm complicated further by the introduction of ancillary factors such as age, infection, size of gland etc.

Elucidating molecular signatures of prostate cancer cells may aid in revealing the intricacies of tumor assessment. Further, molecular profiling may help in determining appropriate molecularly directed therapeutic measures enabling personalized medicine (Samoylova *et al.*, 2003). Creation of cancer molecular profiles engenders the need for an extensive development of specific and selective biocompatible probes which should also be robust, inexpensive and stable. Peptides being in the range of 1-2 kDa and demonstrating acceptable affinity and specificity to their targets represent an attractive platform of probes. They possess impressive tumor penetrating capacity, are generally not recognized by the RES and are less likely to instigate immune responses. In addition, they exhibit a higher activity per mass and greater stability (Ladner *et al.*, 2004). Their undoing, rapid proteolysis as well as poor affinity can be resolved by derivation of peptidomimetics by N and/or C terminal blocking, cyclization and incorporation of D-amino acids (Nilsson *et al.*, 2000; Aina *et al.*, 2002b; Borghouts *et al.*, 2005).

Furthermore, the availability of combinatorial peptide libraries from which potential therapeutics can be extracted adds another availing dimension to the concept of peptidic biopharmaceuticals.

Phage display technology represents a high-through put combinatorial technology for screening billions of random peptides against random targets on the surface of cancer cells or located within them to identify peptides with specific binding properties. The distinctive advantages with this technique are that the target may be unknown and non-immunogenic yet may serve as a delineating character for a particular cell type or tumor type. Not only have phage displayed peptide libraries been used to develop specific probes for prostate cancer but several phage display isolated tumor-specific peptides have been harnessed as putative diagnostic and therapeutic agents. A prostate carcinoma binding peptide, DUP-1, isolated by screening a phage display library against DU-145 cell line was shown to be internalized into prostate cancer cells. Further, radioiodinated DUP-1 accumulated in tumors to a level of 5% injected dose/g within 5 minutes and failed to be removed after perfusion of tumors (Zitzmann *et al.*, 2005). Aggarwal et al identified a peptide binding selectively to Prostate-specific membrane antigen (PSMA) and demonstrated that a dimeric form of this peptide efficiently inhibits the enzymatic activity of PSMA. Furthermore, the dimer was able to bind to PSMA-expressing cell lines (Aggarwal *et al.*, 2005). Phage displayed peptide libraries were used to select for peptides specifically binding to different forms of prostate specific antigen (PSA) and characterized for their effects on the enzymatic activity of PSA. The peptides were found to enhance enzymatic activity of immobilized PSA whereas the capture of PSA by the peptides abolished the enzymatic activity. The authors propose these peptides as potential

tools for recognizing PSA forms more specifically associated with prostate cancer (Ferrieu-Weisbuch *et al.*, 2006). Wang and co-workers created a T7 phage display cDNA library from prostate tumor tissue and panned them against purified IgG from prostate cancer patients to isolate prostate cancer specific phage clones which were then used to create a phage-protein microarray. The microarray thus generated was able to detect malignant sera with considerable specificity and sensitivity and performed better than PSA in doing so (Wang *et al.*, 2006). Phage display derived peptides binding to hepsin (HPN) were used to develop HPN-targeted imaging agents and were able to bind specifically to HPN-expressing LNCaP xenografts in mice. The authors conjugated multiple target-specific peptide molecules to a single nanoparticle to exploit the avidity effect that is generated from the multivalency (Kelly *et al.*, 2008).

Landscape phages afford a natural platform to avail of the avidity effect as they manifest the foreign peptide on all copies of the major coat protein pVIII. The close knit arrangement of the multiple copies of the peptide transforms the phage surface creating novel landscapes to be used in interaction with an almost inexhaustible range of targets and allows for multivalent interactions creating a made-to-order avidity effect (Petrenko *et al.*, 1996). Landscape phage libraries are multibillion collections of such uniquely transformed phage representing a potentially untapped resource for bioactive nanomaterials (Kuzmicheva *et al.*, 2008). Landscape phage libraries have been used to isolate phage probes for malignant glial cells (Samoylova *et al.*, 2003), breast cancer cells (Fagbohun *et al.*, 2008). Romanov and co-workers isolated landscape phages to identify specific ligands to LNCaP cells and demonstrated that a phage designated as pg35 blocked spreading of LNCaP cells as well as their derivatives, C4-2 and C4-2b. The

cognate peptide failed to do so but instead increased the invasiveness of C4-2 and C4-2b as well as activated matrix metalloproteinase MMP-2 and MMP-9 in them (Romanov *et al.*, 2001). Furthermore, a phage, L11 was identified from a landscape library which was involved in attenuating the binding of prostate cancer cells to bone marrow endothelial cells. This phage was found to specifically bind to PSA (Romanov *et al.*, 2004). Apart from cancer related targets, landscape phage or phage peptides have been used in multifarious applications including development of diagnostic probes for bacteria and spores (Brigati *et al.*, 2004; Sorokulova *et al.*, 2005), as a molecular recognition interface in detection devices (Petrenko, 2008b), in gene and drug delivery systems (Mount *et al.*, 2004; Jayanna *et al.*, 2009) demonstrating the enormous flexibility of this technology.

We describe here selection of landscape phage probes for PC3 prostate carcinoma cells using a biased selection scheme in which the pristine library is depleted of non-specific binders by exposure to auxiliary targets prior to exposure to the target cells. Selected phage clones after four rounds of selection were analyzed for their specificity and selectivity towards the target cells using cell association assays. Based on our results we have identified two 8-mer clones which demonstrate 8-9 fold higher selectivity and 15-30 fold higher specificity for PC3 cells than for control cells as well as one 9-mer clone demonstrating 80 fold higher selectivity and 600 times higher specificity towards target cells. Depending on the functional effects of phage-tumor cell associations which are under investigation by us such selective probes may provide an impetus for the development of diagnostic or therapeutic reagents specific for prostate cancer. This gains special importance in light of the fact that prostate tumors especially in the advanced

stages are bereft of treatment options save a few and there is a pressing need for novel therapeutics (Petrylak, 2005b; a) to satisfy the wide spectrum of patient profiles.

3. Materials and Methods

3.1 Cells

Cell lines were obtained from the American Type Culture Collection (ATCC, Manassas, VA). The PC3 (CRL-1435) cells are derived from the bone metastasis of grade IV prostatic adenocarcinoma. HepG2 (HB-8065) cells derived from a human hepatocellular carcinoma and HEK293 (CRL-1573) cells derived from a fetal kidneys were used as controls. WI-38 (CCL-75) cells are normal human lung fibroblasts. All cells were grown as recommended by ATCC and incubated at 37°C, 5% CO_2. For use in phage display selection protocols, all cell types were grown in 25 cm^2 polystyrene flasks for 48 h or in 24/96-well cell culture plates for 24 h to reach sub-confluent or confluent monolayers.

3.2 Landscape phage libraries

Two landscape phage display libraries, f8/8-mer (Petrenko *et al.*, 1996) and f8/9-mer (Kuzmicheva *et al.*, 2009) were used to isolate specific peptide ligands for PC3 prostate carcinoma cells. All general methods of handling phage, including propagation, purification, titering, production of pure phage clone, and isolation of phage DNA have been previously described (Barbas *et al.*, 2001; Brigati *et al.*, 2008).

3.3 Selection of landscape probes

The selection protocol previously described by Samoylova et al incorporating our modifications was adopted to identify phage clones homing to PC3 cells (Samoylova *et al.*, 2003). In an effort to minimize the selection of peptides binding non-specifically and maximize the affinity of target binding peptides, we implemented a rigorous library depletion regimen wherein the naïve library was consecutively exposed to culture flasks, serum treated culture flasks as well as non-target cells (fibroblasts) before being incubated with target PC3 cells. An aliquot of the primary library (100 copies of each phage clone) in 2 ml of blocking buffer (0.5% BSA in serum-free RPMI 1640) was added to an empty cell culture flask (depletion flask) and incubated for 1 h at room temperature. Following the incubation, phage that did not bind to plastic was transferred from the depletion flask to serum-treated culture flasks. At the same time, the WI-38 fibroblast cells were washed twice with serum-free Leibovitz L-15 media and incubated for 1 h at 37°C, 5% CO_2 in serum-free Leibovitz L-15 media that was removed immediately before application of the phage. Phage that did not bind to serum-treated culture flasks was transferred to the fibroblast cell culture flask and incubated for 1 h at room temperature. At the same time, the PC3 cells were washed twice with serum-free RPMI 1640 media and incubated for 1 h at 37°C, 5% CO_2 in serum-free RPMI 1640 media that was removed immediately before application of the phage. Phage that did not bind to fibroblasts was transferred to the PC3 cell culture flask and incubated for 1 h at room temperature. Following the final incubation with PC3 cells phage not associated with tumor cells were washed away by extensive washing with washing buffer (0.5% BSA,

0.1% Tween 20 in serum-free RPMI 1640). Phage bound to the cell surface were collected by treating the PC3 cells with 2 ml of elution buffer (0.1 M glycine-HCl, pH 2.2) for 10 min on ice. After collection, the eluate was neutralized with 376 µl 1 M Tris (pH 9.1). To recover cell internalized phage, after further washing, PC3 cells in the flask were scraped in 5 ml of serum-free RPMI 1640 and pelleted by centrifugation at 130 x *g* for 10 min. RPMI 1640 was removed and the cell pellet was lysed with 200 µl of lysis buffer (2% deoxycholic acid (sodium salt), 10 mM Tris, 2 mM EDTA (pH 8.0)). Phage in eluate were concentrated by centrifugal concentrators (Centricone 100 kDa, Fisher Scientific, Pittsburgh, PA) to an approximate volume of 80 µl. The phage input and output were titered in bacteria and the results of the selection were expressed as the percentage of the ratio of output to input phage. The phage fractions, cell-surface bound phage and cell-internalized phage were amplified separately in bacteria and used in subsequent rounds of selection which were similar to the procedure described above except for the lack of the extensive depletion regimen. Following four rounds of selection, phage DNAs of randomly selected phage probes were PCR amplified, isolated and sequenced to reveal the peptide sequences responsible for target affinity.

3.4 Selectivity of phage probes for PC3 cells

Individual phage clones identified by sequencing were propagated and purified to be used in cell-association assays. Due to the large number of possible candidates, an initial semi-quantitative screening assay was employed where in the association of a selected clone with target PC3 cells as opposed to serum was monitored. The protocol essentially followed that of selection with phage particles (~10^6 cfu/well) being incubated

with target as well as serum treated control wells of a 24-well cell culture plate. Following washing, cell or serum associated phage was collected by lysing the cells, titered in bacteria and presented as a ratio of output to input phage.

A select panel of phage probes identified based on the screening assays was then employed for assays to determine their selectivity. PC3 cells, HEK293 cells and HepG2 cells were grown to confluence in separate wells of a 96-well cell culture plate. As a control, selected wells were treated with media alone. Before application of phage, media in the wells was replaced with serum-free media for 1 h. Each phage probe (~10^6 cfu/well) was added to the designated wells in 100 µl of blocking buffer and incubated for 1 h at room temperature. The buffer containing unbound phage was carefully removed and the cells were washed eight times with 100 µl of cold washing buffer. To collect cell associated phage, 25 µl of lysis buffer (2.5% CHAPS in serum-free media) was then added to each of the wells and incubated for 10 min on a shaker. To the lysate, 125 µl of starved *E.coli* cells was added and incubated for 15 min at room temperature before 180 µl of NZY media containing 0.4 µg/ml of tetracycline was added. After a 45 min incubation at 37°C, the mixtures were plated on NZY plates containing 20 µg/ml tetracycline and incubated overnight. Phage titers so determined were expressed as a ratio of output to input phage. Phage bearing un-related peptide was used as a control. The assays were done in triplicate.

3.5 Mode of interaction of phage probes with PC3 cells

As it is important to definitively identify the cellular localization of the phage probes identified by our assay before we harness them in future applications, we

developed an assay very similar to our first round of selection wherein cells incubated with phage were sequentially treated with acid buffer to recover surface bound phage and then lysed to collect cell-internalized phage. Briefly, PC3 cells were grown to confluence in selected wells of 96-well cell culture plate. Before application of phage, media in the wells was replaced with serum-free media for 1 h. Each phage probe (~10^6 cfu/well) was added to the designated wells in 100 µl of blocking buffer and incubated for 1 h at room temperature. The buffer containing unbound phage was carefully removed and the cells were washed eight times with 100 µl of cold washing buffer for 5 min/wash. To collect surface-bound phage the cells were treated with elution buffer (pH 2.1). The eluate was collected and neutralized with 5 µl 1 M Tris (pH 9.1). The cells were washed two times with 25 µl of cold washing buffer for 5 min/wash and the washes collected. Finally, 25 µl of the lysis buffer (2.5% CHAPS in serum-free media) was added to the cells and incubated for 10 min on a shaker to collect phage internalized into cells. Phage titers were determined by infection of bacteria and presented as a ratio of output to input phage. Phage bearing un-related peptide was used as a control. The assays were done in triplicate.

4. Results

4.1 Selection of phage probes against PC3 cells

We chose to use PC3 cells as our target cells as they closely approach the profile of advanced prostate tumors. We decided to include two landscape libraries, f8/8 (8-mer) and f8/9 (9-mer) in our selection scheme to increase the chances of finding a peptide with

optimal target association properties. Also, since we were interested in isolating phage peptides with high selectivity we adapted a rigorous library depletion protocol in which the naïve library was progressively depleted against plastic, serum and normal fibroblast cells before being allowed to interact with the target cells. Furthermore, a very extensive washing procedure was followed in which the cells were washed 20 times to eliminate unbound phage as well as weak binders. Following incubation, phage associated with the cells were recovered using two different approaches as shown in Figure 11.

Phage bound to tumor cell surface were eluted using an acidic elution buffer of pH 2.1. Following the elution, the cells were washed two times (post-elution wash) and the phage internalized into the tumor cells were recovered following detergent lysis of the tumor cells. Both phage fractions were separately amplified in bacteria and used as input phage in subsequent rounds of selection. In the next round of selection, phage purified from eluate fraction and phage purified from the cell-lysate fraction were added to different flasks containing target cells so that a two-channel selection scheme was set up, one for isolation of cell-binding phage and the other for isolation of cell-internalized phage. The numbers of infective phage particles in input, washes as well as the phage associated with the cells was titered in bacteria and the results of each round presented as the ratio of output phage particles to the input phage particles expressed as a percentage (Yield). The enrichment of phage library for target specific clones manifested by a progressive increase in the yield across consecutive rounds of selection was indicative of a successful selection for tumor cell binders (Figure 12). For both libraries, following four rounds of selection, 40 phage clones each were randomly chosen from the eluate, cell-lysate and post-elution wash fractions respectively for PCR amplification and

sequencing. The sequences are presented in Table 3. Even though we found some familial organization, most of our sequences appear to be unique.

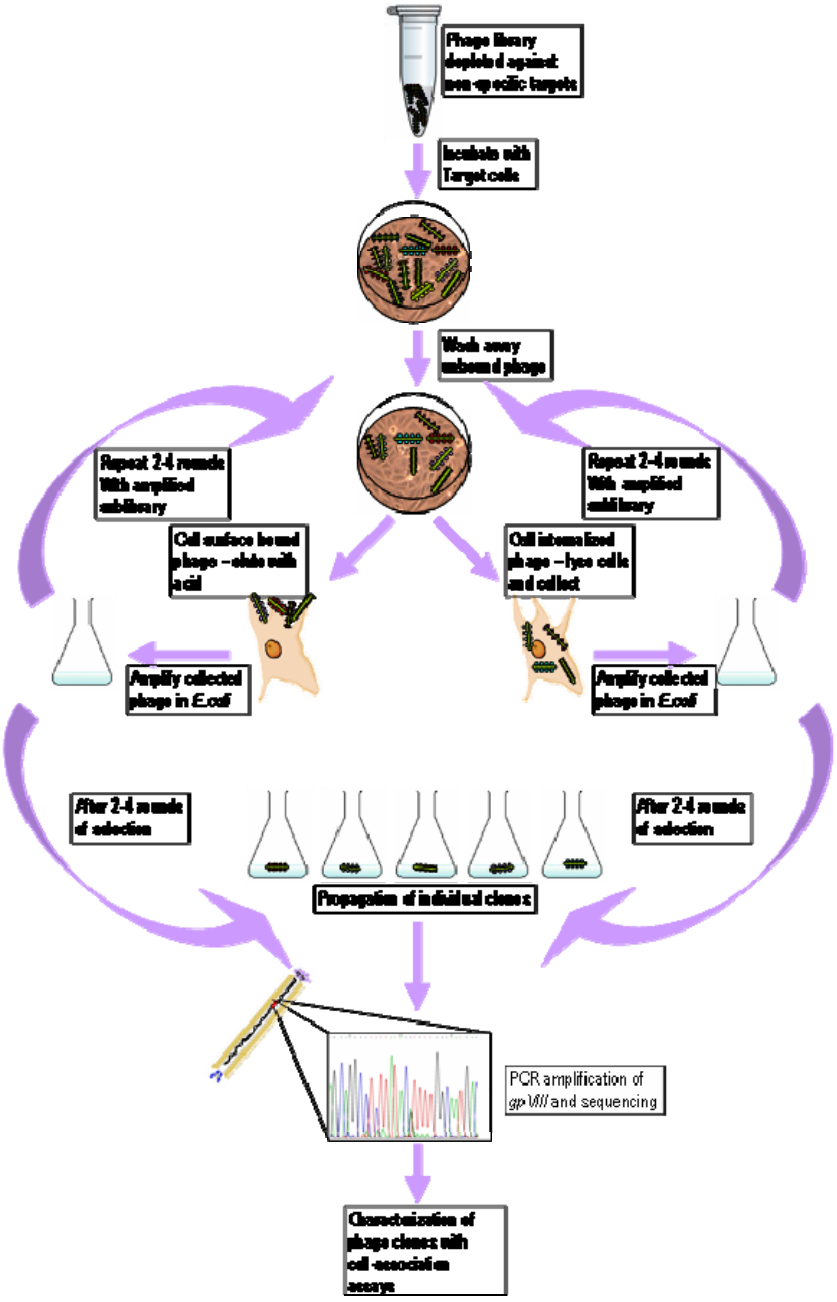

Figure 11: Scheme for affinity selection of landscape phage probes against tumor cells demonstrating the dual channel of phage collection from target to identify cell-surface bound phage as well as cell-internalized phage.

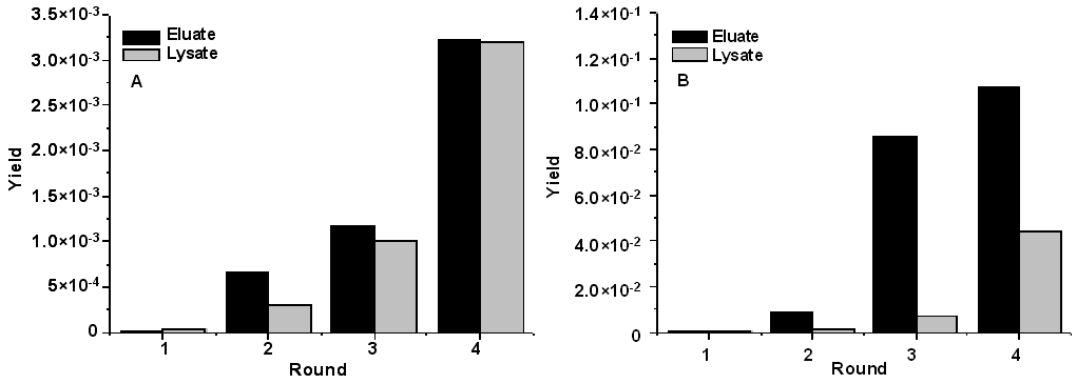

Figure 12: Phage output during successive rounds of selection. X axis – round of selection, Y axis – ratio of phage output to input expressed as percentage and termed as Yield. A progressive increase in the yield across successive rounds indicates selective enrichment of library for target specific clones. A – f8/8 library, B – f8/9 library.

Table 3: Sequences identified after four rounds of selection against PC3 cells

8-mer	9-mer
DTDSHVNL[a]	GAYDVNVND[a]
GDNSHVNL[a]	AEYGERGNA[a]
VSDNTDYS[a]	AEYGESGNA[a]
DTPYDLTG[ab]	AEYGESVLI[a]
ERAPLSVE[abc]	DSDVGWVND[a]
GPDSTWAG[ab]	EAAGANIAP[a]
DSSNKPTG[b]	GPNWAEGDS[a]
DSSRLERV[b]	VADDRDYSD[a]
EGMMYTDV[bc]	VDVSEQMSL[a]
VGQDSDYS[bc]	VGDNVDYMD[a]
AHALTTEE[c]	VGDYDVVDS[a]
APLPTNGE[c]	AEYGESVNA[abc]
ATDHAAPQ[c]	DVVYALSDD[abc]
ATPTTPDP[c]	EGLVWIGMD[bc]
DLTYVNSQ[c]	
EKFASNST[c]	
EVSMYTDV[c]	

a – Eluate

b – Post Elution Wash

c – Lysate

Superscripted alphabets indicate presence of a particular phage peptide in one of the three fractions collected during the course of the selection protocol.

4.2 Specificity and Selectivity of phage probes for PC3 cells

Within the purview of landscape phage display projects, specificity is defined as the ability of a phage probe to associate with its target due to the presence of a specific peptide sequence displayed on the surface of the phage whereas selectivity is defined as the ability of a phage probe to preferentially associate with its target as compared to other targets.

We adopted semi-quantitative screening assays in an attempt to pare down the number of clones that needed to be characterized. Accordingly, the relative affinity of a phage probe to target PC3 cells as opposed to serum (cell-free media) monitored in 24-well cell culture plates was used as a benchmark to select it for further analyis (data not shown). Accordingly, 7 clones from the 8-mer library and 6 clones from the 9-mer library were selected to be used in selectivity assays. The selectivity assays were designed to verify both selectivity and specificity. Selected phage clones (~10^6 cfu/well) were added to designated wells of a 96-well cell culture plate containing target cells, control cells or cell-free media. As we were interested in evaluating the target associating propensity of each rather than localization in this assay, we chose to collect all the phage associated with cells by lysing the cells using lysis buffer (2.5% CHAPS in serum-free media). We had to adopt a lysis buffer different than the one used in our selection scheme as the previous one gave inconsistent results during titering of phage. The collected phage were titered in bacteria and presented as a ratio of output to input phage (Figure 13). Based on our results, we identified two clones from the 8-mer library, DTDSHVNL and DTPYDLTG which were specific and selective for PC3 cells.

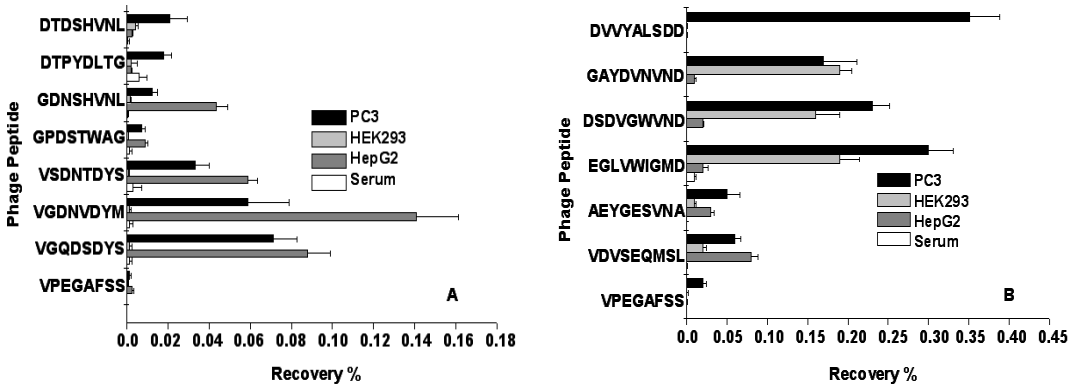

Figure 13: Selectivity and specificity of phage probes. Phage probes selected from preliminary screening assays were incubated with target PC3 cells, control cells or serum treated wells of a 96-well cell culture plate. Phage associated with cells or serum were titered in bacteria and the ratio of phage output to phage input was expressed as recovery % to obtain the measure of the selectivity of a particular clone. The % recovery of the control phage bearing unrelated peptide relative to selected phage probe was indicative of the probe's specificity. Results are the average of three replicates. A – f8/8 library, B – f8/9 library.

The affinity of DTDSHVNL to PC3 cells was ~9 times higher than to either of the control cells and 32 times higher than to serum(cell-free media) whereas the affinity of DTPYLDTG to PC3 cells was ~8 times higher than to either of the control cells and 15 times higher than to serum. The other clones analyzed showed high affinity to target cells as well control cancer cells but not to normal epithelial cells or serum leading us to postulate that these probes may be directed against a universal cancer receptor. A single clone from the 9-mer library was identified, DVVYALSDD, which demonstrated an affinity to PC3 cells that was almost 80 times higher than to the control cells and 600

times than to serum (cell-free media). Surprisingly, the other clones analyzed showed high affinity to target as well as normal epithelial cells but not to control cancer cells or serum indicating that they may directed towards a receptor that is common to both tumor and normal cells. A phage bearing an un-related streptavidin-avid peptide (VPEGAFSS) was used a control to demonstrate specificity of our phage probes.

4.3 Mode of interaction of phage probes with PC3 cells

For efficient use of phage probes it becomes imperative to know if a particular probe has just binding properties or it is internalized following binding to its target. This allows for optimal exploitation of the probes based on their homing propensities. To this end we designed experiments directed towards elucidation of this property of phage probes. The experimental setup was similar to that of selection with selected phage clones (~10^6 cfu/well) being added to designated wells of a 96-well cell culture plate containing target cells. Following incubation, the cells were treated with acid elution buffer followed by washing with a final lysis step to collect the internalized phage particles. The collected phage were titered in bacteria and presented as a ratio of output to input phage (Figure 14). Of the three clones analyzed (DTDSHVNL, DTPYDLTG and DVVYALSDD) the first had been isolated preeminently from the eluate fraction, the second found in both fractions whereas the third had been represented mainly in the lysate fraction. Predictably, DTDSHVNL showed a very high yield in the eluate fraction with moderate yields in the post-elution washes (PEW) and a low yield in the lysate fraction, DTPYDLTG gave comparable yields in both the eluate and lysate fractions whereas DVVYALSDD gave a high yield in eluate fraction as well as lysate fraction. The

presence of DVVYALSDD in the eluate fraction presents questions as to its internalizing capabilities. We feel that the internalizing property is a function of time and/or temperature and modifying either/or both would eliminate the appearance of this phage probe in the eluate fraction as most of it would be internalized. The presence of phage particles in the post-elution washes can be explained on the basis of a phenomenon previously described in cell injury studies as 'pH paradox' (Currin *et al.*, 1991). Here, a fall in pH as observed after cellular injury serves to stabilize the plasma membrane of cells by inhibiting the activity of phospholipases whereas a sudden return to normal pH as occurs following reperfusion creates a spurt in phospholipase activity which in turn damage the cell membrane by cleaving their substrate phospholipids molecules (Harrison *et al.*, 1991). Our experimental setup closely mimics this physiological tableau in that we treat cells with acid elution buffer followed by treatment with washing buffer the pH of which is close to the physiological pH. This sudden change of pH leads to phospholipase activation and subsequent membrane damage allowing for the release of membrane bound components like peptides, phage particles to the medium explaining their presence in the post-elution washes as well as in the lysate fraction.

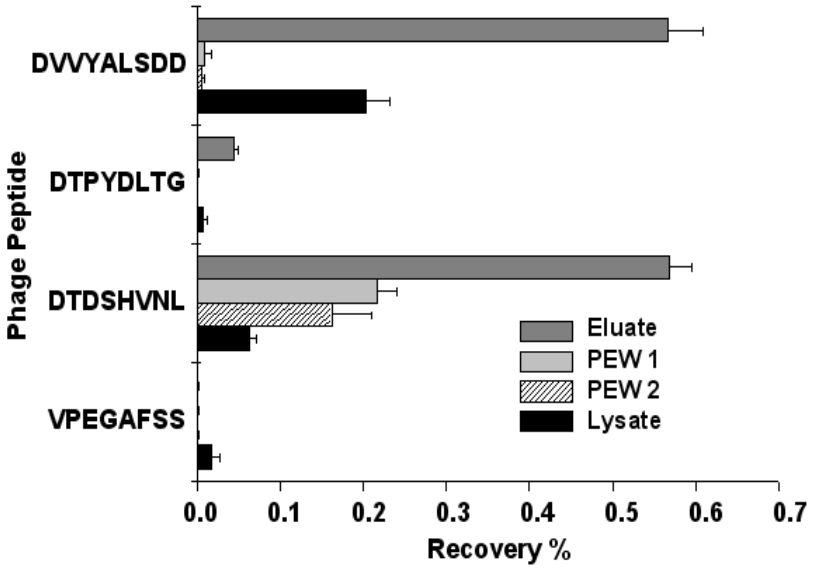

Figure 14: Mode of interaction of selected phage probes with PC3 cells. Selected phage probes were incubated with target PC3 cells. The surface bound phage were eluted with acid elution buffer, the cells washed twice and then lysed with detergent to collect the internalized phage. Phage in all fractions including the Post elution washes (PEW) were titered in bacteria and the ratio of phage output to phage input was expressed as recovery %.

5. Discussion

Phage display, since its conception by Dr. George Smith in 1985 (Smith, 1985) has emerged as a premier tool in molecular biology with widespread applications. The potential of phage display lies in the self-assemblage and self-perpetuation of the query molecules on the viral surface through the expression of the viral life cycle. Additional features are the stability and the longevity of the phage particles which in turn reflects on the peptides they bear on themselves (Brigati and Petrenko, 2005). The surface display of

random peptides creates a high throughput screening system to discover ligands to a host of targets. Also, unique properties of peptides results in high affinity, specificity and selectivity towards their cognate targets. Such characteristics make this technology an ideal molecular tool to extract molecularly directed probes against complex targets such as tumors.

In particular, landscape phage with their intensive surface array of guest peptides represent a potential source of cell-specific probes which can be harnessed in varied drug/gene delivery platforms (Mount *et al.*, 2004; Jayanna *et al.*, 2009). Stringency of our selection conditions was high as the long-term focus was the development of highly selective probes. Amongst the sequences identified, familial structure was not discernable to a great extent probably due to the high stringency during selection which would have precluded the selection of homologous members of a phage clone with moderate affinity allowing for the selection of only clones with high affinity. Furthermore, we were interested in characterizing the mode of cellular interaction of phage probes and hence we collected surface-bound phage separately from the phage internalized into the cells. Also, a very interesting fraction that of the washings obtained after elution was collected and analyzed. There was considerable redundancy of phage probes between the different fractions though there were some notable exceptions like DTDSHVNL and GDNSHVNL which were characteristically found in the eluate fraction. This redundancy can be attributed to dual properties (binding and penetrating) of a phage probe in some cases (DTPYDLTG found 9 times in eluate fraction and 10 times in lysate fraction) or may just be an artifact in other cases (DVVYALSDD found 12 times in lysate fraction but just once in the eluate fraction) arising due to experimental conditions. Also, phage probes

were found in the post-elution washes which led us to hypothesize that the changes in pH occurring during elution and subsequent washings causes membrane perturbations causing the release of non-eluted membrane-bound phage probes to the media.

As a means to narrow down the number of clones to be analyzed, we conducted a screening assay in which the relative affinity of a phage peptide to PC3 cells was measured against its affinity for serum. This assay is semi-quantitative and provides a rough estimate of the putative target-binding properties of a phage probes. Accordingly, 13 clones across both libraries were chosen for further analysis that involved monitoring the selectivity and specificity of a phage probe in a 96-well format. We chose to use hepatocellular carcinoma cell line, HepG2 and Human embryonic kidney cell line, HEK 293 as our non-prostate cell controls to monitor selectivity whereas the control phage bearing an unrelated guest peptide was used to verify specificity. Despite the stringency of selection procedure, our results indicate a selection of some probes which are directed towards receptors shared between normal cells and cancer cells as well as receptors universal to cancer cells. This may be related to the relative abundance of different receptors on tumor cell surface and drives the need for extensive selection protocols with landscape libraries containing different repertoires of guest peptides; an idea which has been previously described (Kuzmicheva *et al.*, 2009).

Earlier research in our laboratory had demonstrated the intrinsic capability of fusion phage proteins to assemble into lipid bilayers and confer an emergent property to the liposomes namely that of target selectivity (Jayanna *et al.*, 2009). These studies were based on the unique structural and biochemical properties of phage major coat protein. The phage major coat protein is an intrinsic membrane protein with a propensity to insert

into lipid bilayers when separated from the phage particle. The amphiphilic nature of the protein drives it to incorporate into liposomes where it forms a transmembrane moiety firmly anchored in the bilayer (Stopar *et al.*, 2003). We propose to harness this property to incorporate tumor specific peptides into therapeutic liposomes thereby deriving tumor targeted liposomes. This simplistic approach coupled with the ability to rapidly obtain tumor-specific phage fusion proteins via phage display allows one to envisage a combinatorial system for the production of targeted liposomal therapeutics. Apart from this example, numerous other studies have shown the possible utility of phage nanoparticles as imaging probes for tumor xenograft models (Petrenko, 2008a). Thus, the probes we have isolated hold promise in respect of their applicability for tumor visualization practices.

Tumors have considerable heterogeneity both between and within tumors (Lleonart *et al.*, 2000) which has complicated tumor diagnostics and therapy but can become a boon if precise molecularly directed therapeutics and diagnostics can be developed to detect and treat the different forms of cancer. Such advancements would enable not only a tumor-specific but a patient-specific profile of diagnosis and treatment (Samoylova *et al.*, 2006).

CHAPTER 4

LIPOSOMES TARGETED BY FUSION PHAGE PROTEINS

1. Abstract

Targeting of nanocarriers has long been sought after to improve the therapeutic indices of anticancer drugs. Here we provide the proof of principle for a novel approach of nanocarrier targeting through their fusion with target-specific phage coat proteins. The source of the targeted phage coat proteins are landscape phage libraries—collections of recombinant filamentous phages with foreign random peptides fused to all 4000 copies of the major coat protein. We exploit in our approach the intrinsic physicochemical properties of the phage major coat protein as a typical membrane protein. Landscape phage peptides specific for specific tumors can be obtained by affinity selection, and purified fusion coat proteins can be assimilated into liposomes to obtain specific drug-loaded nanocarriers. As a paradigm for inceptive experiments, a streptavidin-specific phage peptide selected from a landscape phage library was incorporated into ~100-nm liposomes. Targeting of liposomes was proved by their specific binding to streptavidin-coated beads.

2. Introduction

The concept of using targeted pharmaceutical nanocarriers to enhance the efficiency of anti-cancer drugs has been proven over the past decade both in pharmaceutical research and clinical settings. Examples of a successful realization of this concept are listed in numerous reviews (Torchilin, 2000; Noble *et al.*, 2004; Everts, 2005; Vasir and Labhasetwar, 2005). In particular, it is commonly accepted that selectivity of drug delivery systems can be increased by their coupling with peptide and protein ligands targeted to differentially expressed receptors (Shadidi and Sioud, 2003; Mori, 2004; Krumpe and Mori, 2006). A new challenge, within the frame of this concept, is to develop highly selective, stable, active and physiologically acceptable ligands that would navigate the encapsulated drugs to the site of disease and control unloading of their toxic cargo inside the cancer cells. The development of tumor-specific ligands that respond to above criteria may turn into a routine procedure due to the progress in combinatorial chemistry and phage display (a long list of different target-specific peptides identified by phage display can be found in recent reviews, (Smith and Petrenko, 1997; Nilsson *et al.*, 2000; Aina *et al.*, 2002b; Romanov, 2003)). Detailed protocols for obtaining phages and peptides internalizing into cancer cells (Ivanenkov *et al.*, 1999; Hong and Clayman, 2000; Ivanenkov and Menon, 2000; Zhang *et al.*, 2001; Samoylova *et al.*, 2003; Brigati *et al.*, 2008), and phage homing to tumors of human patients (Krag *et al.*, 2006) have been developed.

A unique extension of phage display technology was the concept of landscape phages in which the phage constructs display the guest peptide on every one of the 4,000 pVIII subunits (Petrenko *et al.*, 1996). It was shown earlier that the tumor-specific peptides fused to the major coat protein pVIII can be affinity selected from multibillion clone landscape phage libraries by their ability to bind very specifically to cancer cells, (Romanov *et al.*, 2001; Samoylova *et al.*, 2003; Fagbohun *et al.*, 2008; Jayanna *et al.*, 2008) demonstrating a high potential of landscape phage libraries as a source of tumor-specific ligands.

To serve as a targeting interface, selected ligands—once identified—have to be harnessed into suitable drug delivery platforms to ensure that their targeting qualities are utilized for a tumor-selective chemotherapy. The development of stealth liposomes and further end-functionalized polyethylene glycol (PEG) derivatives made liposomal formulations a very attractive platform to which target-specific ligands could be coupled to endow the liposomes with specific homing propensities. Several examples of liposomal targeting using phage display derived peptides exist (Koivunen *et al.*, 1999; Medina *et al.*, 2001; Lee *et al.*, 2004; Pastorino *et al.*, 2006; Slimani *et al.*, 2006). In conjunction with the successful realization of peptide-targeted liposomes, the technology required for conjugating the peptides to liposomes has also evolved. A variety of coupling strategies based on different PEG derivatives have been developed, such as pyridyldithiopropionoylamino (PDP)-PEG (Allen *et al.*, 1995), hydrazide (Hz)-PEG (Zalipsky, 1993), maleimido (Mal)-PEG (Kirpotin *et al.*, 1997), and p-nitro-phenylcarbonyl (pNP)-PEG-PE(Torchilin *et al.*, 2001) with their relative merits and demerits. Also, a “postinsertion technique” involving transfer of ligand-coupled PEG

molecules from micellar preparations directly into preformed liposomes has been described (Ishida *et al.*, 1999; Holig *et al.*, 2004) thereby decoupling the conjugation step from the liposome preparation and allowing for a combinatorial synthesis of targeted nanoparticles. In these studies selected peptides have been coupled to the anchor molecules using various techniques, including formation of a disulfide bond, cross-linking between primary amines, reactions between a carboxylic acid and primary amine, between maleimide and thiol, between hydrazide and aldehyde, or between a primary amine and free aldehyde (Nobs *et al.*, 2004).

Chemical conjugation procedures have allowed for a successful realization of the concept of targeted vesicles for tumor chemotherapy. However, they would be prohibitive for a volumetric increase in the targeted liposome preparation, which is required for clinical studies. These considerations led us to study the phage coat proteins as targeting ligands for drug-loaded liposomes. In our approach, disease specific peptides, genetically fused to the phage major coat protein pVIII, are isolated from a phage specific for a target organ, tissue, or cell, and are directly inserted into liposomes exploiting their intrinsic amphiphilic properties (Figure 15). Because the targeting peptide is a natural physical extension of the liposomal membrane-spanning anchor protein, the need for any intervening conjugation procedure is obviated. In essence, the amphiphilic property of the coat protein qualifies the phage fusion protein as a made-to-order liposomal ligand.

The ability of the major coat protein pVIII to incorporate into micelles and liposomes emerges from its intrinsic function as a membrane protein, as judged by its biological, chemical, and structural properties (Lee *et al.*, 2003). The major coat protein pVIII is a 6.5-kDa protein with 55 amino acids in landscape phages used in this study.

Numerous studies have investigated the propensity of the "wild-type" pVIII to insert into micelles and phospholipid bilayers as well its behavior in the same (Chamberlain *et al.*, 1978; Ohkawa and Webster, 1981; Sprujit *et al.*, 1989; Haigh and Webster, 1998). Figure 16 depicts the phospholipids bilayer–spanning conformation of a phage major coat protein. The 16-Å-long amphipathic helix rests on the membrane surface, whereas the 35-Å-long transmembrane helix crosses the membrane at an angle of 26 degrees as far as residue Lys40, where the helix tilt changes. The helix tilt accommodates the thickness of the phospholipid bilayer, which is 31 Å for typical lipids used in liposome construction. The usual size of liposomes being 100 nm, phage fusion proteins would be suitable targeting ligands for liposomes. To this end, we investigated whether target-specific fusion pVIII units of landscape phage retain their targeting properties as components of PEGylated liposomes. For our model experiments we chose to use commercial Doxil (OrthoBiotech, Bridgewater, New Jersey) as a source of lipids because of the ease of availability, standard composition, and the possibility of using constituent doxorubicin as a fluorescent marker. Accordingly, pVIII coat protein units of a streptavidin-specific phage VPEGAFSS (hereafter the phage is designated by the structure of the fusion peptide) were isolated in cholate solution, purified, and allowed to interact with lipid components of Doxil under reconstitution conditions. The resulting liposomes were then tested for streptavidin specificity in a functional test using streptavidin-conjugated colloidal gold particles, which demonstrated that the modified liposomes acquire streptavidin-targeting properties by virtue of the incorporated fusion proteins.

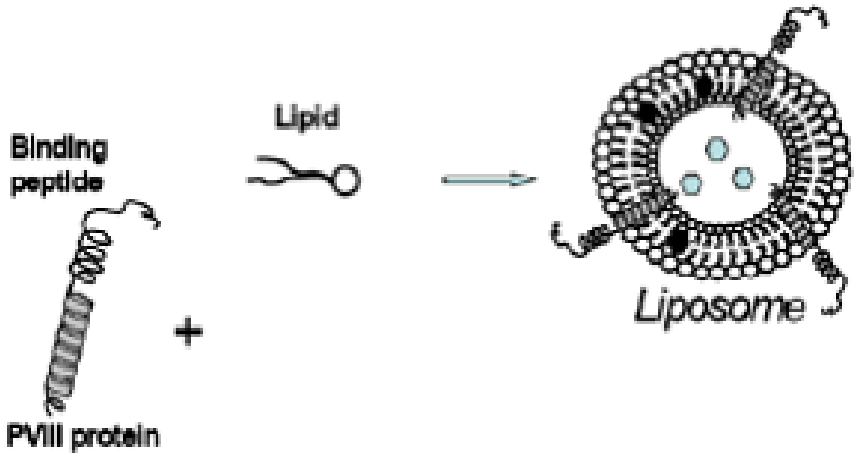

Figure 15: Drug-loaded liposome targeted by the pVIII protein. The hydrophobic helix of the pVIII spans the lipid layer and binding peptide is displayed on the surface of the carrier particles. The drug molecules are shown as hexagons.

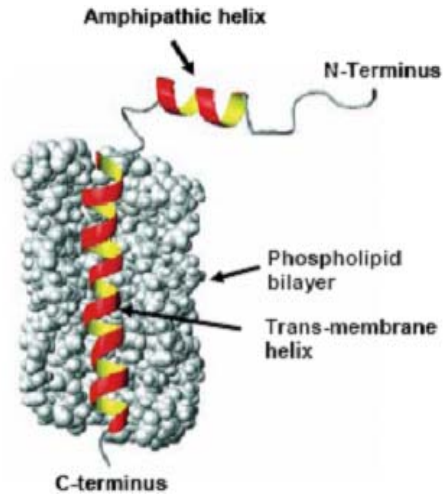

Figure 16: The model of pVIII in the lipid environment (adapted from Stopar et al. Protein–lipid interactions of bacteriophage M13 major coat protein, Biochimica et Biophysica Acta (BBA) - Biomembranes, 2003; 1611:5-15.)

3. Materials and Methods

3.1 Preparation and purification of phage coat protein

Streptavidin-targeting phage selected from the 8mer landscape library, f8/8 (Petrenko *et al.*, 1996; Petrenko and Smith, 2000), was solubilized using the procedure outlined by Sprujit et al (Sprujit *et al.*, 1989). Briefly, 350 µL phage in 1× Tris buffered saline buffer (~1mg/mL) was mixed with 700 µL120 mM cholate in 10 mM Tris-HCl, 0.2 mM EDTA, and chloroform (2.5% v/v final concentration), pH 8.0. The suspension was incubated at 37°C for 1 hour with occasional mixing. The mixture was then applied to a sepharose 6B-CL (AmershamBiosciences,Uppsala, Sweden) column (1cm× 45 cm) and eluted with 10 mM cholate in 10 mM Tris-HCl, 0.2 mM EDTA pH 8.0 to separate major coat protein from viral DNA and traces of bacterial proteins. The chromatographic profile was monitored by Econo UV monitor (Bio-Rad, Hercules, California); 5-mL fractions were collected and stored at 4°C. Concentration of protein in samples was determined spectrophotometrically by use of the formula:

$$1\ A280 = 0.69\ mg/mL$$

and the molar extinction coefficients (8250 ± 412 liters/molecentimeter) predicted by the programProtean (DNASTAR Inc., Madison,Wisconsin) (Gill and von Hippel, 1989). The predicted charge on the protein at pH 8 was +0.5 as determined by the same program.

3.2 Analysis of fusion major coat protein in chromatographic fractions and liposomal preparations by Western Blot

The presence of the fusion major coat protein in relevant fractions/preparations collected was verified by a western blot using biotinylated rabbit anti-fd IgG. Briefly, samples of fractions were mixed with an equal volume of a sample buffer (8% sodium dodecyl sulfate, 24% glycerol, 0.1M Tris pH 6.8, 4% 2-mercaptoethanol, 0.01% Brilliant blue G, 2×) and heated at 95°C for 10 minutes. Ten-microliter aliquots of the denatured samples were then loaded onto a 16% Non-Gradient Tris-Tricine gel (Jule Inc., Milford, Connecticut). Electrophoresis was carried out for 90 minutes at 100 V. Proteins in the gel were transferred to an Immobilon-P PVDF membrane (Millipore, Billerica, Massachusetts). The resulting blots were probed with biotinylated anti-fd IgG (0.12 μg/ mL, prepared according to Barbas et al (Barbas *et al.*, 2001), followed by incubation with NeutrAvidin-horseradish peroxidase (HRP) (Pierce, Rockford, Illinois) and were visualized using a chemiluminescent substrate solution (Pierce).

3.3 Preparation of targeted liposomes

As a source of liposomal constituents we used Doxil containing N-(carbonyl-methoxypolyethylene glycol 2000)-1,2-distearoyl-sn-glycero-3-phosphoethanolamine sodium salt (MPEG-DSPE), 3.19 mg/mL; fully hydrogenated soy phosphatidylcholine (HSPC), 9.58 mg/mL; and cholesterol, 3.19 mg/mL, doxorubicin 2 mg/mL. To incorporate the fusion coat protein into the liposomes, 100 μL of Doxil (~1.6 mg total lipids based on the above composition) were first mixed with 100 μL of 120 mM cholate

in 10 mM Tris-HCl, 0.2 mM EDTA pH 8.0. An aliquot of the solubilized protein (~24 μg protein in 800 μL of 10 mM cholate, 10 mM Tris-HCl, 0.2 mM EDTA pH 8.0) was added to this mixture and incubated for 2 hours at 30°C. The mixture was then dialyzed against a gradually decreasing concentration of cholate as follows (all dialysis steps were carried out in 500 mL of dialysis buffer): 15 mM cholate for 30 minutes, 10 mM cholate for 30 minutes, 7.5 mM cholate for 30 minutes, 5 mM cholate for 30 minutes, 2.5 mM cholate for 30 minutes, followed finally by an overnight dialysis with buffer containing no cholate. The cholate-free liposomes were then purified on a superose 6 column (1 cm × 30 cm; GE Healthcare Bio-Sciences AB, Uppsala, Sweden) using 10 mM Tris-HCl, 0.2 mM EDTA pH 8.0 as eluent. The chromatographic profile was monitored by Econo UV monitor (Bio-Rad); 2.5-mL fractions were collected and stored at 4°C until further analysis.

3.4 Functional test of targeted liposomes with streptavidin-conjugated colloidal gold nanoparticles

To determine whether the fusion coat protein integrated into the liposomes retains its binding activity toward its target streptavidin, we adapted a functional test using streptavidin-conjugated colloidal gold nanoparticles. Briefly, formvar/carbon-coated electron microscopic grids (Ted Pella Inc., Redding, California) were incubated with drops of relevant fractions containing targeted liposomes or nontargeted Doxil liposomes (control) for 20 minutes. The nonspecific binding sites on the grids were then blocked by incubation with separate drops of 2% bovine serum albumin (BSA) in 10 mM Tris-HCl,

0.2 mM EDTA pH 8.0 for 20 minutes. Following the blocking step, the grids were incubated with separate drops of 20-nm streptavidin-conjugated colloidal gold (Ted Pella, Inc.) containing 10^{12} beads/mL in ultrapure water for 60 minutes. The grids were then washed five times with separate drops of 10 mM Tris-HCl, 0.2 mM EDTA pH 8.0 and dried. The grids were negatively stained with 2% phosphotungstic acid containing 0.1% BSA as wetting agent and dried before being visualized by a Phillips transmission electron microscope (FEI Co., Hillsboro Oregon).

4. Results

4.1 Isolation and purification of fusion phage protein

It has been demonstrated elsewhere that deoxycholate-solubilized wild-type bacteriophage f1 can be readily fractionated by gel chromatography into DNA and coat proteins (Makino *et al.*, 1975). Furthermore, it was shown that the phage major coat protein pVIII isolated using sodium cholate displays lower aggregation numbers at least in the fresh state (Sprujit *et al.*, 1989). These observations led us to adapt the cholate isolation method for obtaining fusion phage coat protein from landscape phage. Accordingly, phage particles were disrupted using sodium cholate solution containing chloroform and fractionated as outlined in Methods. Figure 17 shows the elution profile of disrupted phage particles. As expected, DNA eluted first, followed by the phage coat proteins, with a clear distinction between the two peaks. The last peak probably corresponds to cholate micelles as assumed elsewhere (Sprujit *et al.*, 1989). Analysis of

the different chromatographic fractions by western blot (Figure 18) revealed the presence of phage coat protein in the fractions 5 and 6 corresponding to the protein peak.

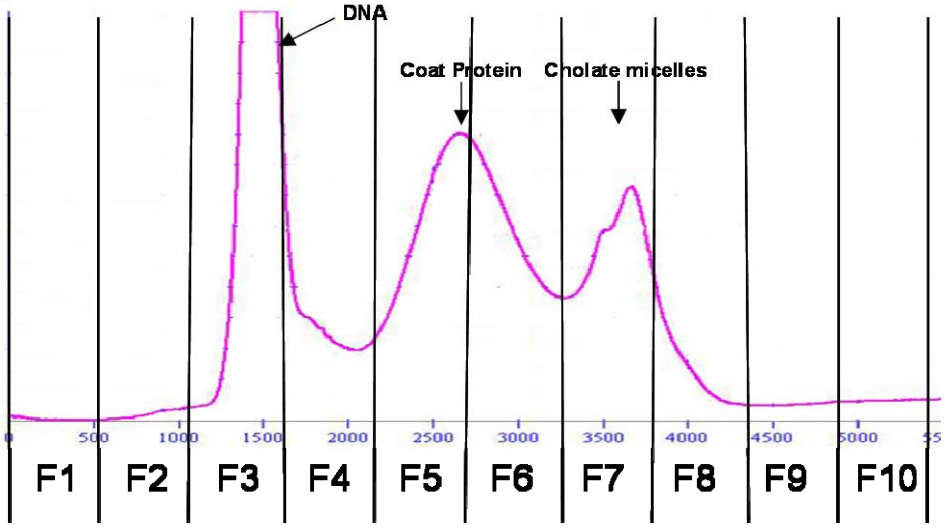

Figure 17: Gel Exclusion Chromatogram of Cholate Solubilized Streptavidin-specific phage. Streptavidin specific phage (VPEGAFSS) was solubilized in Cholate solution as outlined in the experimental section. The mixture was then eluted on a Sepharose 6B-CL column. DNA along with contaminating bacterial components eluted initially followed by phage major coat protein with a final peak of cholate micelles. Lines are drawn to specify the schema of fraction collection.

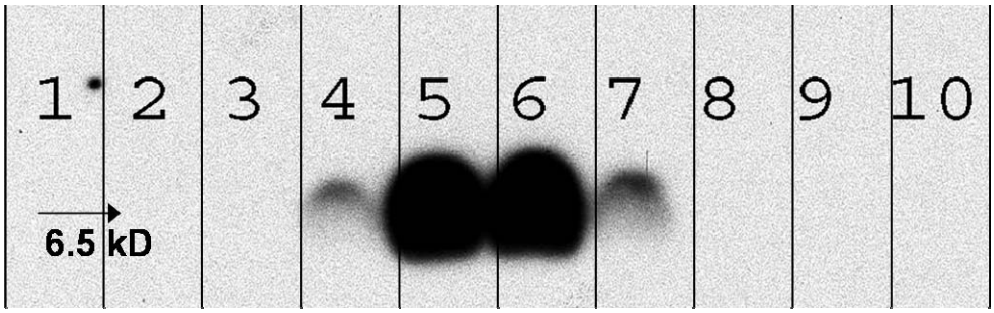

Figure 18: Western Blot Analysis of different fractions collected during gel chromatography of cholate solubilized phage major coat protein. Aliquots of successive

fractions collected during the sepharose 6B-CL chromatography were mixed with an equal volume of Tricine sample buffer, heated to 95°C for 5 min before being loaded onto a 16% Non-gradient Tricine gel. Proteins in the gel were transferred to a PVDF membrane and probed with biotinylated Anti-fd IgG. Visualization was achieved by treatment with Neutravidin-HRP followed by a chemiluminescent substrate. Numbers on the blot indicate the respective fractions to correlate with the fractions shown on Figure 17.

4.2 Preparation of targeted liposomes

Targeted liposomes were prepared by reconstitution of Doxil liposomes in the presence of phage coat proteins as outlined in Methods. Liposomes were initially disrupted in cholate solution, followed by incubation with phage coat protein solution. Controlled uniform integration of phage coat protein into liposomes was achieved by gradient dialysis in decreasing concentration of cholate, conditions that can prevent spontaneous aggregation of coat proteins. The reconstituted liposomes were purified by gel fractionation (Figure 19). The presence of phage coat protein in liposomal fractions 5 and 6 was demonstrated by western blot (Figure 20). Because no free protein was observed during chromatography, the protein content of the liposomes (1.5%) was calculated based on input (24 μg phage coat protein per 1.6 mg lipids) and confirmed by western blot. Doxorubicin content of the preparations at different stages was monitored by absorbance at 491 nm. Not surprisingly, we lost ~95% of the drug during liposome

reconstruction, which proved the reconstruction mechanism of protein insertion into liposomes.

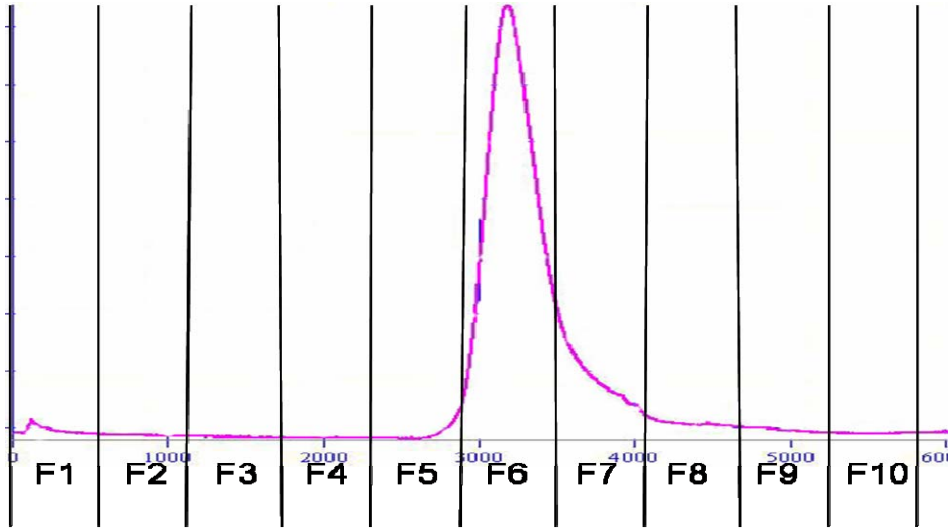

Figure 19: Gel Exclusion Chromatogram of Targeted Liposomes. Liposome carriers in Doxil® were disrupted using 120 mM cholate, mixed with an aliquot of cholate solubilized purified phage major coat protein and incubated. The mixture was then dialyzed against a decreasing concentration of cholate followed by purification on superose 6 prep grade column. The targeted liposomes eluted as a single peak with a broad tail. Lines are drawn to specify the schema of fraction collection.

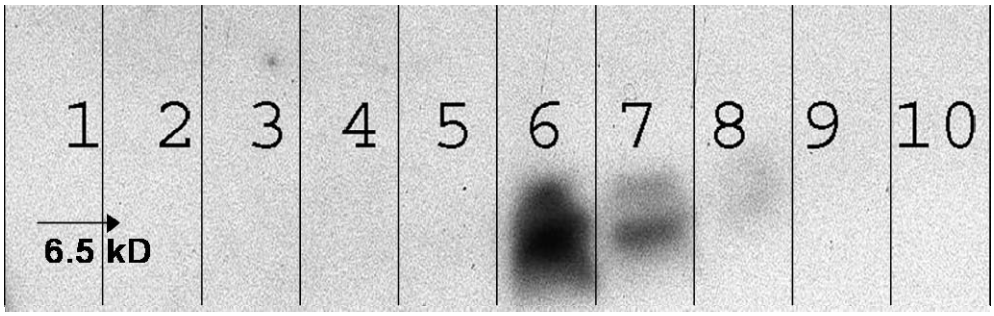

Figure 20: Western Blot Analysis of different fractions collected during gel chromatography of targeted liposomes. Aliquots of successive fractions collected during the superose 6 prep grade chromatography were mixed with an equal volume of Tricine sample buffer, heated to 95^{o}C for 5 min before being loaded onto a 16% Non-gradient Tricine gel. Proteins in the gel were transferred to a PVDF membrane and probed with biotinylated Anti-fd IgG. Visualization was achieved by treatment with Neutravidin-HRP followed by a chemiluminescent substrate. Numbers on the blot indicate the respective fractions to correlate with the fractions shown on Figure 19.

4.3 Functional activity of targeted liposomes

To validate our postulate that decoration of liposomes with target-specific phage proteins allows target recognition by the liposomes, we exposed liposomes targeted with streptavidin-specific fusion proteins to streptavidin-conjugated colloidal gold nanoparticles. Nontargeted liposomes were used as a control. According to Figure 21, targeted liposomes bind streptavidin-coated beads at a much higher level than nontargeted liposomes, as was measured by calculating the ratio of particles to liposomes, which was 1.8 for targeted liposomes and 0.06 for nontargeted liposomes. The

functionality of the streptavidin-specific fusion phage protein in the liposomes as effective targeting ligands has been demonstrated elsewhere by flow cytometry and microarray tests (Petrenko *et al.*, 2006).

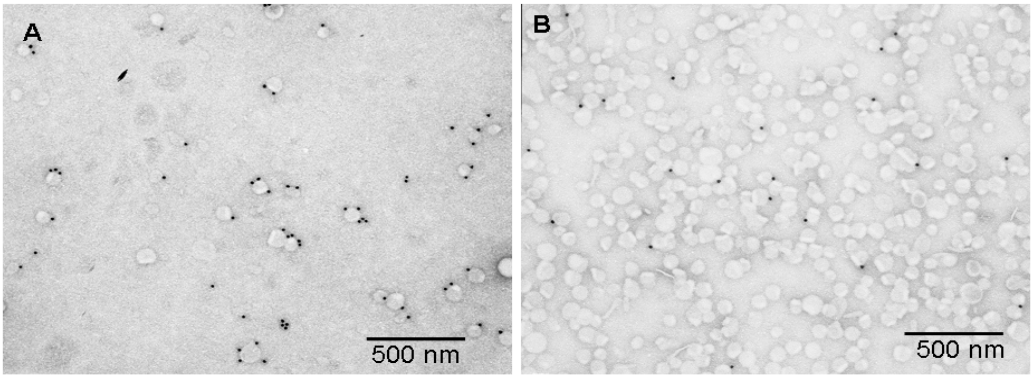

Figure 21: Functional test for targeted liposomes with streptavidin conjugated colloidal gold nanoparticles. Targeted liposomes prepared by co-incubation of purified major coat protein and stealth liposomal carriers of Doxil® were tested using streptavidin conjugated colloidal gold particles for the specificity and functionality of the incorporated phage coat protein. Targeted liposomes were loaded onto formvar/carbon coated E/M grids, incubated with the colloidal gold particles followed by visualization with a Phillips transmission electron microscope (FEI Co., OR). Panel A shows targeted liposomes studded with streptavidin conjugated colloidal gold particles with a particle to liposome ratio of 1.8. Panel B shows non-targeted Doxil® liposomes subjected to the same assay with a particle to liposome ratio of 0.06.

5. Discussion

Phage display libraries have been shown to be the reservoirs of specific peptide binders to tumor vasculature, cancer cells, or their isolated receptors (Craig and Li, 2006). We have in our laboratory isolated phage peptides specific for glioma, breast, and prostate cancer cell lines (Samoylova *et al.*, 2003; Fagbohun *et al.*, 2008; Jayanna *et al.*, 2008). Several peptides selected from phage-displayed peptide libraries have been converted into therapeutics, which validates peptide-targeting potential (Krumpe and Mori, 2006). In these and other studies, selected peptides have been coupled to the surface of the nanocarriers using various chemical techniques mentioned in brief in our introductory remarks. Although these approaches in anchoring peptide ligands on the liposome surface may provide target selectivity in vitro and in vivo, the cost and reproducibility of these derivatives in quality and quantity sufficient for pharmaceutical applications are challenging problems.

Herein we provide the proof of principle for a novel approach for targeting of liposomes through their fusion with purified coat proteins of a target-specific landscape phage, capitalizing on the structural and biochemical properties of phage coat protein. The "membranophilic" nature of phage coat proteins drives them to integrate into liposomes and micelles. Thus, coat protein derived from a tumor-specific landscape phage can be used to create tumor-specific liposomes by co-incubation of the relevant constituents. The drug of choice can then be loaded into the liposomes using any one of the available techniques (Fenske *et al.*, 2003). This modular approach to the production of targeted therapeutic liposomes provides for a combinatorial setup in which different

components can be added in alternate combinations to obtain different drugs. As a continuation of the current study, phage fusion peptides specific for MCF-7 breast cancer cell line were used to prepare targeted liposomes containing Rhodamine-PE (Avanti Polar Lipids, Alabaster, Alabama) and such liposomes were demonstrated to selectively bind cognate target cells (unpublished results). Current studies involve also loading anticancer drug doxorubicin into targeted liposomes and monitoring the stability of the formulations. Therapeutic liposomes targeted to the different cancer cell lines by cognate phage fusion peptides will be prepared and their targeting as well as cytotoxic potential will be evaluated. The simplicity of the approach as demonstrated by our results leads us to believe that this approach has definite potential to contribute to not only a tumor-specific but a patient-specific chemotherapeutic profile.

CHAPTER 5

LANDSCAPE PHAGE FUSION PROTEIN-MEDIATED TARGETING OF PHARMACEUTICAL NANOCARRIERS ENHANCES THEIR PROSTATE TUMOR-CELL ASSOCIATION AND CYTOTOXIC EFFICIENCY

1. Abstract

Cancer chemotherapy is complicated by a lack of selective drug targets. However, tumor chemotoxicity of drugs can be enhanced by precisely targeting them to tumor receptors using tumor-specific probes. Peptide phage display offers a convenient high-throughput approach to screen for tumor-selective probes. Earlier research in our laboratory has been successful in isolating phage peptides selective and specific for PC3 prostate cancer cells. Furthermore, we have demonstrated the proof of concept data for a technique of inserting the tumor-specific peptides into liposomes exploiting the intrinsic physico-chemical properties of the phage coat protein.

Here we describe the production of labeled liposomes targeted to PC3 prostate tumor cells. The targeting was demonstrated using fluorescence microscopy as well as FACS. Furthermore, we describe the modification of commercial Doxil utilizing the above technique with PC3-specific phage peptides so as to obtain targeted Doxil.

The targeted liposomes were shown to exert a higher cytotoxic effect against PC3 cells compared to the control formulations *in vitro* indicating a possible therapeutic advantage.

The simplicity of the approach to produce targeted liposomes coupled with the ability to rapidly obtain tumor-specific phage fusion proteins via phage display allows one to envisage a combinatorial system for the production of targeted liposomal therapeutics which may help overcome the therapeutic adversities associated particularly with complicated clinical entities like advanced prostate tumors.

2. Introduction

The narrow therapeutic windows of most chemotherapeutic agents represent a prohibitive factor in their clinical use, a case in point being the cardiac toxicity of doxorubicin. This results in a clinical threshold dose which cannot be exceeded even if it is warranted as in the case of tumor resistance to drugs. Conceptually, preferential delivery of drugs to pathologic sites should increase the local concentration of the therapeutic in the tumor milieu leading to a higher cytotoxic effect while simultaneously decreasing the side effects. One way to realize this concept is by targeting drugs to their cognate sites of action by way of ligands specific for receptors either uniquely expressed or overexpressed in cancer cells. Targeting results in a precise delivery of drugs to the desired location increasing the bioavailability of the drug while abating non-specific toxicity to normal tissues.

The importance of targeting in enhancing tumoricidal effects of anticancer agents is underscored by the fact that amongst the new anti-neoplastic agents approved by the

FDA since 2000, nearly 75% are targeted therapeutics (Gerber, 2008). The benefits of targeting can be illustrated with numerous examples, an interesting one being the humanized anti-CD74 monoclonal antibody (hLL1 milatuzumab or IMMU-115). This antibody has been used as an anticancer drug by itself, as a carrier for cytotoxic drugs to increase their target localization and also as a navigating ligand for liposomes loaded with doxorubicin thus forming a component of a drug delivery system. The humanized form of the anti-CD74 monoclonal antibody was shown to cause specific growth inhibition and apoptosis of B-cell lines in the presence of a cross-linking reagent. Furthermore, SCID mice bearing multiple myeloma showed a dramatic survival benefit when injected with the antibody, with a single injection given 5 days after the tumor cell injection providing nearly a 75% improvement in the median survival time (Stein *et al.*, 2004). The rapid internalization of the CD74 epitope observed post-binding as well as the fact that CD74 directs transport from the cell surface to endosomes and lysosomes laid the groundwork for the possibility of using this mAB as a carrier of cytotoxic agents. The research group of Goldenberg et al prepared anthracycline conjugates of anti-CD74 monoclonal antibodies with ~ 8-10 doxorubicin molecules on each conjugate and tested their efficacy in a murine model of non-Hodgkin's lymphoma. Both the murine and humanized conjugates of doxorubicin demonstrated a significant survival advantage with all treated animals remaining tumor-free at the end of ~4 months after the initial injection of tumor cells (Griffiths *et al.*, 2003). A similar modular concept was extended to block HIV-1 infection in cell cultures and a HIV-1/MuLV murine challenge model using a doxorubicin-conjugate anti-envelope antibody (Johansson *et al.*, 2006).

A recent review has broadened the perspective of targeting ligands beyond antibodies by enumerating the various applications of the so-called Hunter-Killer peptides (HKPs) in the alleviation of medical conditions like cancer, obesity and arthritis (Ellerby *et al.*, 2008). The concept involves the use of chimeric molecules consisting of two functional domains, one serving as a navigating moiety and the other possessing cytotoxic properties. The targeting ligand helps deliver the cytotoxic payload to specific target areas where the proapoptotic domain kills the cells by the disruption of mitochondrial membranes. One of the earliest applications of this bio-conjugate was in cancer therapeutics (Ellerby *et al.*, 1999) in which a tumor vasculature targeting peptide, CNGRC was affixed to the proapoptotic domain, $(KLAKLAK)_2$ using a glycine linker and its therapeutic efficiency was tested in nude mice bearing MDA-MB-435 derived human breast carcinoma xenografts. Results indicated a dramatic improvement in survival, reduction of tumor growth and metastasis in mice treated with hunter-killer peptide conjugates over control mice. Following this pioneering study, other Hunter-killer peptide combinations were synthesized and utilized as putative therapeutics for prostatic hypertrophy and prostate cancer (Arap *et al.*, 2002), arthritis (Gerlag *et al.*, 2001) and obesity (Kolonin *et al.*, 2004). Peptides were also used to deliver antiproliferative antisense oligonucleotides to tumors (Henke *et al.*, 2008). In this study, it was demonstrated that expressional downregulation of transcriptional factors responsible for tumor invasiveness, metastasis and angiogenesis by a directed delivery of specific antisense molecules mediated by peptides results in the inhibition of primary tumor growth and metastasis. Apart from antibodies and peptides, several other molecules like growth factors, glycoproteins, carbohydrates and receptor ligands have

been employed as targeting ligands with varying measures of success with each (Vasir and Labhasetwar, 2005).

Within the purview of targeting, if one considers the 'payload', the amount of drug reaching the target tissue, the targeting of drug delivery systems will be seen to be more efficient in terms of the stoichiometric ratios of the targeting ligand to drug molecules. Apart from the increased numbers of drug molecules being delivered within a drug delivery vector, such vehicles offer an additional advantage capitalizing on the unique vascular architecture of tumors, a phenomenon referred to as Enhanced Permeation and Retention (EPR). Rapid angiogenesis in tumors results in a compromised capillary system which allows circulating macromolecules to rapidly extravasate into tumor interstitium (Maeda *et al.*, 2000). Furthermore, the extravasated macromolecules remain sequestered within the tumor due to an impaired lymphatic drainage. In addition to the advantages afforded by active and passive targeting of drug vehicles, drug delivery systems like liposomes also provide protection for the drug from degradative mechanisms, favorably alter the pharmacokinetics of the drug and improve solubility of drugs with low solubility.

Liposomes have been by far the most successful of drug delivery system used to date with the success mainly attributable to the biocompatibility of the system. The development of stealth liposomes provided a tremendous impetus for the clinical adaptation of liposomes in cancer chemotherapy with liposomal formulations of doxorubicin (Doxil®, Caelyx®) being used in a variety of tumors. The clinical success and stability of the formulation has led a number of research groups to further improve its performance by grafting the surface of the liposomes with various targeting ligands to

achieve active targeting of Doxil. Hansen et al outlined the criteria for 'ideal' targeted sterically stabilized liposomes and compared the efficiencies of different chemical coupling techniques for attaching antibodies to the surface of sterically stabilized liposomes. Their results indicated that the attachment of antibody molecules to the tip of the PEG polymer is more effective than attachment directly on the surface of the lipsome which results in steric hindrance to the antibody's binding properties. Further, they surmise that of the coupling methods that they evaluated like (maleimidophenyl)butyroyl)dioleoyl-phosphatidylethanolamine (MPB-DOPE), (pyridyldithio)propionoyldioleoylphosphatidylethanolamine (PDP-DOPE), pyridylditiopropionoylamino (PDP)-PEG-DSPE and hydrazide (Hz)-PEG-DSPE, it was the (PDP)-PEG-DSPE which most closely approximated the ideal requirements of a targeted sterically stabilized preparation (Hansen *et al.*, 1995). Torchilin et al developed a simple and rapid method for attaching a variety of ligands containing primary amino groups to the distal ends of PEG chains grafted onto liposomes using *p*-nitrophenylcarbonyl-PEG-1,2-dioleoyl-*sn*-glycero-3-phosphoethanolamine (pNP-PEG-DOPE). The reaction involves the formation of stable and non-toxic urethane (carbamate) with the primary amino groups on the ligands (Torchilin *et al.*, 2001). Yet another technique referred to as the 'post insertion technique' by the authors was developed by Ishida et al. It involved the transfer of ligand-coupled PEG molecules from micellar prepartions directly into pre-formed liposomes thereby decoupling the conjugation step from the liposome preparation allowing for a combinatorial synthesis of targeted nanoparticles (Ishida *et al.*, 1999). Further studies comparing the binding efficacy and cytotoxicity of targeted liposomes prepared by the post-insertion technique with those of

targeted liposomes prepared by conventional ligand conjugation techniques showed no significant differences between the formulations but the facileness associated with post-insertion technique clearly made it ideal for large scale preparations as well as for combinatorial approaches (Iden and Allen, 2001).

An approach similar to that of the post-insertion approach has been developed in our laboratory capitalizing on the unique structural and chemical properties of the landscape phage fusion coat protein. Phage coat protein is an integral membrane protein and when separated from the phage assembly tends to insert spontaneously into lipid bilayers (Sprujit *et al.*, 1989; Kiefer and Kuhn, 1999). We exploited this 'membranophilic' nature of the coat protein to insert streptavidin-specific peptides fused to the N-terminus of the phage coat protein into liposomes. The resulting liposomes were then tested for streptavidin specificity in a functional test using streptavidin-conjugated colloidal gold particles, which demonstrated that the modified liposomes acquire streptavidin-targeting properties by virtue of the incorporated fusion proteins (Jayanna *et al.*, 2009).

Following the proof of concept studies using the streptavidin model system, we used landscape phage libraries to select for landscape phage probes for PC3 prostate carcinoma cells (Brigati *et al.*, 2008). Fusion phage coat proteins bearing the tumor-specific peptides were then harvested from phage particles and inserted into labeled liposomes using the technique described elsewhere (Figure 22) (Jayanna *et al.*, 2009). The orientation and efficiency of insertion of the coat protein units into liposomes were appraised using Western Blot. *In vitro* targeting studies using fluorescence microscopy and FACS was used to demonstrate the PC3-avidity of the targeted liposomes.

Furthermore, PC3-specific peptides were grafted onto commercial Doxil followed by characterization of the targeted preparation with regard to the size distribution and zeta potential. The impact of targeting was evaluated by comparing the cytotoxicites of different liposomal preparations against PC 3 cells *in vitro*.

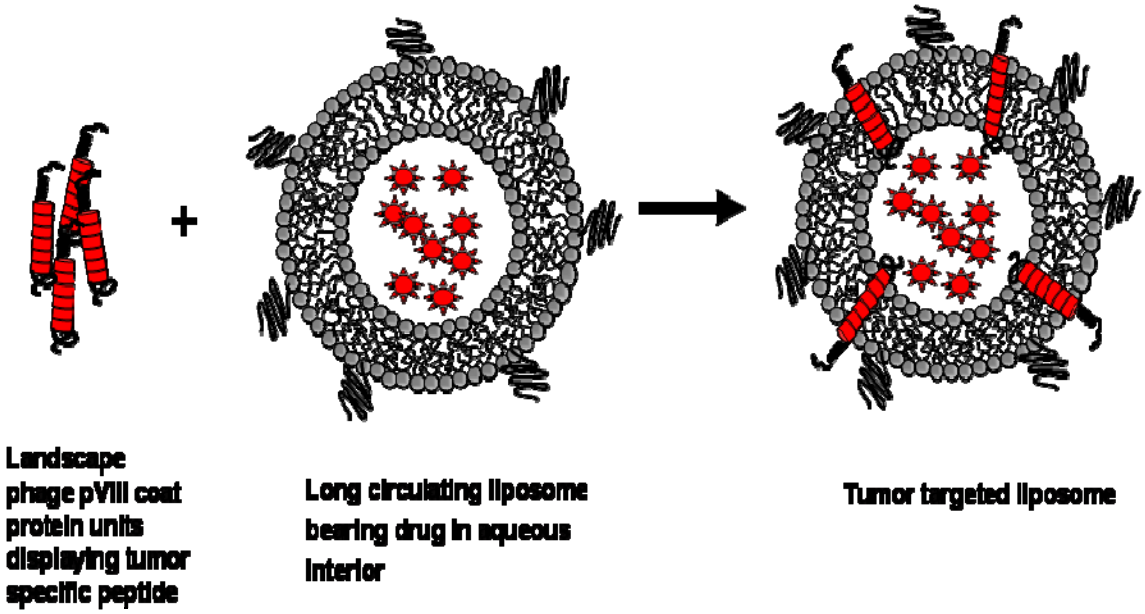

Figure 22: Drug-loaded liposome targeted by the pVIII protein created by exploiting the amphiphilic nature of the phage coat protein. The hydrophobic helix of the pVIII spans the lipid bilayer anchoring it whereas the N-terminal tumor-specific peptide is displayed on the surface of the carrier particles. The drug molecules are pictured as spiked circles.

3. Materials and Methods

3.1 Cells

Cell lines were obtained from the American Type Culture Collection (ATCC, Manassas, VA). The PC3 (CRL-1435) cells are derived from the bone metastasis of grade IV prostatic adenocarcinoma. HEK293 (CRL-1573) cells derived from a fetal kidneys were used as controls in microscopy and fluorescence studies. Cells were grown as recommended by ATCC and incubated at 37°C, 5% CO_2.

3.2 Isolation and Purification of phage fusion protein from PC3-specific phage probes

The selection of phage probes for PC3 cells has been previously described by us (Brigati *et al.*, 2008). Two phage peptides, DVVYALSDD (cell-internalizing ligand designated hereafter as 9-8) and DTDSHVNL (cell-binding ligand designated hereafter as 8-3) demonstrating high specificity and selectivity for PC3 cells were identified for use in further experiments. The PC3-targeting phages were solubilized using the procedure outlined by Sprujit et al (Sprujit *et al.*, 1989). Briefly, 350 µL phage in 1× Tris buffered saline (~1mg/mL) was mixed with 700 µL of 120 mM sodium cholate in 10 mM Tris-HCl, 0.2 mM EDTA, and chloroform (2.5% v/v final concentration), pH 8.0. The suspension was incubated at 37°C overnight. The mixture was then applied to a sepharose 6B-CL (AmershamBiosciences, Uppsala, Sweden) column (1cm× 45 cm) and eluted with 10 mM sodium cholate in 10 mM Tris-HCl, 0.2 mM EDTA pH 8.0 to separate major coat protein from viral DNA and traces of bacterial proteins. The

chromatographic profile was monitored by Econo UV monitor (Bio-Rad, Hercules, CA); 5 mL fractions were collected and stored at 4°C. Concentration of protein in samples was determined spectrophotometrically based on the molar extinction coefficients predicted by the program Protean (DNASTAR Inc., Madison, WI). Phage coat protein from a phage bearing an urelated peptide, VPEGAFSS (streptavidin-specific designated hereafter as 7b1) as well as coat protein from the wild type phage vector (f8-5 designated hereafter as WT) was isolated to be used in the preparation of control liposomes.

3.3 Preparation of labeled liposomes

egg Phosphatidylcholine (ePC), 1,2-Dipalmitoyl-*sn*-Glycero-3-Phosphocholine, 1,2-Dipalmitoyl-*sn*-Glycero-3-(Phospho-*rac*-(1-glycerol)) (Sodium Salt) (DPPG), 1,2-Dioleoyl-3-Trimethylammonium-Propane (Chloride Salt) (DOTAP), 1,2-Distearoyl-*sn*-Glycero-3-Phosphoethanolamine-N-(Amino(Polyethylene Glycol2000) (Ammonium Salt) (PEG2000-PE), 1,2-Dimyristoyl-*sn*-Glycero-3-Phosphoethanolamine-N-(Lissamine Rhodamine B Sulfonyl) (Ammonium Salt) (Rho-PE), Cholesterol (98%) were obtained from Avanti Polar Lipids (Alabaster, AL). For preparation of liposomes the lipid film was obtained from a mixture of ePC, cholesterol, DPPG, DOTAP, PEG2000-PE and Rho-PE in chloroform in the molar ratio (44:30:20:2:3:1). The chloroform was evaporated on a Brinkmann Buchi R-220RW Rotary Evaporator. The film was hydrated with an appropriate volume of 1x PBS. The crude liposome dispersion was then extruded 20 times through polycarbonate filters (pore size 100 nm) by using an Avanti Mini-Extruder (Avanti Polar Lipids, Alabaster, AL). Size and size distribution were measured by the dynamic light scattering using a Coulter N4 MD submicron Particle analyzer

(Beckman Coulter, Inc., Fullerton, CA). Zeta potentials of the liposomal preparations were determined using 90 PLUS particle size analyzer with Zeta PALS system (Brookehaven Corp., Holtsville, NY). Following extrusion, the liposomes were stored at 4°C until further experimental manipulation.

3.4 Preparation of phage fusion protein-targeted labeled liposomes

Labeled liposomes were grafted with PC3-specific phage fusion proteins by mixing the liposomes with appropriate phage fusion protein solution containing 10 mM sodium cholate in 10 mM Tris-HCl, 0.2 mM EDTA pH 8.0 (1% of lipids w/w). The concentration of sodium cholate was increased to 15 mM before incubating the mixture overnight at 37°C. Following the incubation, the sodium cholate in the formulation was removed by gradient dialysis steps in 10 mM, 5 mM and finally 1x PBS solutions. All dialysis steps were done in a volume of 1 L. Liposomes will henceforth be designated based on the grafted phage peptide.

3.5 Targeting of PC3-specific liposomes

PC3 cells and HEK293 cells were grown to subconfluence in 25 cm^2 cell culture flasks, collected by trypsinization and counted. Equal numbers of each line were then re-suspended in 1 ml of GIBCO™ Improved MEM Zn++ Option (Richter's Modification) liquid (Invitrogen, Carlsbad, CA). CellTracker Green CMFDA (5-chloromethylfluorescein diacetate, Molecular Probes, Carlsbad, CA) was then used to stain HEK293 cells using a 1:100 dilution of CellTracker Green CMFDA stock in sterile clear 1× Hanks and then using 1 µl of diluted dye per 1×10^6 cells for 15 min at 37 °C.

The cell suspension was pelleted by centrifugation, resuspended in Improved MEM and incubated for 15 min followed by centrifugation. The pellet was washed 3 times with Improved MEM. Following the labeling, equal numbers of PC3 cells and labeled HEK293 cells were mixed together. The cell mixtures in different tubes were then treated with either PC3-specific liposomes or different control liposomes for 90 min at 37°C. The cells were then washed twice in Improved MEM followed by reconstitution in 500 µl of the same media. The preparations were then used for fluorescence microscopy as well as flow cytometry.

For microscopy, aliquots of the cell mixtures were applied onto microscopic slides (Fisher, Pittsburgh, PA), covered with coverslips (Fisher, Pittsburgh, PA) and visualized with the Cytoviva® microscope system (Cytoviva Inc., Auburn, AL) using FITC, Texas Red and triple band pass (for DAPI, FITC and Texas Red) filters. Images were captured using the DAGE® software.

For flow cytometry, the samples were further filtered through a 50 µm CellTrics filter (Partec GmbH, Germany) before being analyzed on a MoFlo flow cytometer in the green (530 ± 20 nm) and red (700 ± 15 nm) channels. The data was analyzed using Summit 4.3 software (Dako, Carpinteria, CA). The data derived from three separate experiments was analyzed using ANOVA and significance was demonstrated by pair-wise comparisons of means using Tukey's HSD test.

3.6 Preparation of phage fusion protein-targeted Doxil

Doxil was purchased from ORTHO BIOTECH (Bedford, OH). Doxil liposomes were grafted with PC3-specific phage fusion proteins or with control phage fusion proteins in a procedure similar to that outlined for the preparation of targeted labeled liposomes above. Size and size distribution were measured by the dynamic light scattering using a Coulter N4 MD submicron Particle analyzer (Beckman Coulter, Inc., Fullerton, CA). Zeta potentials of the liposomal preparations were determined using 90 PLUS particle size analyzer with Zeta PALS system (Brookehaven Corp., Holtsville, NY). Doxil-entrapped doxorubicin was determined by monitoring absorbance at 485 nm using a Tecan SpectraFluor Plus plate reader (Tecan Systems, Inc., San Jose, CA) after treating the samples with 1% Triton-100. The preparations will henceforth be designated based on the grafted phage peptide.

3.7 Analysis of phage fusion protein in liposomal preparations by western blot

Liposome preparations were treated with 50 µg/ml of proteinase K (Sigma, St. Louis, MO) solution in de-ionized water for 1 h at room temperature. The reaction was stopped by the addition of phenylmethanesulfonyl fluoride (PMSF, final concentration 5 mM) (Sigma, St. Louis, MO). Samples were then mixed with an equal volume of Tricine sample buffer (8% sodium dodecyl sulfate, 24% glycerol, 0.1M Tris pH 6.8, 4% 2-mercaptoethanol, 0.01% Brilliant blue G, 2x) (Jule Inc., Milford, Connecticut) and heated at 95ºC for 40 minutes. 10 µl of the denatured samples were loaded onto 16% Non-gradient Tris-Tricine gel (Jule Inc., Milford, Connecticut). Electrophoresis was carried

out for 30 min at 100V. Proteins in the gel were transferred to an Immobilin-P PVDF membrane (Millipore, Billerica, Massachusetts). The resulting blots were probed with anti-fd IgG (0.594 ng/ml) for detection of N-terminus of peptide or affinity purified anti-pVIII C terminus IgG antibody (3.6 ng/ml) (SigmaGenosys, TX) for C-terminus detection followed by incubation with biotinylated-SP-conjugated Affinitipure goat antirabbit IgG (Jackson Immunoresearch, Westgrove, PA) and subsequently with NeutraAvidin-horseradish peroxidase (HRP) (Pierce, Rockford, Illinois) and were visualized using chemiluminescent substrate solution (Pierce).

3.8 Cytotoxicity Assays

The cytotoxicity of various preparations of the liposomal doxorubicin against PC3 cells was studied using a ready-to-use CellTiter 96® Aqeous One solution of MTS (Promega, Madison, WI) following the protocol suggested by the manufacturer. Liposomal formulations with doxorubicin concentration of up to 200 µg/ml dispersed in cell culture media were added to PC3 cells grown in 96-well cell culture plates to about 60% confluence in three replicates and incubated at 37°C and 5% CO_2 for 48 h. Following the incubation, the cells were washed five times with the cell culture media and treated with 20 µl of CellTiter 96® Aqeous One solution in 80 µl of cell culture media and incubated further at 37°C and 5% CO_2 for 1-2 h. The cell survival rate was estimated by measuring the absorbance of the MTS degradation product at 492 nm using the Tecan SpectraFluor Plus plate reader (Tecan Systems, Inc., San Jose, CA). The data was analyzed using ANOVA and significance was demonstrated by pair-wise comparisons of the means using Tukey's HSD test.

4. Results

We had earlier demonstrated the feasibility of using target-specific phage fusion protein as a navigating module of liposomes (Jayanna *et al.*, 2009). The success of this approach made us expand the proof of concept studies and use it for the preparation of tumor-specific liposomes. Using standard phage display protocols already described (Brigati *et al.*, 2008) we were able to identify highly selective and specific phage probes for PC3 prostate carcinoma cells from landscape phage libraries. The phage coat protein units from these probes with the N-terminally attached target-specific peptides were isolated and purified before being incorporated into Rhodamine-labeled liposomes as well as commercial Doxil®. The addition of the targeting module to liposomes enabled their successful association with their target PC3 cells as well resulted in a higher cytotoxic effect *in vitro* against PC3 cells.

4.1 Preparation and targeting of Rhodamine-labeled PC3-specific liposomes

The tenet underlying the preparation of liposomes targeted with phage fusion protein is the creation of a detergent environment conducive for the transfer of phage coat protein from detergent micelles into the lipid bilayers available. We adopted a 15 mM cholate solution to achieve this objective. Once the coat protein unit is stabilized in the lipid bilayer, the cholate is gradually removed from the mixture to further stabilize the liposomes. Rhodamine-labeled liposomes navigating to PC3 prostate carcinoma cells were prepared via the incorporation of PC3-specific phage fusion proteins using this

technique. The PC3-specific peptides had been previously isolated using standard phage display protocols in our laboratory and their specificity and selectivity evaluated (Brigati *et al.*, 2008). Liposomes modified with an unrelated phage fusion protein (VPEGAFSS, streptavidin-specific) as well as with coat protein from wild type vector phage (f8-5) were used as controls. Surface grafting with the phage coat protein did not significantly affect architecture of the liposomes as indicated by the comparative size distribution and zeta potential data for unmodified and modified preparations (Figure 23). The presence and topography of the PC3-specific phage coat proteins in the liposomes was determined by western blotting and representative results from two preparations are presented in Figure 24. With the antibody specific for the N-terminus of the phage coat protein, we observe a dramatic decrease in the signal after treatment with Proteinase K implying that the structurally mobile N-terminus is exposed at the liposomal surface. However, a similar observation with the antibody specific for the C-terminus implies that the C-terminus is also exposed leading us to conjecture that the coat protein more often associates with the liposomal bilayer in the interfacial region rather than exhibit complete penetration. Similar results were obtained when probing the topology of the coat protein in phage fusion protein modified Doxil.

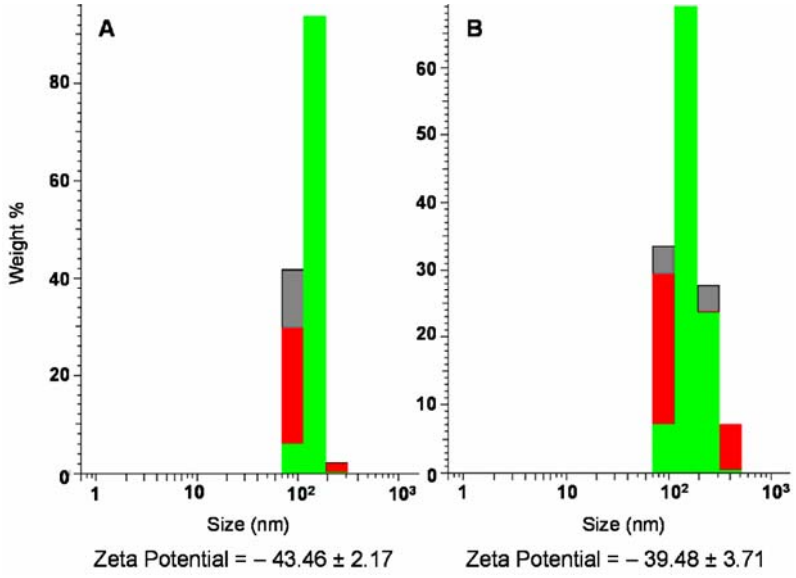

Figure 23: Representative data for the mean size, size distribution and zeta potentials of phage fusion protein-modified liposomes (A) and non-modified liposomes (B).

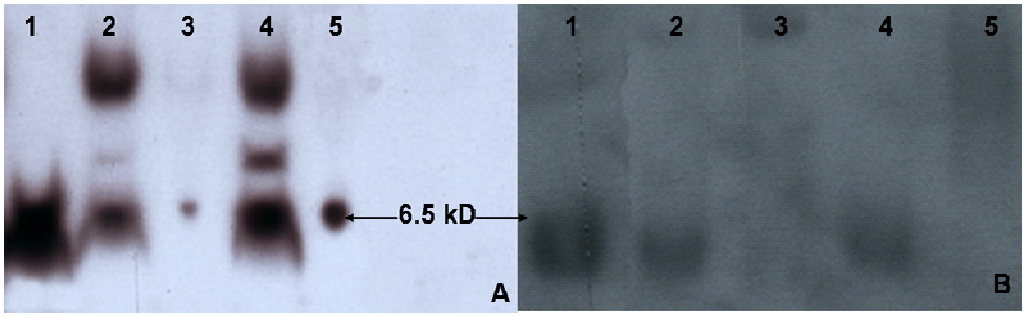

Figure 24: Western blot analysis of phage fusion protein-modified liposomal preparations to determine presence and topology of phage fusion protein. Liposomal preparations were treated with proteinase K and then probed with antibodies specific for either N-terminus (A) or C-terminus (B) of the phage coat protein. Liposomal association does not provide protection from proteolytic degradation to either the N or C termini of the phage coat

protein. Lane 1 – phage coat protein control (~6.5 kD), lane 2 – 8-3 liposomal preparation untreated with proteinase K, lane 3 - 8-3 liposomal preparation treated with proteinase K, lane 4 – 9-8 liposomal preparation untreated with proteinase K, lane 5 – 9-8 liposomal preparation treated with proteinase K.

The targeting efficiency of such PC3-specific liposomes was then evaluated based on their preferential association with PC3 cells in a mixture of target and control cells, conditions approaching the *in vivo* tableau. The control HEK293 cells, representative of a non-cancer cell line, were labeled with a vital dye, CellTracker Green CMFDA to allow for their visualization in microscopy as well separation as a discrete population in flow cytometry whereas the target cells were unlabeled. The principle behind this selective labeling was that only a specific labeling of PC3 cells by the targeted liposomes would result in the visualization and identification of PC3 cells. The results of the fluorescence microscopy are presented in Figure 25. The figures represent the same field of observation under three different filters. Under the FITC filter, we are able to see only the control HEK293 cells stained green with the vital dye, whereas the same field under the Texas Red filter allowed us to envisage the cells stained as a result of liposome binding. A comparison between these two renderings of the same image allows one to distinguish between the target PC3 cells and the control HEK293 cells. Targeted liposomes show an increased avidity for PC3 cells as substantiated by the intense staining of the surface of the PC3 cells. Non-specific staining of control cells is observed but is relatively dim and can be attributed to the affinity of liposomes to cell membranes. The last panel (Figure 4C) used a triple band filter set for DAPI, FITC and Texas Red and thus allows a

visualization of both cell types creating a synoptic image to demonstrate the liposome steering potential of the PC3-specific phage fusion protein.

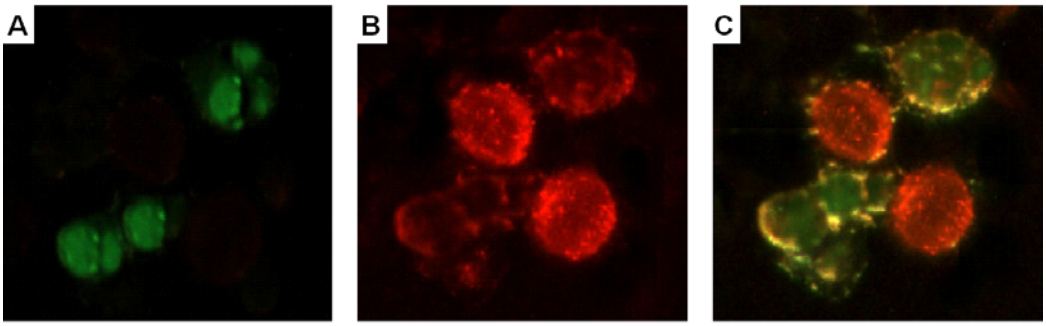

Figure 25: Cancer cell specific association of PC3-targeted Rhodamine-labeled liposomes. Fluorescent microscopy of a mixture of unlabeled target PC3 cells and green-labeled control HEK293 cells treated with PC3-specific Rhodamine-labeled liposomes. Selective association of red liposomes with PC3 cells enables their visualization under relevant filters. Panels represent the same field of observation under different filters; A – Image observed with FITC filter, B – Image observed with Texas Red filter, C – Image observed with a triple band pass filter.

In flow cytometry, the mixture of cells prior to liposomal treatment were resolved into two distinct populations based on the fluorescence intensity in the green channel (y-axis of the depicted scatter plots, Figure 26A), one consisting of labeled control cells (region R1, gated green) and the other unlabeled target cells (region R3, gated grey). Treatment with red Rhodamine-labeled liposomes resulted in the creation of two new populations based on the fluorescence intensity in the red channel (x-axis of the depicted scatter plots, Figure 26B), liposome-labeled PC3 cells (region R4, gated red) and

liposome-labeled HEK293 cells (region R2, gated purple). A predominant shift of the target PC3 cells along the red channel was observed after treatment with PC3-specific liposomes but was not detected with the other control liposomal formulations (Figure 26C, 26D, 26E) indicating a specific targeting afforded by the PC3-specific phage fusion protein adorning the liposomal surface.

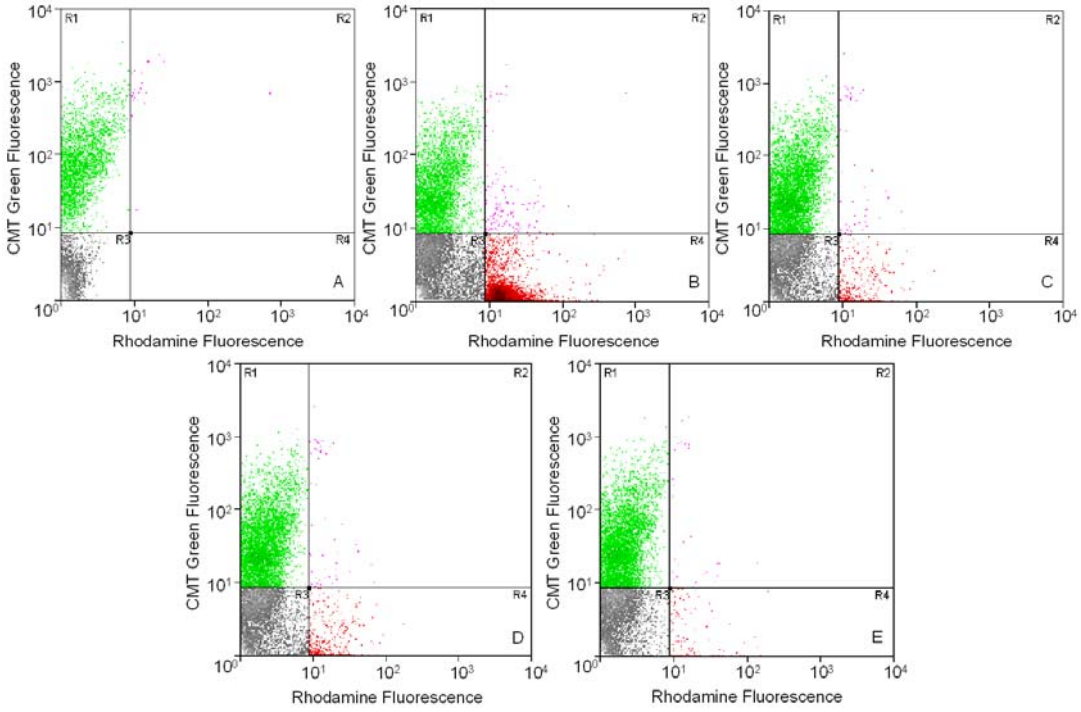

Figure 26: Cancer cell specific association of PC3-targeted Rhodamine-labeled liposomes. Flow cytometric analysis of a mixture of unlabeled target PC3 cells and green-labeled control HEK293 cells without any liposomal treatment (Panel A) differentiated into two distinct populations, based on the fluorescence intensity in the green channel (y-axis), one consisting of labeled control cells (region R1, gated green) and the other unlabeled target cells (region R3, gated grey). Treatment with red Rhodamine-labeled liposomes resulted in the creation of two new populations based on

the fluorescence intensity in the red channel (x-axis), liposome-labeled PC3 cells (region R4, gated red) and liposome-labeled HEK293 cells (region R2, gated purple). A predominant shift of the target PC3 cells along the red channel was observed after treatment with PC3-specific liposomes (Panel B) but was not detected with the other control liposomal formulations (Liposomes targeted with unrelated phage peptide, 7b1, with coat protein from Wild type phage, WT or Untargeted liposomes (Panels C, D and E)) indicating a specific targeting afforded by the PC3-specific phage fusion protein adorning the liposomal surface.

The relative proportions of the target and control cells moving into the regions R4 and R2 after treatment with different liposomal preparations in three separate experiments were then used to obtain quantitative measures termed Targeting Index (TI) according to the following formula;

$$TI = \frac{\mathrm{R4}}{\mathrm{R3}+\mathrm{R4}} \Big/ \frac{\mathrm{R2}}{\mathrm{R1}+\mathrm{R2}}$$

Where,

TI – Targeting index

R4 – liposome labeled PC3 cells

R3+R4 – total number of PC3 cells

R2 – liposome labeled HEK293 cells

R1+R2 – total number of HEK293 cells

The results of this analysis are presented in Figure 27. Liposomes targeted with cell-specific peptide showed a significant preference to associate with their cognate target cells over control cells ($p<0.05$).

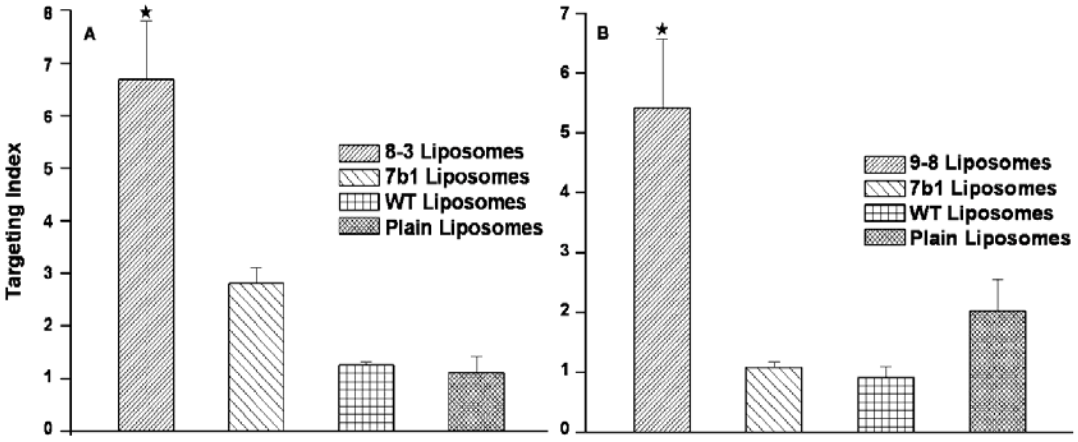

Figure 27: Targeting index of different liposomal preparations. Flow cytometry data (cell counts in a region) was analyzed as outlined in the results to obtain a relative measure of the cell targeting propensities of liposomal preparations. Star denotes significance at $p<0.05$ using one-way ANOVA with Tukey's honestly significant difference *posthoc* test

4.2 Preparation of doxorubicin-loaded phage fusion protein-targeted liposomes

Based on the aforementioned procedure, we were able to graft commercial Doxil® with a variety of phage fusion proteins. Two PC3-targeted liposomal preparations, one decorated with a PC3-binding peptide (DTDSHVNL) and the other decorated with a PC3-internalizing peptide (DVVYALSDD) were prepared. Doxil® modified with phage fusion peptides specific for streptavidin (VPEGAFSS) as well phage

coat protein from the wild type vector phage were also prepared as controls. Surface grafting with the phage coat protein did not significantly affect architecture of the liposomes as indicated by the comparative size distribution and zeta potential data. The presence of phage coat proteins in the liposomal preparations were determined by western blotting as described before. The doxorubicin content of the liposomes decreased during the procedure of ligand incorporation but the amount retained in the preparations allowed for a comparative estimation of their cytotoxic potential.

4.3 Cytotoxicity of doxorubicin-loaded phage fusion protein-targeted liposomes.

Antibody-targeted liposomal preparations have been shown to have a beneficial effect on the cytotoxicity of cytotoxic drugs with a dramatic reduction in IC50 values (Elbayoumi and Torchilin, 2007). We postulated that targeting with tumor-specific peptides would produce similar results. Accordingly, various liposomal formulations with equivalent concentrations of doxorubicin up to 200 μg/ml were evaluated in an *in vitro* cytotoxicity assay. Figure 7A and 8A present the results of these assays. After 48 h of incubation, Doxil targeted with PC3-specific peptides demonstrated higher toxicities in comparison to the control liposomes with a dose-dependent pattern. Comparison of cytotoxicities at 200 μg/ml concentration of doxorubicin confirmed that the survival percentage was significantly lower with PC3-targeted therapeutic liposomes ($p<0.05$).

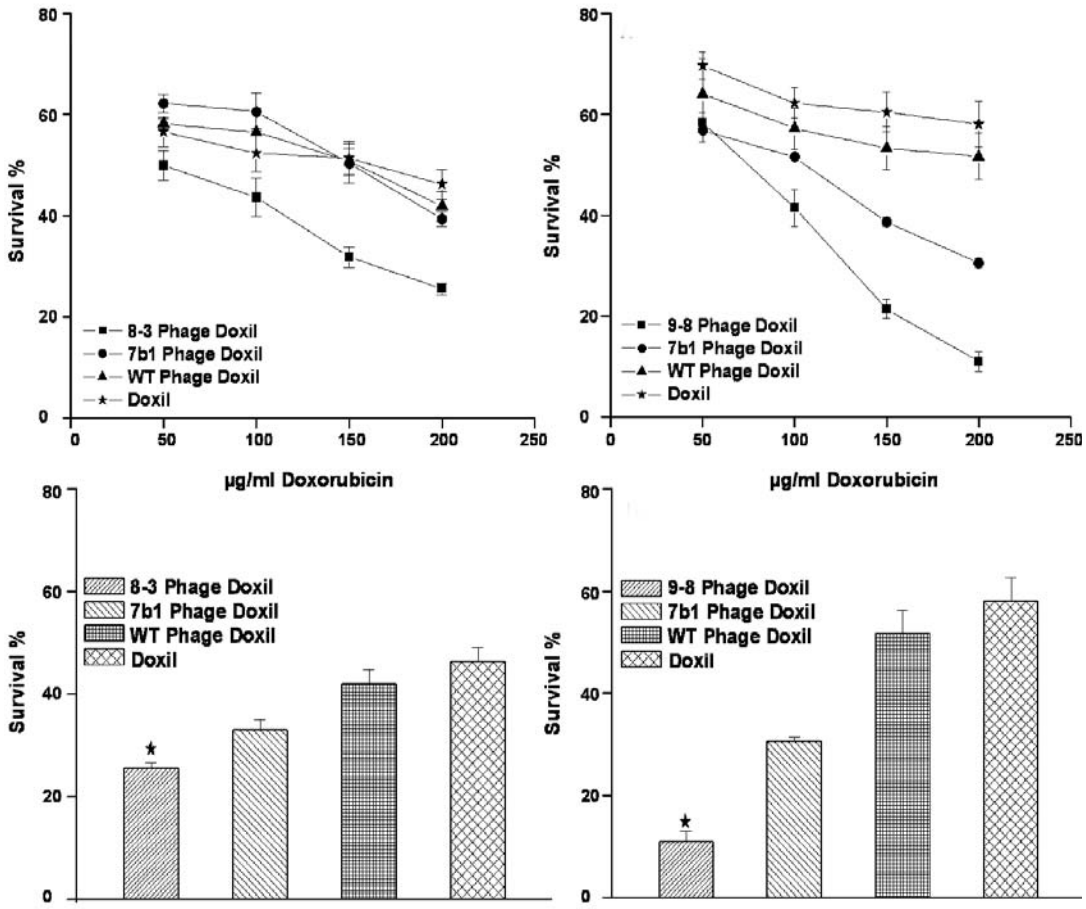

Figure 28: *In vitro* cytotoxicity results of various doxorubicin-loaded liposomal formulations. Commercial Doxil® was grafted with PC3-specific phage fusion proteins (9-8 or 8-3) or control phage fusion proteins (7b1, an unrelated peptide or coat protein from wild type phage, WT) and incubated with PC3 cells for 48 h. The cytotoxicity of each preparation was expressed as survival % with untreated cells being considered as 100%. Upper panels shows the cytotoxicity of the different targeted preparations over a range of concentrations of doxorubicin whereas lower panels compares survival of cells at a fixed concentration of 200 µg/ml of doxorubicin to demonstrate the significant improvement in cytotoxicity achieved with targeting. Star denotes significance at $p<0.05$ using one-way ANOVA with Tukey's honestly significant difference *posthoc* test

5. Discussion

Prostate cancer remains the most common neoplastic disease in the western hemisphere among men and is the second leading cause of mortality. Adoption of widespread screening for Prostate Specific Antigen levels has created a spike in the prevalence of the malignancies as also enabled the detection of earlier and more tractable stages of the disease. Apart from active surveillance, the most common therapeutic options available include radical prostatectomy and androgen ablation. Despite this treatment, approximately 20% of cases proceed to an advanced stage where in the pathology stands independent of its source and becomes oblivious to hormonal manipulation (Chowdhury *et al.*, 2007). This stage, described as Hormone Refractory Prostate Cancer (HRPC), was characterized by a lack of treatment options except those directed towards amelioration of pain up until the groundbreaking results of two multicenter phase III trials that led to the approval of docetaxel as a standard treatment for HRPC (Pomerantz and Kantoff, 2007). However, side effects arising from the excipient, Tween 80, created a need for alternative methods to deliver this drug as well as a need to revisit the utility of targeting other available drugs.

Studies involving the active targeting of doxorubicin-loaded liposomes and Doxil, both *in vitro* and *in vivo* have provided encouraging results. Banerjee et al demonstrated the feasibility of using small molecular weight targeting ligands like anisamide to target liposomes to prostate cancer cell line DU-145 *in vitro* as well as anti-tumor activity of targeted liposomes *in vivo* in a mouse xenograft model of DU-145 (Banerjee *et al.*, 2004). The grafting of nucleosome-specific monoclonal antibody 2C5 (mAB 2C5) onto the

surface of Doxil resulted in enhanced cytotoxicity against a variety of cancer cells in comparison with untargeted Doxil. There was a significant lowering of the IC_{50} values (~8 fold) indicating a lowered toxicity profile with targeted formulations. Furthermore, the targeting antibody allowed for increased internalization of liposomes which may be critical in drug resistant tumors due to the bypass of drug efflux pumps (Elbayoumi and Torchilin, 2007). In an extension of these studies, the *in vivo* tumor accumulation of ^{111}In-labeled 2C5 targeted liposomes in various mouse models of human tumor xenografts was examined. Targeted liposomes showed a preferential accumulation in the tumors over untargeted liposomes (Elbayoumi *et al.*, 2007).Further, the *in vivo* therapeutic efficiency of 2C5 – modified Doxil was evaluated in a PC3 xenograft mouse model. It was observed that treatment with targeted liposomes resulted in lower tumor volumes and tumor weights as compared with non-modified Doxil (ElBayoumi and Torchilin, 2009). Taken together, these results indicate that targeting functions to increase the therapeutic efficiency of drugs at the same time reducing the toxicities associated with them. Thus, targeting may provide the reprieve required to overcome the hurdles facing the use of Doxil in HRPC. In addition, the potential use of targeted Doxil as part of a combination therapy also has to be considered. For example it was shown that doxorubicin amplified the apoptotic properties of Apo2L/TRAIL against PC3 xenograft models in nude mice (El-Zawahry *et al.*, 2005). Thus, we decided to combine two objectives of research within a single module; one, to evaluate the potential of PC3-specific phage fusion protein as a liposomal navigating ligand using commercial Doxil® as a model therapeutic liposome and two, to evaluate if targeting would result in a higher cytotoxicity of doxorubicin *in vitro*.

The targeting studies using Rhodamine-labeled liposomes were able to demonstrate the ability of targeted liposomes to associate with their cognate target cells amidst a mixture of cells, a measure of their selectivity towards PC3 cells. This assay recreated an *in vivo* scenario in which liposomes must be able to distinguish between normal and neoplastic cells based on the molecular differences identified by the targeting peptide grafted on their surface. Flow cytograms testing the association of liposomes modifed with an unrelated phage peptide showed non-significant non-specific association of liposomes with the target cells though the association of liposomes modified with wild type phage coat protein as well as non-targeted liposomes was negligible. These associations may arise due to the natural propensity of liposomes to associate with lipid membranes or due to non-specific binding abilities conferred onto liposomes due to the modification with phage coat proteins.

The association of phage coat protein with liposomes was probed using western blots. Treatment with proteinase K resulted in an elimination of signals of both N-termini and C-termini of the coat proteins imputing the presence of both these termini on the surface of the liposomes. This scenario is possible as according to Stopar et al (Stopar *et al.*, 2006), a protein can associate strongly with a lipid bilayer in three basic modes; through transmembrane anchoring domains or through amphiphilic interfacial domains or through lipidic anchors attached to itself. Thus, the targeting peptide does not, as predicted and expected by us penetrate through the liposomal membrane but probably associates with it in the interfacial region via the amphiphilic N-terminal helix whereas the hydrophobic domain may partially dip into the hydrocarbon core of the bilayer. The C-terminus with positively charged amino acids may form strong electrostatic bonds with

the negatively charged lipid head groups providing further stability but simultaneously precluding its transfer across the hydrocarbon core. This is in accordance with the experiments conducted by Soekarjo et al in which they demonstrated that M13 procoat and coat protein insertion into pre-formed lipid vesicles does not involve transmembrane translocation of the protein but a more likely insertion into the interfacial region (Soekarjo *et al.*, 1996). Further, studies by Kiefer and Kuhn with pf3 coat protein support such a situation as they demonstrated that the transfer of positively charged amino acids across the hydrocarbon core represents an enormous energy sink and cannot be achieved with the available electrophoretic, hydrophobic and electrostatic forces associated with the coat protein unit (Kiefer and Kuhn, 1999). Although, these results do not concur with our proposed mechanism as depicted in Figure 1, evidence of the target-specific homing of the targeted liposomes vindicates our approach for the use of phage fusion protein as a navigating ligand for liposomes.

This view was further sustained by the results of the cytotoxicity assays which showed that target-specific liposomes evinced higher toxicities in PC3 cell cultures than the control liposomes at equivalent concentrations of doxorubicin. The relatively higher cytotoxicity of the liposomes modified with an unrelated phage fusion protein, 7b1, followed the results of the targeting assays in which labeled liposomes modified with the same peptide showed a higher proclivity to associate with target cells than other control liposomes. This observation may be due to a non-specific association of these control liposomes with the cells and creates a need for fine tuning our approach to the production of targeted liposomes. In light of aforementioned studies using targeted Doxil, our results provide additional support for the applicability of targeted liposomes in mitigating

untoward side effects of cytotoxic chemotherapeutics in clinically significant tumor conditions like HRPC.

In synopsis, targeting of drugs/drug carriers has been shown to have definite therapeutic benefits. A limiting factor in the development of targeted liposomal therapeutics has been the chemical conjugation reactions required to append targeting ligands to liposomes. Our approach exploiting the physico-chemical properties of bacteriophage coat protein completely circumvents any chemical modification technique as targeted preparations are obtained by the simple expedient of incubating liposomes and the target-specific phage fusion protein. An additional advantage is the rapid retrieval of target-specific phage probes using high throughput screening with phage display libraries. Thus, targeted liposomal preparations with different drugs for different tumors as well as variants of the same tumor can be rapidly obtained in a combinatorial manner which we hope would provide a modicum of simplicity to the complications associated with the treatment of malignancies.

CHAPTER 6

CONCLUSIONS

Nobel laureate Richard Feynman's speculation that manipulation at the level of atoms and molecules could bring about dramatic changes in our understanding of science and technology was realized with the tremendous progress in molecular visualization and analysis techniques, the outcome of which was the genesis of nanotechnology. The advent and establishment of nanotechnology as an accepted area of technology has created revolutionary changes to approaches adopted to solve problems in diverse domains of human interest.

One such discipline has been that of nanomedicine which has benefited tremendously from the evolution of nanotechnology particularly in the context of tumor chemotherapies. Anti-cancer chemotherapy is blighted by the impartial cytotoxicity of available drugs giving rise to unwanted side effects. Thus identification of the molecular singularity of tumor cells using nanotechnological platforms and further harnessing such differences can achieve a reprieve from non-selective toxicity. Random display of peptide probes on phage particles represents an attractive example of such a platform and serves as a molecular tool to elucidate molecular signatures of different cells. The unique physico-chemical and biological characteristics of different phage particles as well as distinctive processes involved in their life cycle have expanded their utility beyond being

simple scaffolds and genetic carriers of ligands giving rise to the field of phage nanobiotechnology.

Phage nanobiotechnology involves exploiting phage characteristics for orchestrating their use in nanomaterial synthesis and nanodevice fabrication. For example, the extremely precise self assemblage properties of phage particles were used to create tissue-regenerating matrices for directional alignment and growth of neural progenitor cells (Merzlyak *et al.*, 2009). We in turn capitalized on the unique structural properties of phage major coat protein pVIII to recast them as potential targeting ligands for liposomal therapeutics. Our premise was based on the intrinsic membrane avidity of the phage coat protein which allows it to associate with liposomal bilayers. The presence of a target-specific peptide on the N-termini of such liposome-associated coat protein units enables them to steer these liposomes to a cognate target molecule. We hypothesized that such a targeting to cancer cells would improve the therapeutic profile of anti-cancer drugs. Thus, we were able to use landscape phage libraries not only as a source of target-specific probes but also as a source of made-to-order liposomal ligands.

To demonstrate the feasibility of our postulate we successfully used two different landscape phage libraries to isolate phage probes for PC3 cells. The justification behind the use of two libraries lay in our observations that different libraries yield different families of probes as the repertoire of displayed peptides is different in each landscape library and the results of the selection procedure reiterated this concept as we were able to identify diverse phage probes with unique properties with the different libraries. Phage major coat protein units bearing the PC3-specific peptides were then isolated from the PC3-specific phage probes. The peptide units were then grafted onto liposomal surface

by an extremely simple process of co-incubation of pre-formed liposomes and the coat protein solution. The successful association of phage coat protein with the liposomes was demonstrated by western blots. An interesting and critical observation in Western blots designed to probe the topology of the coat protein in liposomes was that the coat protein units were not protected in any way by the liposomal bilayers imputing a lack of insertion of the coat proteins into the lipids which is not surprising given the thermodynamics involved in such an insertion. Despite the deviation from the design proposed in our approach, the results from our targeting studies showed the presence of a functional navigating ligand at the surface of liposomes which is further bolstered by encouraging results from cytotoxicity studies. No doubt the procedure requires further optimization but our results serve to sustain the efforts directed towards future studies. Another area which merits further attention would be techniques for the successful and stable incorporation of therapeutic anti-cancer drugs at requisite concentrations in the targeted liposomes.

Clinical entities like hormone refractory prostate cancer lacking therapeutic avenues requires either novel therapeutic discoveries or the reinvention of existing drug modalities to accommodate their clinical use in HRPC as was the case for this project. The results of this project create a strong basis for the foray of landscape phage technology into the field of targeted drug carriers for prostate tumors. Furthermore, enhanced therapeutic index with decreased side-effects that is observed with targeting would encourage an earlier deployment of chemotherapy improving patient quality of life. The phage technology may be adapted in a short period of time for developing phage-probes on a tumor-specific and patient-specific basis. The specific phage clone can

then used as a navigating ligand for a variety of drug-loaded liposomal or micellar preparations laying the groundwork for the advent of personalized anti-cancer therapy.

BIBLIOGRAPHY

ACS. 2008. Cancer facts and figures. American Cancer Society, Atlanta.

Adams, G.P., and Schier, R. (1999) *Journal of Immunological Methods* **231**, 249-260.

Adams, G.P., Schier, R., McCall, A.M., Simmons, H.H., Horak, E.M., Alpaugh, R.K., Marks, J.D., and Weiner, L.M. (2001) *Cancer Res* **61**, 4750-4755.

Aggarwal, S., Janssen, S., Wadkins, R.M., Harden, J.L., and Denmeade, S.R. (2005) *Biomaterials* **26**, 6077-6086.

Aina, O.H., Sroka, T.C., Chen, M.-L., and Lam, K.S. (2002a) *Peptide Science* **66**, 184-199.

Aina, O.H., Sroka, T.C., Chen, M.L., and Lam, K.S. (2002b) *Biopolymers* **66**, 184-199.

Allen, T.M., Brandeis, E., Hansen, C.B., Kao, G.Y., and Zalipsky, S. (1995) *Biochimica et Biophysica Acta (BBA) - Biomembranes* **1237**, 99-108.

Allen, T.M., and Chonn, A. (1987) *FEBS Letters* **223**, 42-46.

Allen, T.M., Hansen, C., and Rutledge, J. (1989) *Biochimica et Biophysica Acta (BBA) - Biomembranes* **981**, 27-35.

Arap, M.A. (2005) *Genetics and Molecular Biology* **28**, 1-9.

Arap, W., Haedicke, W., Bernasconi, M., Kain, R., Rajotte, D., Krajewski, S., Ellerby, H.M., Bredesen, D.E., Pasqualini, R., and Ruoslahti, E. (2002) *Proceedings of the National Academy of Sciences* **99**, 1527-1531.

Banerjee, R., Tyagi, P., Li, S., and Huang, L. (2004) *International Journal of Cancer* **112**, 693-700.

Barbas, C.F., Burton, D.R., Scott, J.K., and Silverman, G.J. (2001) *Phage display: a laboratory manual* Cold Spring Harbor Laboratory Press New York.

Bhandari, M.S., Crook, J., and Hussain, M. (2005) *Journal of Clinical Oncology* **23**, 8212.

Bill-Axelson, A., Holmberg, L., Ruutu, M., Haggman, M., Andersson, S.O., Bratell, S., Spangberg, A., Busch, C., Nordling, S., and Garmo, H. 2005. Radical prostatectomy versus watchful waiting in early prostate cancer, pp. 1977-1984.

Borghouts, C., Kunz, C., and Groner, B. (2005) *Journal of Peptide Science* **11**, 713-726.

Brawer, M.K. (2006) *Reviews in Urology* **8**, S35.

Brigati, J., Williams, D.D., Sorokulova, I.B., Nanduri, V., Chen, I.H., Turnbough, C.L., Jr., and Petrenko, V.A. (2004) *Clin Chem* **50**, 1899-1906.

Brigati, J.R., and Petrenko, V.A. (2005) *Anal Bioanal Chem* **382**, 1346-1350.

Brigati, J.R., Samoylova, T.I., Jayanna, P.K., and Petrenko, V.A. (2008) In Coligan J.E., D.B.M., Speicher D.W., Wingfield P.T. (eds), *Current Protocols in Protein Science*. John Wiley & Sons, Inc, New Jersey. pp. p.1-27.

Byar, D.P., and Corle, D.K. (1988) *NCI monographs: a publication of the National Cancer Institute*, 165.

Calais Da Silva, F.M., Calais Da Silva, F., Bono, A., Brausi, M., Whelan, P., Queimadelos, A., Portillo, J., Kirkali, Z., and Robertson, C. 2006. Phase III intermittent MAB vs continuous MAB, pp. 4513.

Caparon, M.H., Deciechi, P.A., Devine, C.S., Olins, P.O., and Lee, S.C. (1996) *Molecular Diversity* **1**, 241-246.

Carnazza, S., Gioffre, G., Felici, F., and Guglielmino, S. (2007) *Journal of Physics: Condensed Matter*, 395011.

Chamberlain, B.K., Nozaki, Y., Tanford, C., and Webster, R.E. (1978) *Biochim Biophys Acta* **510**, 18-37.

Chowdhury, S., Burbridge, S., and Harper, P.G. (2007) *International Journal of Clinical Practice* **61**, 2064-2070.

Collins, A.T., and Maitland, N.J. (2006) *European Journal of Cancer* **42**, 1213-1218.

Cortez-Retamozo, V., Backmann, N., Senter, P.D., Wernery, U., De Baetselier, P., Muyldermans, S., and Revets, H. (2004) *Cancer Res* **64**, 2853-2857.

Craig, R., and Li, S. (2006) *Mini Reviews in Medicinal Chemistry* **6**, 757-764.

Crawford, E.D., Eisenberger, M.A., McLeod, D.G., Spaulding, J.T., Benson, R., Dorr, F.A., Blumenstein, B.A., Davis, M.A., and Goodman, P.J. 1989. A controlled trial of leuprolide with and without flutamide in prostatic carcinoma, pp. 419-424.

Currin, R.T., Gores, G.J., Thurman, R.G., and Lemasters, J.J. (1991) *FASEB J.* **5**, 207-210.

D'Amico, A.V., Manola, J., Loffredo, M., Renshaw, A.A., DellaCroce, A., and Kantoff, P.W. 2004. 6-month androgen suppression plus radiation therapy vs radiation therapy alone for patients with clinically localized prostate cancer A randomized controlled trial, pp. 821-827. Am Med Assoc.

de Wit, R. (2008) *BJU international* **101**, 11-15.

Devlin, J.J., Panganiban, L.C., and Devlin, P.E. (1990) *Science* **249**, 404-406.

Dijkman, G.A., Janknegt, R.A., De Reijke, T.M., and Debruyne, F.M.J. (1997) *The Journal of urology* **158**, 160-163.

El-Zawahry, A., McKillop, J., and Voelkel-Johnson, C. (2005) *BMC Cancer* **5**, 2.

Elbayoumi, T.A., Pabba, S., Roby, A., and Torchilin, V.P. (2007) *Journal of Liposome Research* **17**, 1-14.

Elbayoumi, T.A., and Torchilin, V.P. (2007) *European Journal of Pharmaceutical Sciences* **32**, 159-168.

ElBayoumi, T.A., and Torchilin, V.P. (2009) *Clin. Cancer. Res.* **15**, 1973.

Ellerby, H.M., Arap, W., Ellerby, L.M., Kain, R., Andrusiak, R., Rio, G.D., Krajewski, S., Lombardo, C.R., Rao, R., Ruoslahti, E., et al. (1999) *Nat. Med.* **5**, 1032-1038.

Ellerby, H.M., Bredesen, D.E., Fujimora, S., and John, V. (2008) *J. Med. Chem.* **51**, 5887-5892.

Everts, M. (2005) *Drugs of the future* **30**, 1067-1076.

Fagbohun, O.A., Bedi, D., Jayanna, P.K., Deinnocentes, P., Bird, R.C., and Petrenko, V.A. 2008. Landscape phage probes for Breast cancer cells. In *NSTI Nanotech*, Boston.

Feldman, B.J., and Feldman, D. (2001) *Nature Reviews Cancer* **1**, 34-45.

Felici, F., Castagnoli, L., Musacchio, A., Jappelli, R., and Cesareni, G. (1991) *Journal of Molecular Biology* **222**, 301-310.

Fenske, D.B., Maurer, N., and Cullis, P.R. (2003) In Torchilin, V.P. et al. (eds), *Liposomes: A Practical Approach*. Oxford University Press, New York. pp. 173-180.

Ferrieu-Weisbuch, C., Michel, S., Collomb-Clerc, E., Pothion, C., Deléage, G., and Jolivet-Reynaud, C. (2006) *Journal of Molecular Recognition* **19**, 10-20.

Flynn, C.E., Lee, S.-W., Peelle, B.R., and Belcher, A.M. (2003) *Acta Materialia* **51**, 5867-5880.

Fodor, S.P., Dunker, A.K., Ng, Y.C., Carsten, D., and Williams, R.W. (1981) *Prog Clin Biol Res* **64**, 441-455.

Fujimori, K., Covell, D.G., Fletcher, J.E., and Weinstein, J.N. (1989) *Cancer Res* **49**, 5656-5663.

Gabizon, A., Shmeeda, H., Horowitz, A.T., and Zalipsky, S. (2004) *Advanced Drug Delivery Reviews* **56**, 1177-1192.

Gao, H., Ouyang, X., Banach-Petrosky, W.A., Shen, M.M., and Abate-Shen, C. (2006) *Cancer Research* **66**, 7929.

Garde, S.V., Forté, A.J., Ge, M., Lepekhin, E.A., Panchal, C.J., Rabbani, S.A., and Wu, J.J. (2007) *Anti-Cancer Drugs* **18**, 1189.

Gerber, D.E. (2008) *Am. Fam. Physician* **77**, 311.

Gerlag, D.M., Borges, E., Tak, P.P., Ellerby, H.M., Bredesen, D.E., Pasqualini, R., Ruoslahti, E., and Firestein, G.S. (2001) *ARTHRITIS RESEARCH* **3**, 357-361.

Giebel, L.B., Cass, R.T., Milligan, D.L., Young, D.C., Arze, R., and Johnson, C.R. (1995) *Biochemistry* **34**, 15430-15435.

Gill, S.C., and von Hippel, P.H. (1989) *Analytical Biochemistry* **182**, 319-326.

Goldstraw, M.A., and Kirby, R.S. (2006) *ANNALS-ROYAL COLLEGE OF SURGEONS OF ENGLAND* **88**, 439.

Goren, D., Horowitz, A.T., Tzemach, D., Tarshish, M., Zalipsky, S., and Gabizon, A. 2000. Nuclear Delivery of Doxorubicin via Folate-targeted Liposomes with Bypass of Multidrug-resistance Efflux Pump 1, pp. 1949-1957. AACR.

Greenwood, J., Willis, A.E., and Perham, R.N. (1991) *Journal of Molecular Biology* **220**, 821-827.

Griffiths, G.L., Mattes, M.J., Stein, R., Govindan, S.V., Horak, I.D., Hansen, H.J., and Goldenberg, D.M. 2003. Cure of SCID mice bearing human B-lymphoma xenografts by an anti-CD74 antibody-anthracycline drug conjugate, pp. 6567-6571. AACR.

Haigh, N.G., and Webster, R.E. (1998) *Journal of Molecular Biology* **279**, 19-29.

Haley, B., and Frenkel, E. (2008) *Urologic Oncology: Seminars and Original Investigations* **26**, 57-64.

Hansen, C.B., Kao, G.Y., Moase, E.H., Zalipsky, S., and Allen, T.M. (1995) *Biochimica et Biophysica Acta (BBA) - Biomembranes* **1239**, 133-144.

Harrison, D.C., Lemasters, J.J., and Herman, B. (1991) *Biochem Biophys Res Commun* **174**, 654-659.

Heidenreich, A., Sommer, F., Ohlmann, C.H., Schrader, A.J., Olbert, P., Goecke, J., and Engelmann, U.H. (2004) *Cancer* **101**.

Henke, E., Perk, J., Vider, J., de Candia, P., Chin, Y., Solit, D.B., Ponomarev, V., Cartegni, L., Manova, K., and Rosen, N. (2008) *Nature Biotechnology* **26**, 91.

Hofschneider, P.H. (1963) *Z. Naturforschg.* **18b**, 203-205.

Holig, P., Bach, M., Volkel, T., Nahde, T., Hoffmann, S., Muller, R., and Kontermann, R.E. (2004) *Protein Engineering, Design and Selection* **17**, 433-441.

Hong, F.D., and Clayman, G.L. (2000) *Cancer Res* **60**, 6551-6556.

Huang, S.K., Lee, K.D., Hong, K., Friend, D.S., and Papahadjopoulos, D. (1992) *Cancer Res* **52**, 5135-5143.

Huang, W., Beharry, Z., Zhang, Z., and Palzkill, T. (2003) *Protein Eng.* **16**, 853-860.

Hubert, A., Lyass, O., Pode, D., and Gabizon, A. (2000) *Anti-Cancer Drugs* **11**, 123.

Huggins, C., Stevens Jr, R.E., and Hodges, C.V. (1941) *Archives of surgery* **43**, 209.

Hughes, C., Murphy, A., Martin, C., Sheils, O., and O'Leary, J. (2005) *British Medical Journal* **58**, 673-684.

Hunter, G.J., Rowitch, D.H., and Perham, R.N. (1987) *Nature* **327**, 252-254.

Iannolo, G., Minenkova, O., Gonfloni, S., Castagnoli, L., and Cesareni, G. (1997) *Biological Chemistry* **378**, 517-521.

Iannolo, G., Minenkova, O., Petruzzelli, R., and Cesareni, G. (1995) *Journal of Molecular Biology* **248**, 835-844.

Iden, D.L., and Allen, T.M. (2001) *BBA-Biomembranes* **1513**, 207-216.

Ilyichev, A.A., Minenkova, O.O., Tatkov, S.I., Karpyshev, N.N., Eroshkin, A.M., Petrenko, V.A., and Sandakhchiev, L.S. (1989) *Doklady Biochemistry (ProcAcad Sci USSR) - EnglTr* **307**, 196-198.

Immordino, M.L., Brusa, P., Arpicco, S., Stella, B., Dosio, F., and Cattel, L. (2003) *Journal of Controlled Release* **91**, 417-429.

Immordino, M.L., Dosio, F., and Cattel, L. (2006) *Int J Nanomedicine* **1**, 297-315.

Ishida, T., Iden, D.L., and Allen, T.M. (1999) *FEBS Lett.* **460**, 129-133.

Ivanenkov, V.V., Felici, F., and Menon, A.G. (1999) *Biochimica et Biophysica Acta (BBA) - Molecular Cell Research* **1448**, 463-472.

Ivanenkov, V.V., and Menon, A.G. (2000) *Biochemical and Biophysical Research Communications* **276**, 251-257.

Iversen, P., Tveter, K., and Verenhorst, E. (1996) *Scandinavian journal of urology and nephrology* **30**, 93-98.

Iyer, A.K., Khaled, G., Fang, J., and Maeda, H. (2006) *Drug Discovery Today* **11**, 812-818.

Jain, R.K. (1990) *Cancer Res* **50**, 814-819.

Janknegt, R.A., Abbou, C.C., Bartoletti, R., Bernstein-Hahn, L., Bracken, B., Brisset, J.M., Calais da Silva, F., Chisholm, G., Crawford, E.D., and Debruyne, F.M.J. (1993) *The Journal of urology* **149**, 77-83.

Jayanna, P.K., Deinnocentes, P., Bird, R.C., and Petrenko, V.A. 2008. Landscape phage probes for PC3 prostate carcinoma cells. In *NSTI Nanotech*, Boston.

Jayanna, P.K., Torchilin, V.P., and Petrenko, V.A. (2009) *Nanomed. Nanotechnol. Biol. Med.* **5**, 83-89.

Johansson, S., Goldenberg, D.M., Griffiths, G.L., Wahren, B., and Hinkula, J. (2006) *AIDS* **20**, 1911.

Kaisary, A.V., Tyrrell, C.J., Beacock, C., Lunglmayr, G., and Debruyne, F. (1995) *European Urology* **28**, 215-222.

Kantoff, P.W., Halabi, S., Conaway, M., Picus, J., Kirshner, J., Hars, V., Trump, D., Winer, E.P., and Vogelzang, N.J. (1999) *Journal of Clinical Oncology* **17**, 2506.

Kassouf, W., Tanguay, S., and Aprikian, A.G. (2003) *The Journal of urology* **169**, 1742-1744.

Kay, B.K., Adey, N.B., He, Y.S., Manfredi, J.P., Mataragnon, A.H., and Fowlkes, D.M. (1993) *Gene* **128**, 59-65.

Kehoe, J.W., and Kay, B.K. (2005) *Chem. Rev.* **105**, 4056-4072.

Kelly, K.A., Setlur, S.R., Ross, R., Anbazhagan, R., Waterman, P., Rubin, M.A., and Weissleder, R. (2008) *Cancer Res* **68**, 2286-2291.

Kiefer, D., and Kuhn, A. (1999) *Embo J* **18**, 6299-6306.

Kirpotin, D., Park, J.W., Hong, K., Zalipsky, S., Li, W.-L., Carter, P., Benz, C.C., and Papahadjopoulos, D. (1997) *Biochemistry* **36**, 66-75.

Klibanov, A.L., Maruyama, K., Torchilin, V.P., and Huang, L. (1990) *FEBS Letters* **268**, 235-237.

Klotz, L. (2005) *Journal of Clinical Oncology* **23**, 8165.

Koivunen, E., Arap, W., Valtanen, H., Rainisalo, A., Medina, O.P., Heikkila, P., Kantor, C., Gahmberg, C.G., Salo, T., Konttinen, Y.T., et al. (1999) **17**, 768-774.

Kolonin, M.G., Saha, P.K., Chan, L., Pasqualini, R., and Arap, W. (2004) *Nat. Med.* **10**, 625-632.

Krag, D.N., Fuller, S.P., Oligino, L., Pero, S.C., Weaver, D.L., Soden, A.L., Hebert, C., Mills, S., Liu, C., and Peterson, D. (2002) *Cancer Chemother Pharmacol* **50**, 325-332.

Krag, D.N., Shukla, G.S., Shen, G.-P., Pero, S., Ashikaga, T., Fuller, S., Weaver, D.L., Burdette-Radoux, S., and Thomas, C. (2006) *Cancer Res* **66**, 7724-7733.

Krumpe, L., and Mori, T. (2006) *International Journal of Peptide Research and Therapeutics* **12**, 79-91.

Kuzmicheva, G.A., Jayanna, P.K., Sorokulova, I.B., and Petrenko, V.A. (2009) *Protein Engineering, Design and Selection* **22**, 9-18.

Kuzmicheva, G.A., Sorokulova, I.B., Jayanna, P.K., and Petrenko, V.A. 2008. Landscape phage libraries as a source of bioselective nanomaterials. In *NSTI Nanotech*, Boston.

Ladner, R.C., Sato, A.K., Gorzelany, J., and de Souza, M. (2004) *Drug Discovery Today* **9**, 525-529.

Lamla, T., and Erdmann, V.A. (2003) *Journal of Molecular Biology* **329**, 381-388.

Lee, S., M.F.[1], M., and S.J.[1][2], O. (2003) *Journal of Biomolecular NMR* **26**, 327-334.

Lee, T.-Y., Lin, C.-T., Kuo, S.-Y., Chang, D.-K., and Wu, H.-C. (2007) *Cancer Res* **67**, 10958-10965.

Lee, T.-Y., Wu, H.-C., Tseng, Y.-L., and Lin, C.-T. (2004) *Cancer Res* **64**, 8002-8008.

Legendre, D., and Fastrez, J. (2002) *Gene* **290**, 203-215.

Li, Z., Koch, H., and DÃ¼beh, S. (2003) *Journal of Molecular Microbiology & Biotechnology* **6**, 57.

Lleonart, M.E., Martin-Duque, P., Sanchez-Prieto, R., Moreno, A., and Ramon y Cajal, S. (2000) *Histol Histopathol* **15**, 881-898.

Loeb, T. (1960) *Science* **131**, 932-933.

Lukyanov, A.N., Elbayoumi, T.A., Chakilam, A.R., and Torchilin, V.P. (2004) *Journal of Controlled Release* **100**, 135-144.

Maeda, H., Wu, J., Sawa, T., Matsumura, Y., and Hori, K. (2000) *Journal of Controlled Release* **65**, 271-284.

Makino, S., Woolford, J.L., Jr, Tanford, C., and Webster, R.E. (1975) *J. Biol. Chem.* **250**, 4327-4332.

Makowski, L., and Soares, A. (2003) *Bioinformatics* **19**, 483-489.

Malik, P., Terry, T.D., Bellintani, F., and Perham, R.N. (1998) *FEBS Letters* **436**, 263-266.

Mandava, S., Makowski, L., Devarapalli, S., Uzubell, J., and Rodi, D.J. (2004) *PROTEOMICS* **4**, 1439-1460.

Mao, C., Solis, D.J., Reiss, B.D., Kottmann, S.T., Sweeney, R.Y., Hayhurst, A., Georgiou, G., Iverson, B., and Belcher, A.M. (2004) *Science* **303**, 213-217.

Maruyama, K., Huang, L., and Kennel, S.J. (1990) *Proceedings of the National Academy of Sciences of the United States of America ; Vol/Issue: 87:15; DOE Project*, Pages: 5744-5748.

Marvin, D.A. (1998) *Current Opinion in Structural Biology* **8**, 150-158.

Marvin, D.A., Hale, R.D., Nave, C., and Helmer-Citterich, M. (1994) *J Mol Biol* **235**, 260-286.

Marvin, D.A., and Hoffman-Berling, H. (1963) *Nature (London)* **197**, 517-518.

Marvin, D.A., Welsh, L.C., Symmons, M.F., Scott, W.R.P., and Straus, S.K. (2006) *Journal of Molecular Biology* **355**, 294-309.

Matsuo, T., Matsuo, T., Yamamoto, T., Niiyama, K., Yamazaki, N.A.Y.N., Ishida, T.A.I.T., Kiwada, H.A.K.H., Shinohara, Y.A.S.Y., and Kataoka, M.A.K.M. 2007. Design, preparation and directional insertion of peptides into lipid bilayer membrane and their application for the preparation of liposome of which surface

could be coated by externally added antibody. In *Micro-NanoMechatronics and Human Science, 2007.* , pp. 73-78.

Mazhar, D., and Waxman, J. (2002) *Postgrad. Med. J.* **78**, 590-595.

McLafferty, M.A., Kent, R.B., Ladner, R.C., and Markland, W. (1993) *Gene* **128**, 29-36.

McLeod, D., Zinner, N., Tomera, K., Gleason, D., Fotheringham, N., Campion, M., and Garnick, M.B. (2001) *Urology* **58**, 756-761.

McMenemin, R., Macdonald, G., Moffat, L., and Bissett, D. (2002) *Investigational new drugs* **20**, 331-337.

Medina, O.P., Soderlund, T., Laakkonen, L.J., Tuominen, E.K.J., Koivunen, E., and Kinnunen, P.K.J. (2001) *Cancer Res* **61**, 3978-3985.

Meissner, P.S., Sisk, W.P., and Berman, M.L. (1987) *Proceedings of National Academy of Sciences* **84**, 4171-4175.

Merzlyak, A., Indrakanti, S., and Lee, S.W. (2009) *Nano Letters* **9**, 846-852.

Merzlyak, A., and Lee, S.-W. (2006) *Current Opinion in Chemical Biology* **10**, 246-252.

Messing, E.M., Manola, J., Sarosdy, M., Wilding, G., Crawford, E.D., and Trump, D. 1999. Immediate hormonal therapy compared with observation after radical prostatectomy and pelvic lymphadenectomy in men with node-positive prostate cancer, pp. 1781-1788.

Mori, T. (2004) *Current Pharmaceutical Design* **10**, 2335-2343.

Mount, J.D., Samoylova, T.I., Morrison, N.E., Cox, N.R., Baker, H.J., and Petrenko, V.A. (2004) *Gene* **341**, 59-65.

Nellis, D.F., Ekstrom, D.L., Kirpotin, D.B., Zhu, J., Andersson, R., Broadt, T.L., Ouellette, T.F., Perkins, S.C., Roach, J.M., Drummond, D.C., et al. (2005a) *Biotechnol. Prog.* **21**, 205-220.

Nellis, D.F., Kirpotin, D.B., Janini, G.M., Shenoy, S.R., Marks, J.D., Tsai, R., Drummond, D.C., Hong, K., Park, J.W., Ouellette, T.F., et al. (2005b) *Biotechnol. Prog.* **21**, 221-232.

Nieto, M., Finn, S., Loda, M., and Hahn, W.C. (2007) *International Journal of Biochemistry and Cell Biology* **39**, 1562-1568.

Nilsson, F., Tarli, L., Viti, F., and Neri, D. (2000) *Advanced Drug Delivery Reviews* **43**, 165-196.

Noble, C.O., Kirpotin, D.B., Hayes, M.E., Mamot, C., Hong, K., Park, J.W., Benz, C.C., Marks, J.D., and Drummond, D.C. (2004) *Expert Opin Ther Targets* **8**, 335-353.

Nobs, L., Buchegger, F., Gurny, R., and Allemann, E. (2004) *J Pharm Sci* **93**, 1980-1992.

Nobs, L., Buchegger, F., Gurny, R., and Allemann, E. (2006) *Drugs and the Pharmaceutical Sciences* **158**, 123-148.

Ohkawa, I., and Webster, R. (1981) *J. Biol. Chem.* **256**, 9951-9958.

Olofsson, L., Ankarloo, J., and Nicholls, I.A. (1998) *Journal of Molecular Recognition* **11**, 91-93.

Olsen, E.V., Sorokulova, I.B., Petrenko, V.A., Chen, I.H., Barbaree, J.M., and Vodyanoy, V.J. (2006) *Biosensors and Bioelectronics* **21**, 1434-1442.

Papahadjopoulos, D., Allen, T.M., Gabizon, A., Mayhew, E., Matthay, K., Huang, S.K., Lee, K., Woodle, M.C., Lasic, D.D., Redemann, C., et al. (1991) *Proceedings of the National Academy of Sciences* **88**, 11460-11464.

Paschke, M. (2006) *Appl Microbiol Biotechnol* **70**, 2-11.

Pastorino, F., Brignole, C., Di Paolo, D., Nico, B., Pezzolo, A., Marimpietri, D., Pagnan, G., Piccardi, F., Cilli, M., Longhi, R., et al. (2006) *Cancer Res* **66**, 10073-10082.

Petrenko, V.A. (2008a) *Expert Opinion on Drug Delivery* **5**, 825-836.

Petrenko, V.A. (2008b) *Microelectronics Journal* **39**, 202-207.

Petrenko, V.A., and Brigati, J.R. (2007) In J.M.V, E. (eds), *Immunoassay and other Bioanalytical Techniques*. CRC press, Taylor & Francis Group, Boca Raton, FL

Petrenko, V.A., and Smith, G.P. (2000) *Protein Engineering* **13**, 589-592.

Petrenko, V.A., and Smith, G.P. (2005) In Sidhu, S.S. (eds), *Phage Display in Biotechnology and Drug Discovery*. CRC Press, Taylor & Francis Group, Boca Raton, FL

Petrenko, V.A., Smith, G.P., Gong, X., and Quinn, T. (1996) *Protein Engineering* **9**, 797-801.

Petrenko, V.A., Smith, G.P., Mazooji, M.M., and Quinn, T. (2002) *Protein Engineering* **15**, 943-950.

Petrenko, V.A., Ustinov, S.N., and Chen, I. 2006. Fusion Phage as a Bioselective Nanomaterial: Evolution of the concept. In *European Nano Systems 2006*, pp. 89-94, Paris.

Petrylak, D.P. (2005a) *Urology* **65**, 3-7.

Petrylak, D.P. (2005b) *Urology* **65**, 8-12.

Petrylak, D.P., Tangen, C.M., Hussain, M.H., Lara, P.N., Jr., Jones, J.A., Taplin, M.E., Burch, P.A., Berry, D., Moinpour, C., Kohli, M., et al. (2004) *N Engl J Med* **351**, 1513-1520.

Picus, J., and Schultz, M. 1999. Docetaxel (Taxotere) as monotherapy in the treatment of hormone-refractory prostate cancer: preliminary results, pp. 14.

Pomerantz, M., and Kantoff, P. (2007) *Annual Review of Medicine* **58**, 205-220.

Reilly, R.M., Sandhu, J., Alvarez-Diez, T.M., Gallinger, S., Kirsh, J., and Stern, H. (1995) *Clin Pharmacokinet* **28**, 126-142.

Reiss, B.D., Mao, C., Solis, D.J., Ryan, K.S., Thomson, T., and Belcher, A.M. (2004) *Nano Letters* **4**, 1127-1132.

Ridder, A.N.J.A., van de Hoef, W., Stam, J., Kuhn, A., de Kruijff, B., and Killian, J.A. (2002) *Biochemistry* **41**, 4946-4952.

Roberts, D., Guegler, K., and Winter, J. (1993) *Gene* **128**, 67-69.

Rodi, D.J., Mandava, S., and Makowski, L. (2005) In Sidhu, S.S. (eds), *Phage display in biotechnology and drug discovery*. CRC press, Taylor & Francis Group, Boca Raton, FL. pp. 1-61.

Romanov, V.I. (2003) *Curr Cancer Drug Targets* **3**, 119-129.

Romanov, V.I., Durand, D.B., and Petrenko, V.A. (2001) *Prostate* **47**, 239-251.

Romanov, V.I., Whyard, T., Adler, H.L., Waltzer, W.C., and Zucker, S. (2004) *Cancer Res* **64**, 2083-2089.

Rosner, B. (2006) *Fundamentals of Biostatistics*. Thomson Brooks/Cole, Belmont, CA.

Samoylova, T.I., Cox, N.R., Morrison, N.E., Globa, L.P., Romanov, V., Baker, H.J., and Petrenko, V.A. (2004) *Biotechniques* **37**, 254-260.

Samoylova, T.I., Morrison, N.E., Globa, L.P., and Cox, N.R. (2006) *Anti-Cancer Agents in Medicinal Chemistry (Formerly Current Medicinal Chemistry - Anti-Cancer Agents)* **6**, 9-17.

Samoylova, T.I., Petrenko, V.A., Morrison, N.E., Globa, L.P., Baker, H.J., and Cox, N.R. (2003) *Mol Cancer Ther* **2**, 1129-1137.

Sawant, R.M., Cohen, M.B., Torchilin, V.P., and Rokhlin, O.W. (2008) *Journal of Drug Targeting* **16**, 601-604.

SchrÖDer, F.H., Kurth, K.H., FossÅ, S.D., Hoekstra, W., Karthaus, P.P.M., Debois, M., and Collette, L. (2004) *The Journal of urology* **172**, 923-927.

Schulze, H., and Senge, T. (1990) *The Journal of urology* **144**, 934.

Shadidi, M., and Sioud, M. (2003) *Drug Resistance Updates* **6**, 363-371.

Shannon, C.E. (1948) *The Bell System Technical Journal* **27**, 379-423, 623-656.

Shukla, G.S., and Krag, D.N. (2005a) *Journal of Drug Targeting* **13**, 7 - 18.

Shukla, G.S., and Krag, D.N. (2005b) *Oncol Rep* **13**, 757-764.

Sidhu, S.S. (2000) *Current Opinion in Biotechnology* **11**, 610-616.

Slimani, H., Guenin, E., Briane, D., Coudert, R., Charnaux, N., Starzec, A., Vassy, R., Lecouvey, M., Perret, Y.G., and Cao, A. (2006) *Journal of Drug Targeting* **14**, 694 - 706.

Small, E.J., Halabi, S., Dawson, N.A., Stadler, W.M., Rini, B.I., Picus, J., Gable, P., Torti, F.M., Kaplan, E., and Vogelzang, N.J. (2004) *Journal of Clinical Oncology* **22**, 1025.

Smith, G.P. (1985) *Science* **228**, 1315-1317.

Smith, G.P. (1988) *Virology* **167**, 156-165.

Smith, G.P., and Petrenko, V.A. (1997) *Chemical Reviews* **97**, 391-410.

Smith, G.P., and Scott, J.K. (1993) *Methods in Enzymology* **217**, 228-257.

Soekarjo, M., Eisenhawer, M., Kuhn, A., and Vogel, H. (1996) *Biochemistry* **35**, 1232-1241.

Sorokulova, I.B., Olsen, E.V., Chen, I.H., Fiebor, B., Barbaree, J.M., Vodyanoy, V.J., Chin, B.A., and Petrenko, V.A. (2005) *Journal of Microbiological Methods* **63**, 55-72.

Sprujit, R.B., Wolfs, C.J.A.M., and Hemminga, M. (1989) *Biochemistry (Mosc).* **28**, 9158-9165.

Stein, R., Qu, Z., Cardillo, T.M., Chen, S., Rosario, A., Horak, I.D., Hansen, H.J., and Goldenberg, D.M. (2004) *Blood* **104**, 3705-3711.

Stopar, D., Spruijt, R.B., and Hemminga, M.A. (2006) *Chem. Phys. Lipids* **141**, 83-93.

Stopar, D., Spruijt, R.B., Wolfs, C.J.A.M., and Hemminga, M.A. (2003) *Biochimica et Biophysica Acta (BBA) - Biomembranes* **1611**, 5-15.

Taichman, R.S., Loberg, R.D., Mehra, R., and Pienta, K.J. (2007) *J. Clin. Invest.* **117**, 2351.

Tanne, J.H. (2008) *BMJ* **336**, 66.

Tannock, I.F., de Wit, R., Berry, W.R., Horti, J., Pluzanska, A., Chi, K.N., Oudard, S., Theodore, C., James, N.D., Turesson, I., et al. (2004) *N Engl J Med* **351**, 1502-1512.

Tannock, I.F., Osoba, D., Stockler, M.R., Ernst, D.S., Neville, A.J., Moore, M.J., Armitage, G.R., Wilson, J.J., Venner, P.M., and Coppin, C.M. (1996) *Journal of Clinical Oncology* **14**, 1756.

Thiaudiere, E., Soekarjo, M., Kuchinka, E., Kuhn, A., and Vogel, H. (1993) *Biochemistry* **32**, 12186-12196.

Torchilin, V.P. (1985) *Crit Rev Ther Drug Carrier Syst* **2**, 65-115.

Torchilin, V.P. (2000) *European Journal of Pharmaceutical Sciences* **11**, S81-S91.

Torchilin, V.P., Levchenko, T.S., Lukyanov, A.N., Khaw, B.A., Klibanov, A.L., Rammohan, R., Samokhin, G.P., and Whiteman, K.R. (2001) *BBA-Biomembranes* **1511**, 397-411.

Vasir, J.K., and Labhasetwar, V. (2005) *Technol Cancer Res Treat* **4**, 363-374.

Walsh, P.C. (1997) *The Journal of urology* **158**, 1623.

Wang, Q.W., Lu, H.L., Song, C.C., Liu, H., and Xu, C.G. (2005) *World J Gastroenterol* **11**, 4003-4007.

Wang, X., Yu, J., Sreekumar, A., Varambally, S., Shen, R., Giacherio, D., Mehra, R., Montie, J.E., Pienta, K.J., Sanda, M.G., et al. (2006) *The Journal of Urology* **175**, 1706-1706.

Waxman, J., Man, A., Hendry, W.F., Whitfield, H.N., Besser, G.M., Tiptaft, R.C., Paris, A.M., and Oliver, R.T. (1985) *British Medical Journal* **291**, 1387.

Webster, R. (2001) In Carlos F.Barbas III et al. (eds), *Phage display : a laboratory manual.* Cold Spring Harbor Laboratory Press., NY

Wilt, T.J., Abrahamsson, P.A., Crawford, E.D., Lucia, M.S., Sakr, W.A., and Schalken, J. (2003) *Reviews in Urology* **5**, S3.

Yagoda, A., and Petrylak, D. (1993) *Cancer* **71**, 1098-1109.

Zalipsky, S. (1993) *Bioconjugate Chem.* **4**, 296-299.

Zeri, A.C., Mesleh, M.F., Nevzorov, A.A., and Opella, S.J. (2003) *Proceedings of the National Academy of Sciences* **100**, 6458-6463.

Zhang, J., Spring, H., and Schwab, M. (2001) *Cancer letters* **171**, 153-164.

Zitzmann, S., Mier, W., Schad, A., Kinscherf, R., Askoxylakis, V., Kramer, S., Altmann, A., Eisenhut, M., and Haberkorn, U. (2005) *Clin Cancer Res* **11**, 139-146.